

Monoterpenoid indole alkaloid dimers from *Kopsia arborea* inhibit cyclin-dependent kinase 5 and tau phosphorylation

Chen Chen^a, Jian-Wen Liu^a, Ling-Li Guo^a, Feng Xiong^a, Xiao-Qian Ran^{b,d}, Ya-Rong Guo^{b,e}, Yong-Gang Yao^{b,d}, Xiao-Jiang Hao^{a,c,***}, Rong-Can Luo^{b,d,**}, Yu Zhang^{a,*}

^a State Key Laboratory of Phytochemistry and Plant Resources in West China, Kunming Institute of Botany, Chinese Academy of Sciences, Kunming, 650201, Yunnan, China

^b Key Laboratory of Animal Models and Human Disease Mechanisms of the Chinese Academy of Sciences & Yunnan Province, And KIZ-CUHK Joint Laboratory of Bioresources and Molecular Research in Common Diseases, Kunming Institute of Zoology, Chinese Academy of Sciences, Kunming, 650204, Yunnan, China

^c Research Unit of Chemical Biology of Natural Anti-Virus Products, Chinese Academy of Medical Sciences, Beijing, 100730, China

^d Kunming College of Life Science, University of Chinese Academy of Sciences, Kunming, 650201, Yunnan, China

^e School of Life Sciences, Division of Life Sciences and Medicine, University of Science and Technology of China, Hefei, 230026, Anhui, China

ARTICLE INFO

Keywords:

Kopsia arborea Blume
Apocynaceae
Monoterpenoid indole alkaloids
Kopoffines A-C
Cyclin-dependent kinase 5
Tau phosphorylation

ABSTRACT

Three undescribed monoterpenoid indole alkaloid dimers (kopoffines A-C, which are connected via a methylene unit) and with nine known alkaloids were isolated and identified from the fruits of *Kopsia arborea* Blume. Their structures, including their absolute configurations, were established by HRESIMS, NMR, single-crystal X-ray diffraction, and ECD analyses. Kopoffines A-C showed significant inhibition against cyclin-dependent kinase 5 (IC_{50} : 0.34–2.18 μ M). Western blotting analyses showed that kopoffines A-C significantly decreased the protein levels of CDK5 and phospho-CDK5 (Tyr15) (pCDK5) at concentrations of 2.5 and 10 μ M. The levels of phospho-Tau (Thr217) (pTau217, a new biomarker of AD), and phospho-Tau (Ser396) (pTau396), which play major roles in the formation of neurofibrillary tangles, were decreased by the kopoffines A-C treatment. Molecular docking studies indicated that kopoffines A-C could form stable interactions with CDK5.

1. Introduction

Alzheimer's disease (AD) is the distinguishing form of senile dementia that can obstruct normal cognitive function (Selkoe, 2021). Since it impacts the memory, thinking, and social autonomy, AD affects approximately 50 million individuals worldwide and is now among the 10 most common fatal diseases (Gauthier et al., 2021; Wang et al., 2017). Despite intensive studies, the pathogenesis of this tragic illness has not been elucidated, and effective therapies remain to be discovered (Scheltens et al., 2021). The formation of neurofibrillary tangles (NFTs) and senile plaques (SPs) are the major pathological hallmarks of AD (Lacosta et al., 2017). NFT consists of paired helical filaments whose

main component is hyperphosphorylated tau, and SP is caused by the abnormal metabolism and accumulation of amyloid- β (A β) (Lacosta et al., 2017).

Although invariant pathological hallmarks, plaques, tangles and neuronal death are common to AD, the mechanistic relationship among these features remains largely unknown. One molecular mediator that can link these events is proline-directed serine-threonine protein kinase cyclin-dependent kinase 5 (CDK5), which is a kinase in tau phosphorylation (Cruz and Tsai, 2004; Lopes and Agostinho, 2011). CDK5 is involved in the regulation of neurite extension, synapse formation, and synaptic transmission (Cicero and Herrup, 2005; Patrick et al., 1999; Zhang et al., 2008; Zhou et al., 2020). The activity of CDK5 is regulated

* Corresponding author. State Key Laboratory of Phytochemistry and Plant Resources in West China, Kunming Institute of Botany, Chinese Academy of Sciences, Kunming, 650201, Yunnan, China.

** Corresponding author. Key Laboratory of Animal Models and Human Disease Mechanisms of the Chinese Academy of Sciences & Yunnan Province, And KIZ-CUHK Joint Laboratory of Bioresources and Molecular Research in Common Diseases, Kunming Institute of Zoology, Chinese Academy of Sciences, Kunming, 650204, Yunnan, China.

*** Corresponding author. State Key Laboratory of Phytochemistry and Plant Resources in West China, Kunming Institute of Botany, Chinese Academy of Sciences, Kunming, 650201, Yunnan, China.

E-mail addresses: haoxj@mail.kib.ac.cn (X.-J. Hao), luorongcan@mail.kiz.ac.cn (R.-C. Luo), zhangyu@mail.kib.ac.cn (Y. Zhang).

by its binding with activator proteins p35 and p25 (Chow et al., 2014; Lopes and Agostinho, 2011). Increasing evidence supports that the deregulation of CDK5 is neurotoxic and contributes to the pathogenesis of AD (Cheung and Ip, 2012; Cruz and Tsai, 2004). p25 is more stable and able to activate CDK5 than p35 under physiological conditions, which allows CDK5 to be continuously overactivated (Noble et al., 2003; Cruz et al., 2003). The CDK5/p25 complex catalyzes the hyperphosphorylation of serine/threonine at specific sites in its substrate tau, and the structure of tau is altered, which misfolds and aggregates tau and forms NFT (Lopes and Agostinho, 2011; Seo et al., 2017). Therefore, CDK5 has been suggested as an appealing drug target for AD (Allnutt et al., 2020; Huang et al., 2020; Malhotra et al., 2021; Sundaram et al., 2013; Zheng et al., 2005).

Monoterpene indole alkaloids (MIAs) are an attractive class of alkaloids with complex structures and intriguing biological activities, and reserpine and vincristine are outstanding representatives among them (De Luca et al., 2012). *Kopsia arborea* Blume (Apocynaceae) is one of

three species of the *Kopsia* genus that are rich in MIAs and some of them possess novel skeletons and significant activities (Jin et al., 2022; Li et al., 1995; Wong et al., 2019, 2021). Previously we found that 5 β -O-angelate-20-deoxynggenol (HEP14) and harpertrioate A exhibited potential in the treatment of AD via novel mechanisms (Li et al., 2016; Tang et al., 2021). In our ongoing search for bioactive natural products (Huo et al., 2021; Yi et al., 2020; Yuan et al., 2017; Zhang et al., 2018, 2020), three undescribed MIA dimers (kopoffines A-C (1–3)), and nine known alkaloids were obtained from the fruits of *K. arborea* (see Fig. 1). The present study aimed to elucidate the structures and clarify their potential effects on CDK 5 and tau phosphorylation.

2. Results and discussion

Kopoffine A (**1**) was isolated as colorless crystals. Its molecular formula of C₄₁H₄₈N₄O₃ was established by its HRESIMS data at 645.3807 [M + H]⁺ (calcd for C₄₁H₄₈N₄O₃ + H, 645.3799), which indicated 20

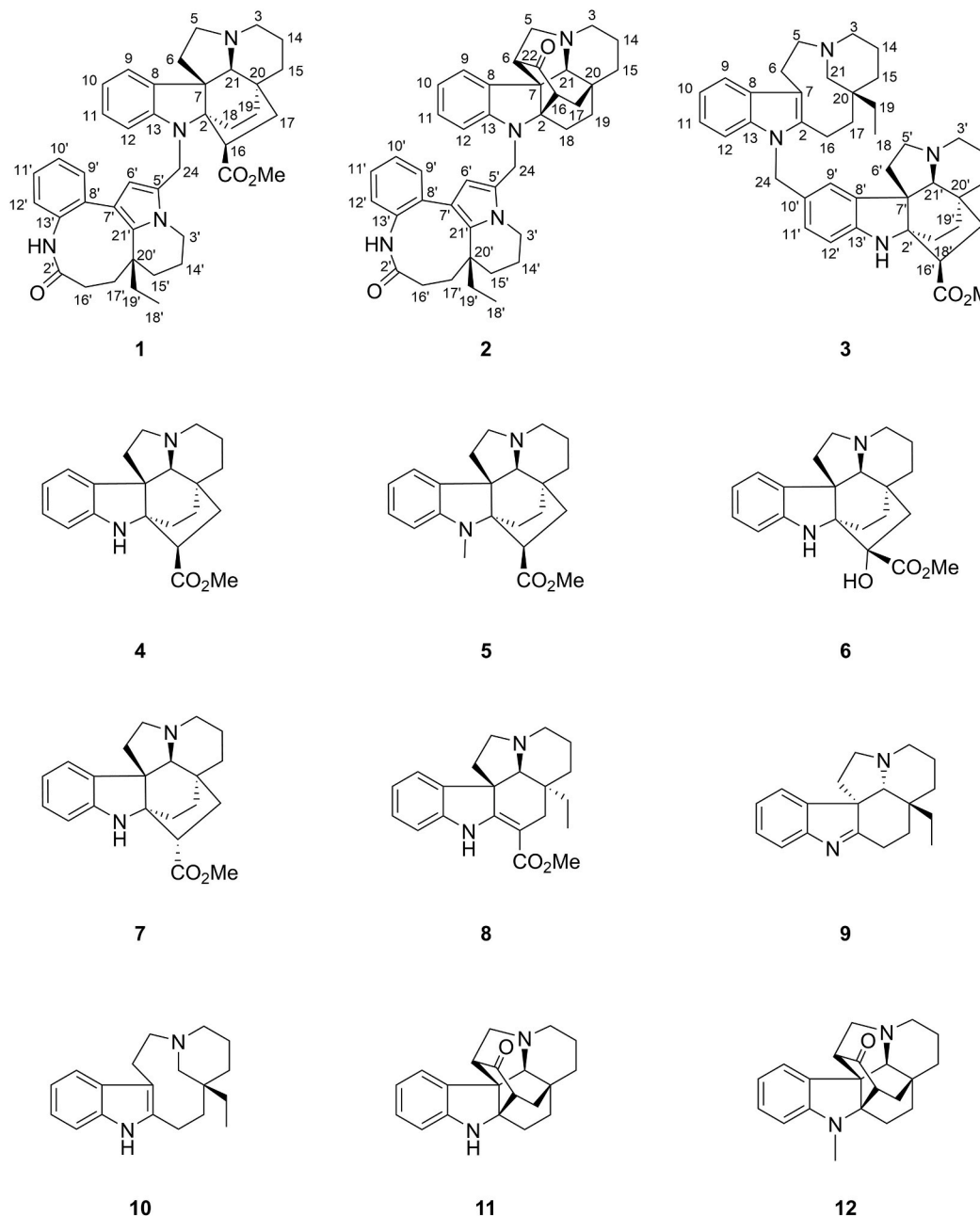


Fig. 1. Molecular structures of alkaloids 1–12.

indices of hydrogen deficiency. IR absorption bands at 3434, 1731 and 1660 cm^{-1} suggested the presence of NH, ester carbonyl and lactam carbonyl groups, respectively. The ^{13}C NMR data (Table 2) indicated that **1** was a bisindole alkaloid, and 41 carbon atoms were classified as two methyls (one methoxy), 15 sp^3 methylenes, 11 methines (nine sp^2 and two sp^3 ones), and 13 nonprotonated carbons (nine sp^2 and four sp^3 ones). The observation of three characteristic nonprotonated carbons resonating at δ_{C} 72.1, 57.1, and 31.1 and one unsubstituted indole moiety (δ_{H} 6.32–7.10) demonstrated that one monomer shared the same skeleton as aspidofractinine-type MIAs, kopsinine (Wong et al., 2021). Meanwhile, the presence of one methyl (δ_{H} 0.73, t, J = 7.5 Hz; δ_{C} 8.3), one quaternary carbon (δ_{C} 38.9), one amide carbonyl (δ_{C} 177.3), and two sp^2 nonprotonated carbons (δ_{C} 116.9, 129.2) indicated that the other monomer was the rhazinilam-type MIA rhazinilam (Gan et al., 2013; Goh et al., 1989). The striking difference was that the sp^2 methine (δ_{C} 118.9) at C-5 in rhazinilam was replaced by an sp^2 nonprotonated carbon at δ_{C} 128.4 in **1**, which indicated that the position might be a linkage point of the dimer. In addition to the aforementioned signals observed in the NMR spectrum, methylene (δ_{H} 3.71, 4.39, each 1 H with doublet, J = 15.5 Hz; δ_{C} 43.2) might be the probable linkage between the two monomers. The key HMBC correlations of H-24 b (δ_{H} 4.39) to δ_{C} 72.1, 150.7, 128.4, and 109.1 confirmed that the two units were linked through the methylene moiety with N-1 and C-5' as terminal junctions (Fig. 2A). The planar structure was finally established as an aspidofractinine-rhazinilam-type bisindole alkaloid with a methylene moiety as a linker, which was verified through ^1H - ^1H COSY, HSQC, and HMBC data analyses (Fig. 2A).

The relative configuration of **1** was established by an analysis of its ROESY spectrum (Fig. 2B). The ROESY correlations of H-21 (δ_{H} 2.98) with H-18a (δ_{H} 1.44) and H-19 b (δ_{H} 1.38), and of H-16 (δ_{H} 2.96) with H-18 b (δ_{H} 1.53) indicated that these protons were co-facial and arbitrarily assigned as α -oriented. Therefore, the ester carbonyl at C-16 was β -oriented. However, the relative configuration of the ethyl group at C-20' in unit B could not be assigned due to the limited ROESY correlations. Finally, the absolute configuration of (2R,7R,16R,20R,21S,20'R)-**1** was established by X-ray diffraction analysis with a Flack parameter of 0.01 (12) (Fig. 3).

Kopoffine B (**2**) was obtained as a white powder. The HRESIMS data (m/z 613.3539 [$\text{M} + \text{H}$] $^+$, calcd for $\text{C}_{40}\text{H}_{44}\text{N}_4\text{O}_2 + \text{H}$, 613.3537) showed that the molecular formula of compound **2** was $\text{C}_{40}\text{H}_{44}\text{N}_4\text{O}_2$. The IR

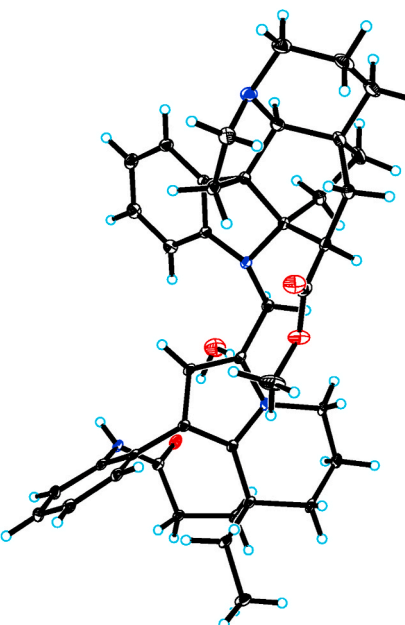
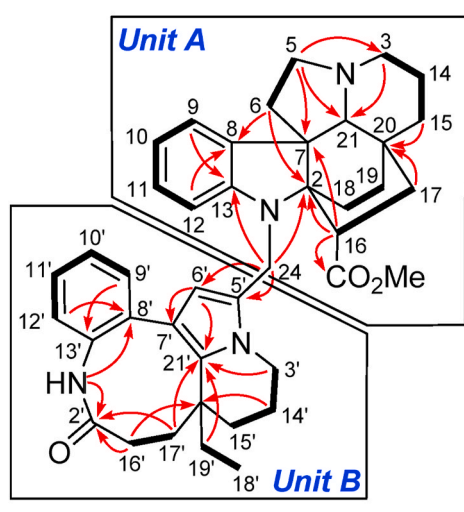
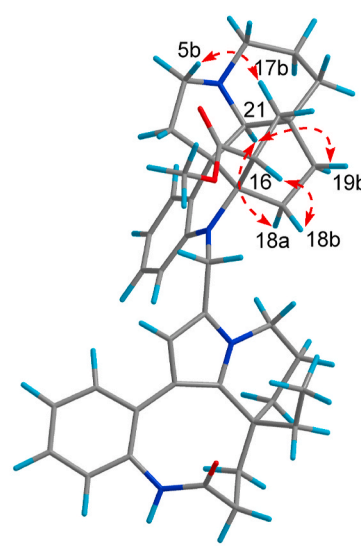


Fig. 3. X-ray ORTEP drawing of **1**.

spectrum showed absorption bands at 3429, 1739 and 1665 cm^{-1} , which corresponded to NH, carbonyl and lactam carbonyl groups, respectively. Comprehensive analysis of its NMR data suggested that **2** was a bisindole alkaloid and had a similar skeleton to **1**. In addition to the unsubstituted indole moiety (δ_{H} 6.69–7.36), HMBC correlations of H-6 (δ_{H} 2.40) and H-16 (δ_{H} 1.83) to the carbonyl carbon (δ_{C} 219.6), and of H-18 b (δ_{H} 2.14) to C-2 (δ_{C} 75.6) and C-7 (δ_{C} 64.2), as well as correlations of H-15a (δ_{H} 1.28) and H-19 b (δ_{H} 1.36) to C-20 (δ_{C} 31.6) confirmed the presence of a kopsanone unit instead of kopsinine in **2** (Jones et al., 2011). A notable observation of the sp^2 quaternary carbon (δ_{C} 126.0) at C-5' in the rhazinilam unit and the additional methylene (δ_{H} 3.78, 4.39; δ_{C} 41.8) indicated that the dimer might have an identical linkage pattern to alkaloid **1**. Key HMBC correlations from H-24 (δ_{H} 3.78) to C-2 (δ_{C} 75.6), C-13 (δ_{C} 153.0), C-5' (δ_{C} 126.0), and C-6' (δ_{C} 112.6) suggested the linkage of the two units from the indolic nitrogen



A



B

Fig. 2. ^1H - ^1H COSY (A: real bold lines), selected HMBC (A: red arrows), and ROESY (B: dashed red arrows) correlations of **1**. (For interpretation of the references to color in this figure legend, the reader is referred to the Web version of this article.)

of the kopsine-type monomer to C-5' of the rhazinilam-type monomer. Thus, the complete planar structure of **2** was determined (Fig. 4A).

The ROESY correlations of H-5a (δ_H 3.13) and H-17 b (δ_H 1.89) and of H-21 (δ_H 3.28) with H-19a (δ_H 1.19) deduced that CH₂-18, CH₂-19, and H-21 were α -oriented, whereas the bridge C-2-C-16-C-17-C-20 was β -oriented, and unit A had an identical configuration to kopsanone (Jones et al., 2011). However, unit B had only one chiral quaternary carbon atom at C-20', and no corresponding ROESY correlations were observed, so the configuration of unit B could not be determined. Finally, time-dependent density functional theory (TDDFT) ECD calculations were applied to clarify the absolute configuration of **2**. Since the relative configuration of unit B was unassigned, it has two possible absolute configurations: 20'R or 20'S. Thus, two possible isomers of (2R, 6R, 7R, 16R, 20R, 21S, 20'R)-2 and (2R, 6R, 7R, 16R, 20R, 21S, 20'S)-2 were used as primary geometries. The results showed that the calculated ECD curve for (2R, 6R, 7R, 16R, 20R, 21S, 20'R)-2 well matched its experimental ECD spectrum (Fig. 5), which established the absolute configuration of **2**.

Kopoffine C (**3**) was isolated as a white powder. Its molecular formula was determined to be C₄₁H₅₂N₄O₂ by HRESIMS at *m/z* 633.4153 [M + H]⁺ (calcd for C₄₁H₅₂N₄O₂ + H, 633.4163), which corresponds to 18 degrees of unsaturation. The ¹H NMR data (Table 1) indicated the presence of seven aromatic resonances of the indole moiety (δ_H 6.45–7.41), which indicated that alkaloid **3** could be an indole dimer. Synthetic application of ¹H and ¹³C NMR data led to recognition of one aspidosperma and one aspidofractinine type. The existence of three sp³ nonprotonated carbons (δ_C 67.9, 59.4, 32.5) was similar to alkaloid **1**, which signified that the monomer was an aspidofractinine-type MIA, kopsinine (Wong et al., 2021). In addition, one characteristic sp³ quaternary carbon at δ_C 38.5 and one ethyl group (δ_C 32.9, 8.4) revealed that the other monomer had the same skeleton as quebrachamine (Wenkert et al., 1976). The conspicuous differences between **3** and kopsinine were the loss of aromatic signals H-10' in kopsinine and the appearance of an aromatic quaternary carbon signal (δ_C 131.9), which indicated the possible connection mode. Moreover, HMBC correlations from methylene (δ_H 5.13, 5.27) to C-2 (δ_C 142.9), C-13 (δ_C 137.9), C-9' (δ_C 121.4), C-10' (δ_C 131.9), and C-11' (δ_C 126.3) suggested that the methylene group linked the two moieties at the indolic nitrogen in units A and C-10' in unit B. Further analysis of the 2D NMR (HSQC, HMBC, and ¹H-¹H COSY) spectrum determined the planar structure of **3** (Fig. 6A).

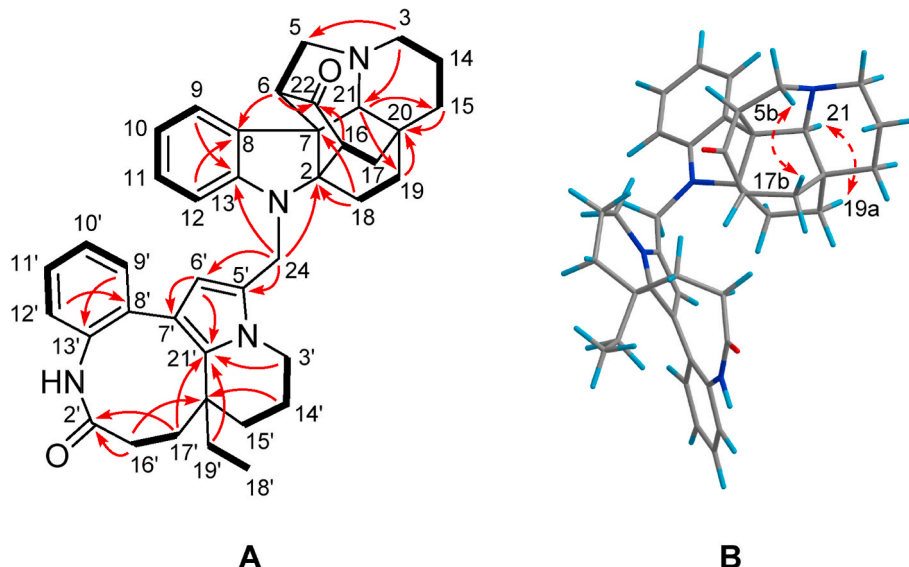


Fig. 4. ¹H-¹H COSY (A: real bold lines), selected HMBC (A: red arrows), and ROESY (B: dashed red arrows) correlations of **2**. (For interpretation of the references to color in this figure legend, the reader is referred to the Web version of this article.)

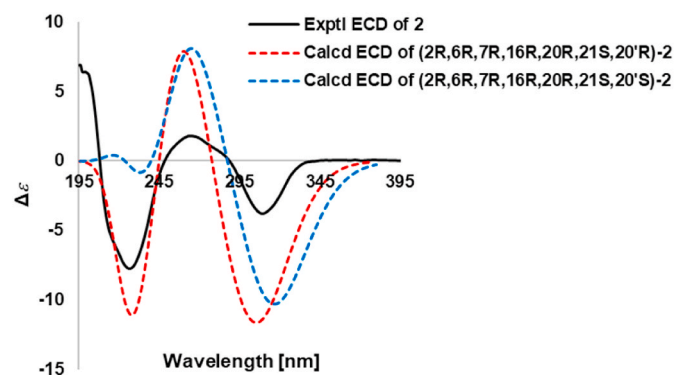


Fig. 5. Comparison of the experimental ECD and calculated ECD spectra of (2R,6R,7R,16R,20R,21S,20'R)-2 (A) and (2R,6R,7R,16R,20R,21S,20'S)-2 (B).

The relative configuration of **3** was deduced from the analysis of its ROESY spectrum (Fig. 6B). The observed ROESY correlations between H-21' (δ_H 3.01) and H-18'b (δ_H 1.81), H-19'a (δ_H 1.19), and between H-16' (δ_H 2.96) and H-18'a (δ_H 1.52) indicated that the aspidofractinine-type monomer had an identical relative configuration to kopsinine (Wong et al., 2021) and left the relative configuration of the aspidosperma-type unit unassigned due to the chiral center. The specific optical value of **3** was nearly zero, which indicated the possibility of a racemate. Then, HPLC analysis using a Chiraldak IC column was performed, and the results demonstrated that **3** was an optically pure compound (Fig. S3.12), which was confirmed by the obvious observation of Cotton effects at 220 ($\Delta\epsilon$, -3.5) and 239 ($\Delta\epsilon$, +19.8) nm in the ECD spectrum (Fig. S3.9). In an attempt to assign the absolute configuration of **3**, we performed time-dependent density functional theory (TDDFT) ECD calculations on two possible geometries: (20R, 2'R, 7'R, 16'R, 20'R, 21'S)-3 and (20S, 2'R, 7'R, 16'R, 20'R, 21'S)-3. The calculated ECD curve for (20R, 2'R, 7'R, 16'R, 20'R, 21'S)-3 well matched its experimental ECD spectrum (Fig. S3.10) and finally established the absolute configuration of **3**.

By comparison of experimental and reported physical data, nine known alkaloids were identified: kopsinine (**4**) (Wong et al., 2021), pleiocarpinine (**5**) (Kuehne and Seaton, 1985), kopsinine B (**6**) (Kitajima et al., 2012), 16-epikopsinine (**7**) (Subramaniam et al., 2017), vinca-difformine (**8**) (Abouzeid et al., 2017), eburenine (**9**) (Wenkert et al.,

Table 1¹H NMR Data of Alkaloids 1–3 at 500 MHz (δ in ppm, J in Hz).

Position	1 ^a	2 ^b	3 ^b
3a	2.94 (m) ^c	2.96 (m)	2.21 (dd, 10.0, 4.0)
3 b	3.12 (br d, 13.5)	3.02 (m)	2.34 (dd, 10.0, 5.0)
5a	2.93 (m) ^c	3.13 (dd, 10.0, 5.0)	2.25 (dd, 11.0, 3.5)
5 b	3.34 (q, 8.0)	3.42 (t, 10.0)	2.41 (dd, 11.0, 3.0)
6a	1.52 (m)	2.40 (dd, 5.0, 2.0)	2.84 (dd, 15.0, 2.5)
6 b	2.77 (ddd, 14.0, 8.0, 3.5)		2.96 (m) ^c
9	7.10 (d, 7.0)	7.36 (d, 7.5) ^c	7.41 (d, 7.5)
10	6.69 (t, 7.0)	6.75 (t, 7.5)	6.95 (t, 7.5)
11	7.02 (t, 7.0)	7.10 (td, 7.5, 1.0)	7.00 (t, 7.5)
12	6.32 (d, 7.0)	6.69 (d, 7.5)	7.24 (d, 7.5)
14a	1.27 (m)	1.23 (m) ^c	1.19 (m) ^c
14 b	1.89 (m)	1.91 (m) ^c	1.45 (m) ^c
15a	1.29 (m)	1.28 (m)	1.05 (dd, 15.0, 7.0)
15 b	1.57 (m)	1.49 (m)	1.11 (m) ^c
16a	2.96 (m) ^c	1.83 (br d, 10.5)	2.59 (dd, 15.0, 6.0)
16 b			2.71 (dd, 15.0, 6.0)
17a	1.35 (m)	1.52 (m) ^c	1.25 (m)
17 b	2.84 (ddd, 13.5, 9.0, 3.0)	1.89 (m)	1.38 (m)
18a	1.44 (m)	1.48 (m)	0.82 (t, 7.5)
18 b	1.53 (m) ^c	2.14 (td, 12.5, 4.0)	
19a	1.23 (m)	1.19 (m)	1.10 (m) ^c
19 b	1.38 (m)	1.36 (td, 12.5, 4.0)	1.23 (m)
21a	2.98 (s)	3.28 (s)	1.41 (d, 12.0)
21 b			3.39 (d, 12.0)
23	3.41 (s)		
24a	3.71 (d, 15.0)	3.78 (d, 14.0)	5.13 (d, 16.5)
24 b	4.39 (d, 15.0)	4.39 (d, 14.0)	5.27 (d, 16.5)
NH'	6.46 (s)		
3'a	3.57 (ddd, 12.5, 12.5, 5.0)	3.50 (td, 12.0, 5.0)	2.96 (m) ^c
3'b	4.03 (td, 12.0, 5.0)	3.97 (dd, 12.0, 5.0)	3.09 (dt, 13.5, 2.0)
5'a			2.94 (m) ^c
5'b			3.42 (q, 8.0)
6'a	5.55 (s)	5.74 (s)	1.51 (m)
6'b			2.76 (ddd, 14.0, 8.5, 2.0)
9'	7.29 (m)	7.35 (d, 7.5)	7.29 (s)
10'	7.23 (t, 7.5)	7.36 (td, 7.5, 2.0) ^c	
11'	7.28 (t, m)	7.29 (td, 7.5, 2.0)	6.45 (d, 7.5) ^c
12'	7.14 (d, 7.5)	7.21 (d, 7.5)	6.46 (d, 7.5) ^c
14'a	1.93 (m)	1.73 (m)	1.29 (m)
14'b	2.32 (m)	2.44 (m)	1.93 (m)
15'a	1.54 (m)	1.52 (m) ^c	1.31 (m)
15'b	1.72 (td, 13.5, 3.0)	1.73 (m)	1.60 (m)
16'a	1.95 (m)	1.91 (m) ^c	2.96 (m) ^c
16'b	2.38 (t, 13.5)	2.42 (ddd, 11.0, 6.0, 2.0)	
17'a	1.47 (m)	1.54 (dd, 14.0, 9.0)	1.37 (m)
17'b	2.54 (t, 13.0)	2.77 (t, 14.0)	2.74 (m)
18'a	0.73 (t, 7.5)	0.70 (t, 7.0)	1.52 (m)
18'b			1.81 (m)
19'a	1.21 (m)	1.22 (m) ^c	1.19 (m)
19'b	1.49 (m)	1.46 (m)	1.44 (m)
21'			3.01 (s)
23'			3.71 (s)

^a Measured in CDCl₃.^b Measured in Methanol-d₄.^c Overlapped.

1976), quebrachamine (10) (Wu et al., 2010), (−)-kopsanone (11) (Jones et al., 2011), and *N*-methylkopsanone (12) (Kuehne and Seaton, 1985).

A possible biogenetic pathway for alkaloids 1–3 is presented in Fig. 9. Biogenetically, the N-1 methyl of pleiocarpinine (5) or *N*-methylkopsanone (12) is oxidized to form N1-Me iminium ions and yield intermediates i and ii, respectively. Then, C-5 of rhazinilam undergoes electrophilic substitution with intermediates i and ii to give dimers 1 and 2, respectively. Similarly, quebrachamine (10) is oxidized at N-1 to yield intermediate iii, which undergoes electrophilic substitution with C-10 of kopsinine (4) and eventually forms alkaloid 3.

Table 2¹³C NMR Data of Alkaloids 1–3 at 125 MHz (δ in ppm).

Position	1 ^a	2 ^b	3 ^b
2	72.1	75.6	142.9
3	47.7	47.7	56.4
5	50.7	55.1	54.6
6	34.9	58.7	23.4
7	57.1	64.2	109.7
8	140.5	135.9	129.1
9	120.1	123.1	117.9
10	118.8	120.3	119.4
11	127.0	128.9	121.0
12	110.1	110.5	110.2
13	150.7	153.0	137.9
14	17.4	16.1	23.8
15	36.4	34.8	36.0
16	42.3	51.4	19.8
17	32.2	34.5	33.7
18	26.1	18.5	8.4
19	33.5	36.5	32.9
20	31.1	31.6	38.5
21	68.4	71.9	57.7
22	175.2	219.6	
23	52.2		
24	43.2	41.8	47.6
2'	177.3	178.9	67.9
3'	43.3	44.4	48.4
5'	128.4	126.0	51.8
6'	109.1	112.6	35.2
7'	116.9	118.1	59.4
8'	140.7	141.0	142.0
9'	130.8	132.6	121.4
10'	127.2	129.2	131.9
11'	127.8	127.9	126.3
12'	126.9	127.7	112.0
13'	138.1	139.6	150.2
14'	19.1	19.9	17.4
15'	32.4	34.4	37.3
16'	28.2	29.0	44.7
17'	37.1	38.5	33.5
18'	8.3	8.6	33.7
19'	30.4	31.0	35.1
20'	38.9	40.3	32.5
21'	129.2	133.1	69.5
22'			176.6
23'			52.5

^a Measured in CDCl₃.^b Measured in Methanol-d₄.

To understand the potential biological activities of alkaloids 1–3 against AD, we conducted cellular analyses using human glioma U251 cells, which stably express the human APP mutant (APP-p. M671L) (U251-APP cells), a cellular AD model that was used in our previous studies (Luo et al., 2020, 2021; Zhang et al., 2016). DMSO (dimethyl sulfoxide) was used as the solvent and negative control. Dinaciclib, which is a CDK5 selective inhibitor (Kumar et al., 2015), was used as a positive control in this assay. At concentrations of 2.5 and 10 μ M, alkaloids 1–3 showed no apparent toxicity to U251-APP cells (Fig. 7A). Alkaloids 1–3 showed potent inhibition against cyclin-dependent kinase 5 (IC₅₀: 0.34–2.18 μ M) (Table 3) when dinaciclib was used as a positive control. Moreover, Western blotting analyses showed that 1–3 significantly decreased the protein levels of CDK5 and phospho-CDK5 (Tyr15) (pCDK5) at concentrations of 2.5 and 10 μ M (Fig. 7B–G), although p25/p35 was not significantly changed, which suggested their potential inhibitory effects on the CDK5 enzymatic activity. Western blotting analyses showed that the levels of phospho-Tau (Thr217) (pTau217, which is a new biomarker of AD) (Mattsson-Carlgren et al., 2020; Palmqvist et al., 2020;), and phospho-Tau (Ser396) (pTau396), which play major roles in the formation of NFT (Stathas et al., 2021), were decreased by the 1–3 treatment. These results suggested that the three alkaloids could inhibit the phosphorylation of tau and its downstream consequences. We measured the levels of A β 42 species, which play

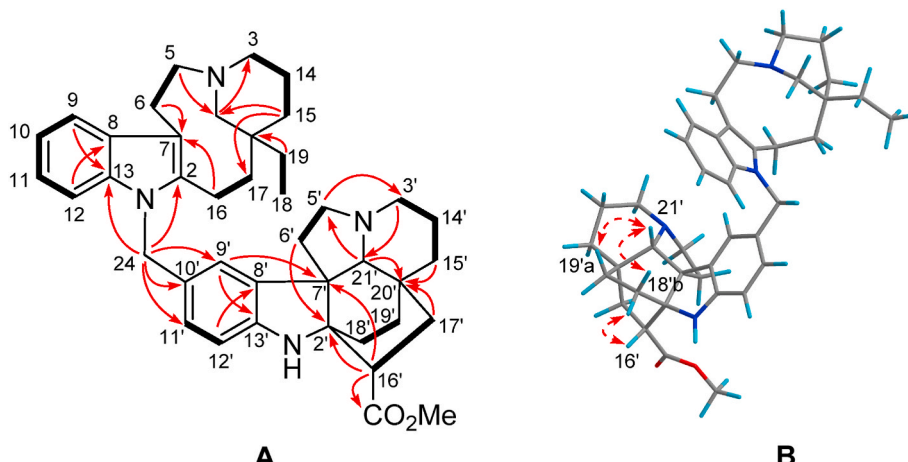


Fig. 6. ^1H - ^1H COSY (A: real bold lines), selected HMBC (A: red arrows), and ROESY (B: dashed red arrows) correlations of **3**. (For interpretation of the references to color in this figure legend, the reader is referred to the Web version of this article.)

major synaptotoxic roles in AD (Mucke and Selkoe, 2012; Dunys et al., 2018; Jan et al., 2017). However, in the culture supernatant of U251-APP cells treated with **1–3**, the levels of $\text{A}\beta_{42}$ did not change, as determined by ELISA (Fig. 7H).

As described above, alkaloids **1–3** exerted strong inhibitory effects on CDK5. To better understand the possible interaction of alkaloids **1–3** with CDK5, docking studies were performed using Schrodinger 2020-3 software. For the CDK5-**1** complex (Fig. 8), the observed amide carbonyl group formed a hydrogen bond with the LYS89 residue. Meanwhile, in the CDK5-**3** complex, a hydrogen bond formed between the ester carbonyl group in alkaloid **3** and the GLU12 residue (Fig. S3.13). These *in silico* results might account for the observed inhibitory efficiency against CDK5 by alkaloids **1–3**.

3. Conclusions

In summary, three undescribed monoterpenoid indole alkaloid dimers (kopoffines A-C (**1–3**)) and nine known alkaloids were isolated and identified from the fruits of *K. arborea*, which were linked by a methylene bridge. Their structures including absolute configurations were established by HRESIMS, NMR, single-crystal X-ray diffraction, and ECD analyses. Alkaloids **1–3** showed potent inhibitory effects on cyclin-dependent kinase 5 (IC_{50} : 0.34–2.18 μM). The cellular assays showed that **1–3** could inhibit the tau phosphorylation and CDK5 activities, which suggested their potential against Alzheimer's disease.

4. Experimental

4.1. General experimental procedures

IR spectra data were done with a Bio-Rad FTS-135 spectrometer from KBr pellets. NMR spectra were performed on Bruker 500 MHz spectrometers with TMS as the internal standard. Optical rotations were recorded on a JASCO P-1020 digital polarimeter, and the ECD spectral data were performed on the optical physical chirascan spectrometer. Mass spectra were measured on VG Auto Spec-3000 or API-Qstar-Pulsar instruments. X-ray data were collected using a Bruker APEX DUO instrument. Column chromatography was performed on silica gel H (10–40 μm , Qingdao Marine Chemical Inc., China) and silica gel (60–80 and 200–300 mesh, Qingdao Marine Chemical Inc., China), and Sephadex LH-20 (40–70 μm , Amersham Pharmacia Biotech AB). Semi-preparative HPLC was performed on a Waters X-bridge (5 μm ; 10 mm \times 150 mm), C18 reversed-phase column. The chiral HPLC was performed on a Daicel Chiral IC column (5 μm ; 10 mm \times 250 mm).

4.2. Plant material

The fruits of *Kopsia arborea* Blume (Apocynaceae) were collected in Guangzhou, Guangdong Province, China (23°59'41.5"N/113°18'4.2"E) in November 2018 and were identified by Dr. Gui-Hua Tang. The voucher specimen (ZY20181101) is preserved in Kunming Institute of Botany, Chinese Academy of Sciences (CAS).

4.3. Extraction and isolation

The dried fruits of *K. arborea* (3.5 kg) were extracted 3 times with 95% EtOH and then distill under reduced pressure to obtain the extract. Crude alkaloid (180 g) was obtained subsequently from the extract according to the methods described previously (Yuan et al., 2017). Then the crude alkaloid was separated on silica gel column chromatography eluted with dichloromethane/methanol (100:1 \rightarrow 1:1) gradient elution to obtain four major fractions (Fr. A-Fr. D). Fr. B (47 g) was separated on a RP C18 column and eluted with MeOH/H₂O (30:70 \rightarrow 100:0, v/v) to obtain three subfractions (Fr. B1–Fr. B3). Fr. B1 (11 g) was further separated on a silica gel column chromatography eluted with petroleum ether/acetone (9:1), followed by semi-preparative HPLC with MeOH/H₂O (65:35, 0.1% Et₂NH, 3.0 ml/min) to give compound **1** (8.7 mg, $t_{\text{R}} = 28.2$ min). Fr. B2 (15 g) was subjected to Sephadex LH-20 eluted with MeOH and followed by semi-preparative HPLC with CH₃CN/H₂O (70:30, 0.1% Et₂NH, 3.0 ml/min) to give compound **2** (5.7 mg, $t_{\text{R}} = 36.0$ min). Fr. C (40 g) was further divided into four subfractions (C_I–IV) by silica gel column chromatography (petroleum ether/acetone, 9:1:0.1). Fr. C_{II} (5.2 g) was subsequently separated by semi-preparative HPLC with MeOH/H₂O (55:45, 0.1% Et₂NH, 3.0 ml/min) to give compound **3** (14.8 mg, $t_{\text{R}} = 43.0$ min). Detailed isolation procedures for the known compounds are described in Supplementary Material.

4.4. Compound characterization

Kopoffine A (1). Colorless crystals; $[\alpha]_{28} \text{D} -61$ (c 0.1, MeOH); ECD (0.00040 M, MeOH) λ_{max} ($\Delta\epsilon$) 212 (-20.4) nm; IR (KBr) ν_{max} 3434, 2925, 1731, 1660, 1475, 1199, 755 cm⁻¹; ^1H and ^{13}C NMR data, see Tables 1 and 2, respectively; HRESIMS m/z 645.3807 [M + H]⁺ (calcd for C₄₁H₄₈N₄O₃ + H, 645.3799).

Kopoffine B (2). White powder; $[\alpha]_{28} \text{D} -26$ (c 0.1, MeOH); ECD (0.00049 M, MeOH) λ_{max} ($\Delta\epsilon$) 227 (-7.6), 264 ($+1.8$), 309 (-3.7) nm; IR (KBr) ν_{max} 3429, 2926, 1739, 1665, 1459, 1236 cm⁻¹; ^1H and ^{13}C NMR data, see Tables 1 and 2, respectively; HRESIMS m/z 613.3539 [M + H]⁺ (calcd for C₄₀H₄₄N₄O₂ + H, 613.3537).

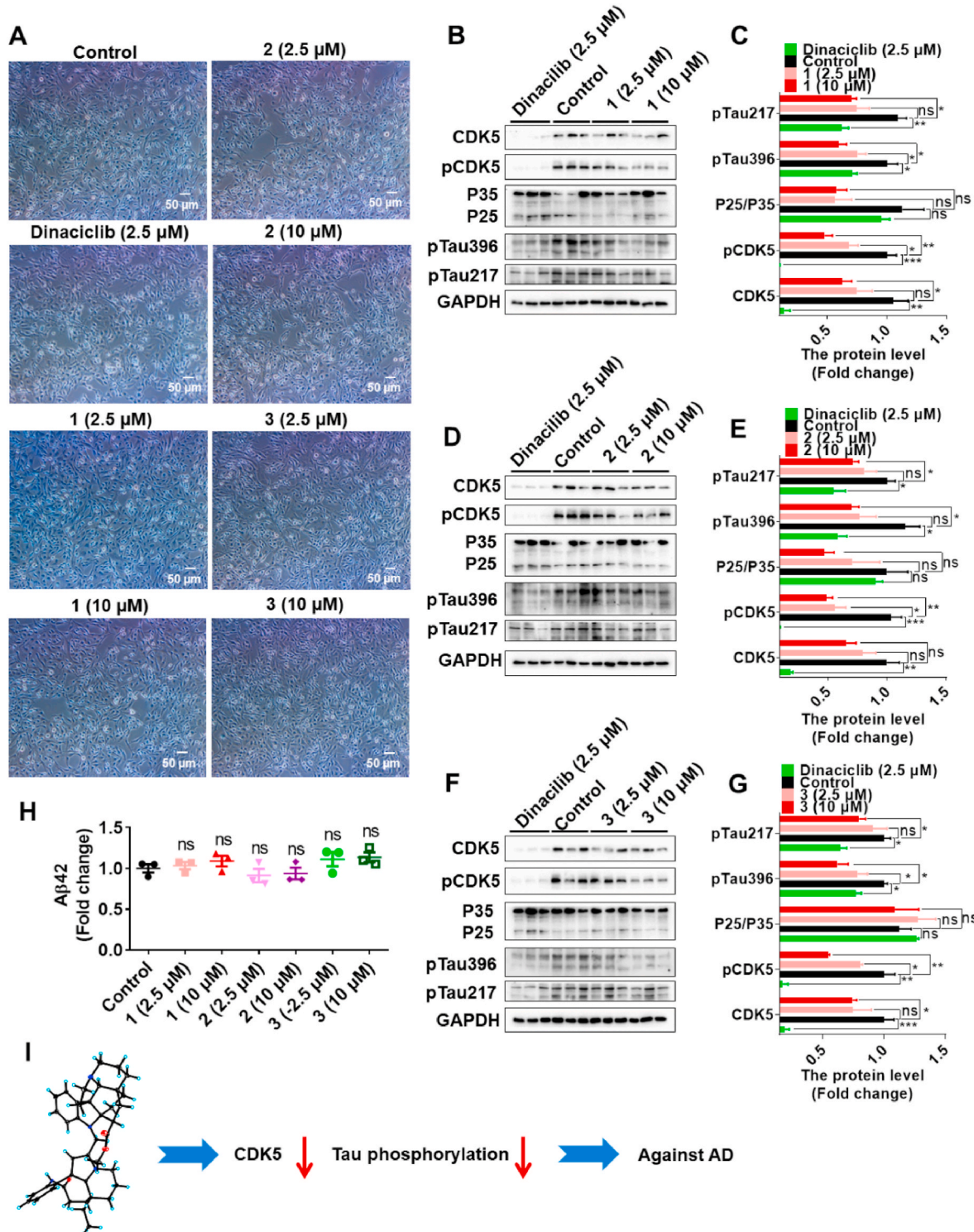


Fig. 7. Results of biological activity assays. (A) The morphology of the U251-APP cells treated with or without compounds (2.5 μM or 10 μM) or Dinacilib (2.5 μM, as a positive control) for 24 h. (B–G) Western blotting assays showing the protein levels of CDK5, pCDK5, p25/p35, pTau396, and pTau217 in the U251-APP cells treated with or without compounds. Shown data are a representative Western blotting result (B, D, F) and quantification of protein levels (C, E, G) based on 3 independent experiments. (H) Level of extracellular A_β42/A_β1-42 in the supernatant of U251-APP cells treated with compounds or DMSO (Control) as determined by ELISA. (I) A proposed role of compounds against AD by downregulating CDK5 activities and decreasing Tau phosphorylation. Data are presented as the means ± SEM. ns, not significant; ***, P < 0.001; **, P < 0.01; *, P < 0.05; one-way ANOVA with the Bonferroni's post-hoc test.

Kopoffine C (3). White powder; [α]25 D +6 (c 0.1, MeOH); ECD (0.00026 M, MeOH) λ_{max} ($\Delta\epsilon$) 220 (-3.5), 239 (+19.8) nm; IR (KBr) ν_{max} 3428, 2926, 1731, 1639, 1467, 1206 cm⁻¹; ¹H and ¹³C NMR data, see Tables 1 and 2, respectively; HRESIMS m/z 633.4153 [M + H]⁺ (calcd for $C_{41}H_{52}N_4O_2 + H$, 633.4163).

Crystal data for **kopoffine A (1)**: $C_{41}H_{48}N_4O_3 \bullet H_2O$, $M = 662.85$, $a = 8.3245$ (2) Å, $b = 16.4573$ (5) Å, $c = 25.0171$ (8) Å, orthorhombic, $V = 3427.31$ (17) Å³, $T = 100$ (2) K, space group $P212121$, $Z = 4$, $\mu(\text{Cu K}\alpha) = 0.657$ mm⁻¹, 31,679 reflections measured, 6722 independent reflections ($R_{int} = 0.0859$). The final R_1 values were 0.0406 ($I > 2\sigma(I)$). The

Table 3
CDK5 kinase inhibitory activity of alkaloids 1–3.

Compounds	1	2	3	Dinaciclib ^b
IC ₅₀ (nM) ^a	2183	666.4	341.4	3.511

^a IC₅₀: 50% inhibitory concentration.

^b Positive control.

final *wR* (F^2) values were 0.1014 ($I > 2\sigma(I)$). The final R_1 values were 0.0492 (all data). The final *wR* (F^2) values were 0.1050 (all data). The goodness of fit on F^2 was 1.058. Flack parameter = 0.01 (12). CCDC 2177407 (www.ccdc.cam.ac.uk).

4.5. Kinase preparations and assays

CDK protein enzyme (CDK5/p25, C33-10G-05), CDK kinase assay substrates (Histone H1 Protein, H10-54 N, Rb Protein, R05-55G), Kinase Dilution Buffer III (K23-09-0), Kinase Assay Buffer I (K01-09-05), and ATP Stock Solution (A50-09-200) were purchased from SignalChem. ADP-Glo kinase assay reagent (V6930) was purchased from Promega. Proxiplate-384 plates (6,008,280) were purchased from PerkinElmer. Stock compounds (5 mM) were diluted 1/2 log to the desired concentrations with DMSO. Three microliters of diluted compound dose and blank (DMSO) were added to 997 μ l of 1x assay buffer to obtain a 3x (15 μ M) reaction compound solution A. Then, 100 ng/ μ l of enzyme stock was diluted with kinase dilution buffer to obtain a 3x reaction enzyme solution B. Then, 10 mM of ATP stock and protein substrate stock were diluted to obtain a 6x solution; we mixed equal volumes of ATP and substrate to obtain a 3x solution C. After 2 μ l of solutions A and B were mixed and incubated at room temperature (RT) for 15 min, 2 μ l of solution C was added and incubated at RT for another 45 min. After the 1-h incubation, we terminated the reaction by spotting 6 μ l of ADP-Glo reagent and depleted the remaining ATP via further incubation at RT for 40 min. Then, we added 12 μ l of kinase detection reagent, incubated it at RT for 30 min, and detected the luminescence signal using an EnVision® 2015 Multimode Plate Reader (61,004,648). Dinaciclib (GLPBIO, 779,353-01-4) was used as the positive control.

4.6. Cell culture and treatment

The U251-APP cells were created in Kunming Institute of Zoology, Chinese Academy of Science, and were cultured in Roswell RPMI-1640

medium (HyClone, C11875500BT) supplemented with 10% fetal bovine serum (Gibco-BRL, 10,099–141) at 37 °C in a humidified atmosphere incubator with 5% CO₂ and 95% humidity, as described in our previous studies (Luo et al., 2020, 2021; Xiang et al., 2017; Zhang et al., 2016). Cells were seeded in pre-warmed growth medium in 6-well plates. Chemicals including Dinaciclib (GLPBIO, 779,353-01-4), were applied directly to the culture medium for treatment, and cells were harvested at 24 h after treatment.

4.7. Western blot analysis

Western blotting for target proteins was performed using the common approach described in our previous studies (Luo et al., 2020, 2021; Su et al., 2017; Zhang et al., 2016). In brief, cell lysates of U251-APP cells were prepared using protein lysis buffer (Beyotime Institute of Biotechnology, P0013). The protein concentration was determined by a BCA protein assay kit (Beyotime Institute of Biotechnology, P0012). In total, 20 μ g of protein was separated by 12% sodium dodecyl sulfate-polyacrylamide gel electrophoresis and transferred to a polyvinylidene difluoride membrane (Bio-Rad, L1620177 Rev D). The membrane was soaked with 5% (w:v) skim milk at RT for 2 h. The membrane was incubated with primary antibodies overnight at 4 °C. The antibodies were GAPDH, glyceraldehyde-3-phosphate dehydrogenase [Proteintech, 60004-1-Ig], CDK5 [Santa Cruz Biotechnology, sc-6247], phospho-CDK5 (Tyr15) (pCDK5) [Absin, abs130996], phospho-Tau (Ser396) (pTau396, PHF13) [Cell Signaling Technology, 9632 S], phospho-Tau (Thr217) [Abcam, ab192665], and p35/25 (C64B10) [Cell Signaling Technology, 2680 S]. The membranes were washed 3 times with TBST (Tris-buffered saline [Cell Signaling Technology, 9997] with Tween 20 [0.1%; Sigma, P1379]), each time 5 min, and subsequently incubated with peroxidase-conjugated anti-mouse (474–1806) or anti-rabbit (474–1516) IgG (1:5000; KPL) at RT for 1 h. The epitope was visualized using an ECL Western blot detection kit (Millipore, WBKLS0500). ImageJ software (National Institutes of Health, Bethesda, Maryland, USA) was used to evaluate the densitometry. GAPDH was used as a loading control to measure the densitometry of target protein.

4.8. Enzyme linked immunosorbent assay (ELISA) for A β 42

The level of A β 42/A β 1–42 in the supernatant of U251-APP cells was measured using a commercial ELISA kit (Elabscience, E-EL-H0543c), as

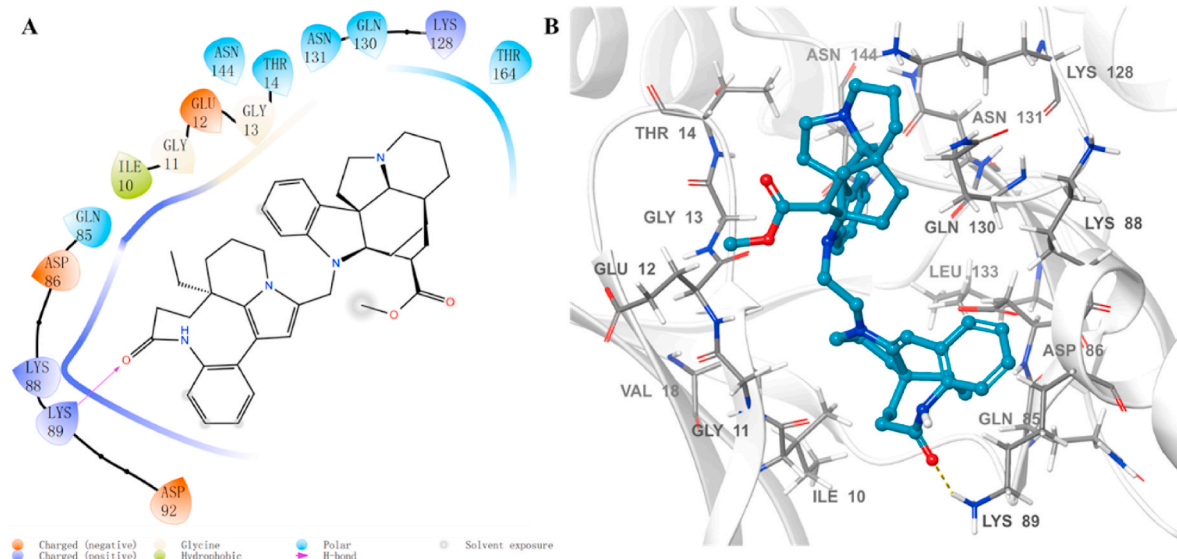


Fig. 8. The molecular docking results of alkaloid 1 with CDK5. (A) Two-dimensional ligand interaction diagram of alkaloid 1 with the residues in the active site of CDK5. (B) Site view of the interactions observed between the residues in the active cavity of CDK5 and alkaloid 1.

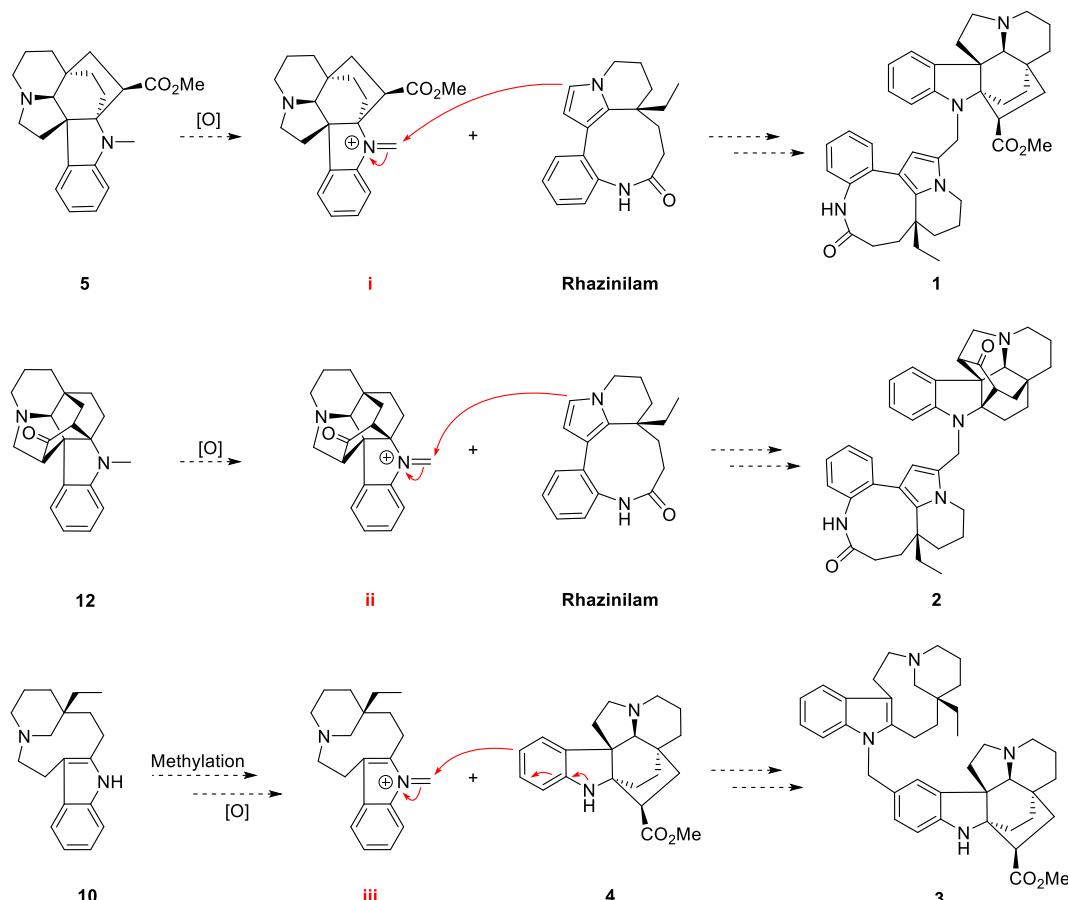


Fig. 9. Proposed biogenetic pathway for alkaloids 1–3.

described in our recent study (Luo et al., 2020, 2021; Tang et al., 2021; Zhang et al., 2016).

4.9. Molecular docking

The docking process was performed by Schrodinger 2020-3 software. The crystal structure of CDK5 (PDB ID: 1UNL resolution: 2.20 Å) was downloaded from the RCSB protein data bank (Berman et al., 2000) (<http://www.pdb.org>). The crystal structure of CDK5 was prepared by Protein Prepare module of Schrodinger software. The preparation process includes adding hydrogen atoms, adding missing side chains, removing water molecules, assigning protonated state and performing energy minimization. Ligands was prepared by generating 3D coordinates, assigning protonated state and performing energy minimization using LigPrep module of Schrodinger software. The location and size of grid box were automatically set based on the location and size of original crystal ligand. The XP docking mode was used to generate docking poses.

Declaration of competing interest

The authors declare that they have no known competing financial interests or personal relationships that could have appeared to influence the work reported in this paper.

Data availability

No data was used for the research described in the article.

Acknowledgments

We thank the National Natural Science Foundation of China (81874295 to Y. Z, 32170988 and 31900737 to R. C. L.), Yunan Revitalization Talents Support Plan-Young Talent Project (to Y. Z.), DR PLANT, Basic Research Program of Yunnan Province (202201AW070010 and 202001AT070107 to R. C. L.), the Youth Innovation Promotion Association of CAS (2021000011 to R. C. L.), the Original Innovation Project “from 0 to 1” of the Basic Frontier Scientific Research Program, CAS (ZDBS-LY-SM031 to R. C. L.), the CAS “Light of West China” Program (2020000023 to R. C. L.), and the Young scientific and technological talents promotion project of Yunnan Association for Science and Technology (2022000043 to R. C. L) for financial support.

Appendix A. Supplementary data

Supplementary data to this article can be found online at <https://doi.org/10.1016/j.phytochem.2022.113392>.

References

- Abouzeid, S., Beutling, U., Surup, F., Bar, F.M.A., Amer, M.M., Badria, F.A., Yahyazadeh, M., Bronstrup, M., Selmar, D., 2017. Treatment of *Vinca minor* leaves with methyl jasmonate extensively alters the pattern and composition of indole alkaloids. *J. Nat. Prod.* 80, 2905–2909. <https://doi.org/10.1021/acs.jnatprod.7b00424>.
- Allnutt, A.B., Waters, A.K., Kesari, S., Yenugonda, V.M., 2020. Physiological and pathological roles of Cdk5: potential directions for therapeutic targeting in neurodegenerative disease. *ACS Chem. Neurosci.* 11, 1218–1230. <https://doi.org/10.1021/acscchemneuro.0c00096>.
- Berman, H.M., Westbrook, J., Feng, Z., Gilliland, G., Bhat, T.N., Weissig, H., Shindyalov, I.N., Bourne, P.E., 2000. The protein data bank. *Nucleic Acids Res.* 28, 235–242. <https://doi.org/10.1093/nar/28.1.235>.

- Cheung, Z.H., Ip, N.Y., 2012. Cdk5: a multifaceted kinase in neurodegenerative diseases. *Trends Cell Biol.* 22, 169–175. <https://doi.org/10.1016/j.tcb.2011.11.003>.
- Cruz, J.C., Tseng, H.C., Goldman, J.A., Shih, H., Tsai, L.H., 2003. Aberrant Cdk5 activation by p25 triggers pathological events leading to neurodegeneration and neurofibrillary tangles. *Neuron* 40, 471–483. [https://doi.org/10.1016/S0896-6273\(03\)00627-5](https://doi.org/10.1016/S0896-6273(03)00627-5).
- Chow, H.M., Guo, D., Zhou, J.C., Zhang, G.Y., Li, H.F., Herrup, K., Zhang, J., 2014. CDK5 activator protein p25 preferentially binds and activates GSK3 β . *Proc. Natl. Acad. Sci. U. S. A.* 111, E4887–E4895. <https://doi.org/10.1073/pnas.1402627111>.
- Ciceri, S., Herrup, K., 2005. Cyclin-dependent kinase 5 is essential for neuronal cell cycle arrest and differentiation. *J. Neurosci.* 25, 9658–9668. <https://doi.org/10.1523/JNEUROSCI.1773-05.2005>.
- Cruz, J.C., Tsai, L.H., 2004. Cdk5 deregulation in the pathogenesis of Alzheimer's disease. *Trends Mol. Med.* 10, 452–458. <https://doi.org/10.1016/j.molmed.2004.07.001>.
- De Luca, V., Salim, V., Atsumi, S.M., Yu, F., 2012. Mining the biodiversity of plants: a revolution in the making. *Science* 336, 1658–1661. <https://doi.org/10.1126/science.1217410>.
- Gauthier, S., Rosa-Neto, P., Morais, J.A., Webster, C., 2021. *World Alzheimer Report 2021: Journey Through the Diagnosis of Dementia*. Alzheimer's Disease International, London, England.
- Dunys, J., Valverde, A., Checler, F., 2018. Are N- and C-terminally truncated A β species key pathological triggers in Alzheimer's disease? *J. Biol. Chem.* 293, 15419–15428. <https://doi.org/10.1074/jbc.R118.003999>.
- Gan, C.Y., Low, Y.Y., Thomas, N.F., Kam, T.S., 2013. Rhazinilam-leuconolam-leuconoxine alkaloids from *Leuconotis griffithii*. *J. Nat. Prod.* 76, 957–964. <https://doi.org/10.1021/np400214y>.
- Goh, S.H., Razak Mohd Ali, A., Wong, W.H., 1989. Alkaloids of *Leuconotis griffithii* and *L. eugenifolia* (apocynaceae). *Tetrahedron* 45, 7899–7920. [https://doi.org/10.1016/S0040-4020\(01\)85802-6](https://doi.org/10.1016/S0040-4020(01)85802-6).
- Huang, Y., Huang, W., Huang, Y., Song, P., Zhang, M., Zhang, H.T., Pan, S., Hu, Y., 2020. Cdk5 inhibitory peptide prevents loss of neurons and alleviates behavioral changes in p25 transgenic mice. *J. Alzheimers Dis.* 74, 1231–1242. <https://doi.org/10.3233/JAD-191098>.
- Huo, Z.Q., Zhao, Q., Zhu, W.T., Hao, X.J., Zhang, Y., 2021. Bousmekines A-E, new alkaloids from two *bousigonie* species: *B. angustifolia* and *B. mekongensis*. *Nat. Prod. Bioprospect.* 11, 207–213. <https://doi.org/10.1007/s13659-020-00278-6>.
- Jan, A., Janusson, B., Delaiellini, A., Somasekharan, S.P., Bhanshali, F., Vandal, M., Negri, G.L., Moerman, D., MacKenzie, I., Calon, F., Hayden, M.R., Taubert, S., Sorensen, P.H., 2017. eEF2K inhibition blocks A β 42 neurotoxicity by promoting an NRF2 antioxidant response. *Acta Neuropathol.* 133, 101–119. <https://doi.org/10.1007/s00401-016-1634-1>.
- Jin, Q., Zhao, Y.L., Liu, Y.P., Zhang, R.S., Zhu, P.F., Zhao, L.Q., Qin, X.J., Luo, X.D., 2022. Anti-inflammatory and analgesic monoterpenoid indole alkaloids of *Kopsia officinalis*. *J. Ethnopharmacol.* 285, 114848. <https://doi.org/10.1016/j.jep.2021.114848>.
- Jones, S.B., Simmons, B., Mastracchio, A., MacMillan, D.W.C., 2011. Collective synthesis of natural products by means of organocascade catalysis. *Nature* 475, 183–188. <https://doi.org/10.1038/nature10232>.
- Kitajima, M., Ohara, S., Kogure, N., Wu, Y.Q., Zhang, R.P., Takayama, H., 2012. New indole alkaloids from *Melodinus henryi*. *Heterocycles* 85, 1949–1959. <https://doi.org/10.3987/COM-12-12511>.
- Kuehne, M.E., Seaton, P.J., 1985. Studies in biomimetic alkaloid syntheses. 13. Total syntheses of racemic aspidofractine, pleiocarpine, pleiocarpinine, kopsinine, N-methylkopsanone, and kopsanone. *J. Org. Chem.* 50, 4790–4796. <https://doi.org/10.1021/jo00224a027>.
- Kumar, S.K., LaPlant, B., Chng, W.J., Zonder, J., Callander, N., Fonserca, R., Fruth, B., Roy, V., Erlichman, C., Stewart, A.K., 2015. Dinaciclib, a novel CDK inhibitor, demonstrates encouraging single-agent activity in patients with relapsed multiple myeloma. *Blood* 125, 443–448. <https://doi.org/10.1182/blood-2014-05-573741>.
- Lacosta, A.M., Insua, D., Badi, H., Pesini, P., Sarasa, M., 2017. Neurofibrillary tangles of A β -40 in Alzheimer's disease brains. *J. Alzheimers Dis.* 58, 661–667. <https://doi.org/10.3233/JAD-170163>.
- Li, P.T., Leeuwenberg, A.J.M., Middleton, D.J., 1995. *Flora of China*, vol. 16. Science Press, Beijing, pp. 162–163.
- Li, Y., Xu, M., Ding, X., Yan, C., Song, Z.Q., Chen, L.W., Huang, X.H., Wang, X., Jian, Y.L., Tang, G.H., Tang, C.Y., Di, Y.T., Mu, S.Z., Liu, X.Z., Liu, K., Li, T., Wang, Y.C., Miao, L., Guo, W.X., Hao, X.J., Yang, C.L., 2016. Protein kinase C controls lysosome biogenesis independently of mTORC1. *Nat. Cell Biol.* 18, 1065–1077. <https://doi.org/10.1038/ncb3407>.
- Lopes, J.P., Agostinho, P., 2011. Cdk5: multitasking between physiological and pathological conditions. *Prog. Neurobiol.* 94, 49–63. <https://doi.org/10.1016/j.pneurobio.2011.03.006>.
- Luo, R., Fan, Y., Yang, J., Ye, M., Zhang, D.F., Guo, K., Li, X., Bi, R., Xu, M., Yang, L.X., Li, Y., Ran, X., Jiang, H.Y., Zhang, C., Tan, L., Sheng, N., Yao, Y.G., 2021. A novel missense variant in ACAA1 contributes to early-onset Alzheimer's disease, impairs lysosomal function, and facilitates amyloid- β pathology and cognitive decline. *Signal Transduct. Targeted Ther.* 6, 325. <https://doi.org/10.1038/s41392-021-00748-4>.
- Luo, R., Su, L.Y., Li, G., Yang, J., Liu, Q., Yang, L.X., Zhang, D.F., Zhou, H., Xu, M., Fang, Y., Li, J., Yao, Y.G., 2020. Activation of PPAR α -mediated autophagy reduces Alzheimer disease-like pathology and cognitive decline in a murine model. *Autophagy* 16, 52–69. <https://doi.org/10.1080/15548627.2019.1596488>.
- Malhotra, N., Gupta, R., Kumar, P., 2021. Pharmacological relevance of CDK inhibitors in Alzheimer's disease. *Neurochem. Int.* 148, 105115. <https://doi.org/10.1016/j.neuint.2021.105115>.
- Mattsson-Carlgren, N., Janelidze, S., Palmqvist, S., Cullen, N., Svenssonsson, A.L., Strandbergh, O., Mengel, D., Walsh, D.M., Stomrud, E., Dage, J.L., Hansson, O., 2020. Longitudinal plasma p-tau217 is increased in early stages of Alzheimer's disease. *Brain* 143, 3234–3241. <https://doi.org/10.1093/brain/awaa286>.
- Mucke, L., Selkoe, D.J., 2012. Neurotoxicity of amyloid β -protein: synaptic and network dysfunction. *Cold Spring Harb. Perspect. Med.* 2 (7), a006338. <https://doi.org/10.1101/cshperspect.a006338>.
- Noble, W., Olm, V., Takata, K., Casey, E., O, M., Meyerson, J., Gaynor, K., LaFrancois, J., Wang, L.L., Kondo, T., Davies, P., Burns, M., Nixon, V.R., Dickson, D., Matsuoaka, Y., Ahljanian, M., Lau, L.F., Duff, K., 2003. Cdk5 is a key factor in tau aggregation and tangle formation in vivo. *Neuron* 38, 555–565. [https://doi.org/10.1016/S0896-6273\(03\)00259-9](https://doi.org/10.1016/S0896-6273(03)00259-9).
- Palmqvist, S., Janelidze, S., Quiroz, Y.T., Zetterberg, H., Lopera, F., Stomrud, E., Su, Y., Chen, Y.H., Serrano, G.E., Leuzy, A., Mattsson-Carlgren, N., Strandbergh, O., Smith, R., Villegas, A., Sepulveda-Falla, D., Chai, X.Y., Proctor, N.K., Beach, T.G., Blennow, K., Dage, J.L., Reiman, E.M., Hansson, O., 2020. Discriminative accuracy of plasma phospho-tau217 for Alzheimer disease vs other neurodegenerative disorders. *JAMA*, J. Am. Med. Assoc. 324, 772–781. <https://doi.org/10.1001/jama.2020.12134>.
- Patrick, G.N., Zukerberg, L., Nikolic, M., Monte, S., Dilkes, P., Tsai, L.H., 1999. Conversion of p35 to p25 deregulates Cdk5 activity and promotes neurodegeneration. *Nature* 402, 615–622. <https://doi.org/10.1038/45159>.
- Scheltens, P., De Strooper, B., Kivipelto, M., Holstege, H., Chételat, G., Teunissen, C.E., Cummings, J., van der Flier, W.M., 2021. Alzheimer's disease. *Lancet* 397, 1577–1590. [https://doi.org/10.1016/S0140-6736\(20\)32205-4](https://doi.org/10.1016/S0140-6736(20)32205-4).
- Selkoe, D.J., 2021. Treatments for Alzheimer's disease emerge. *Science* 373, 624–626. <https://doi.org/10.1126/science.abi6401>.
- Seo, J., Kritskiy, O., Watson, L.A., Barker, S.J., Dey, D., Raja, W.K., Lin, Y.T., Ko, T., Cho, S., Penney, J., Silva, X.C., Sheridan, S.D., Lucente, D., Gusella, J.F., Dickerson, B.C., Haggarty, S.J., Tsai, L.H., 2017. Inhibition of p25/cdk5 attenuates tauopathy in mouse and iPSC models of frontotemporal dementia. *J. Neurosci.* 37, 9917–9924. <https://doi.org/10.1523/JNEUROSCI.0621-17.2017>.
- Stathas, S., Alvarez, V.E., Xia, W., Nicks, R., Meng, G., Daley, S., Pothast, M., Shah, A., Kelley, H., Esnault, C., McCormack, R., Dixon, E., Fishbein, L., Cherry, J.D., Huber, B.R., Tripodis, Y., Alosco, M.L., Mez, J., McKee, A.C., Stein, T.D., 2021. Tau phosphorylation sites serine 202 and serine 396 are differently altered in chronic traumatic encephalopathy and Alzheimer's disease. *Alzheimers Dement* 18, 1511–1522. <https://doi.org/10.1002/alz.12502>.
- Su, L.Y., Luo, R.C., Liu, Q.J., Su, J.R., Yang, L.X., Ding, Y.Q., Xu, L., Yao, Y.G., 2017. Atg 5- and Atg7-dependent autophagy in dopaminergic neurons regulates cellular and behavioral responses to morphine. *Autophagy* 13, 1496–1511. <https://doi.org/10.1080/15548627.2017.1332549>.
- Subramaniam, G., Hiraku, O., Hayashi, M., Koyano, T., Komiyama, K., Kam, T.S., 2017. Biologically active aspidofractinine, rhazinilam, akuumiline, and vincorine alkaloids from *Kopsia*. *J. Nat. Prod.* 70, 1783–1789. <https://doi.org/10.1021/np0703747>.
- Sundaram, J.R., Poore, C.P., Sulaimee, N.H., Pareek, T., Asad, A.B., Rajkumar, R., Cheong, W.F., Wenk, M.R., Dawe, G.S., Chuang, K.H., Pant, H.C., Kesavapany, S., 2013. Specific inhibition of p25/cdk5 activity by the Cdk5 inhibitory peptide reduces neurodegeneration in vivo. *J. Neurosci.* 33, 334–343. <https://doi.org/10.1523/JNEUROSCI.3593-12.2013>.
- Tang, X.H., Luo, R.C., Ye, M.S., Tang, H.Y., Ma, Y.L., Chen, Y.N., Wang, X.M., Lu, Q.Y., Liu, S., Li, X.N., Yan, Y., Yang, J., Ran, X.Q., Fang, X., Zhou, Y., Yan, Y.G., Di, Y.T., Hao, X.J., 2021. Harpertrioate A, an A,B,D-seco-Limonoid with promising biological activity against Alzheimer's disease from twigs of *Harrisonia perforata* (blanco). *Merr. Org. Lett.* 23, 262–267. <https://doi.org/10.1021/acs.orglett.0c03460>.
- Wang, J., Gu, B.J., Masters, C.L., Wang, Y.J., 2017. A systemic view of Alzheimer disease—insights from amyloid- β metabolism beyond the brain. *Nat. Rev. Neurol.* 13, 612–623. <https://doi.org/10.1038/nrneurol.2017.111>.
- Wenkert, E., Cochran, D.W., Gottlieb, H.E., Hagaman, E.W., Brazfilho, R., Matos, F.J.A., Madruga, M.I.L.M., 1976. ^{13}C -NMR Spectroscopy of Naturally Occurring Substances. XLII. Conformational analysis of quebrachamine-like indole alkaloids and related substances. *Helv. Chim. Acta* 59, 2711–2723. <https://doi.org/10.1002/hcl.19760590810>.
- Wong, S.K., Wong, S.P., Sim, K.S., Lim, S.H., Low, Y.Y., Kam, T.S., 2019. A cytotoxic indole characterized by incorporation of a unique carbon–nitrogen skeleton and two pentacyclic corynanthean alkaloids incorporating a substituted tetrahydrofurane ring from *Kopsia arborea*. *J. Nat. Prod.* 82, 1902–1907. <https://doi.org/10.1021/acs.jnatprod.9b00255>.
- Wong, S.K., Yeap, J.S.Y., Tan, C.H., Sim, K.S., Lim, S.H., Low, Y.Y., Kam, T.S., 2021. Arbolidinines A–C, biologically-active aspidofractinine-aspidofractinine, aspidofractinine-strychnan, and kopsine-strychnan bisindole alkaloids from *Kopsia arborea*. *Tetrahedron* 78, 131802. <https://doi.org/10.1016/j.tet.2020.131802>.
- Wu, Y.Q., Kitajima, M., Kogure, N., Wang, Y.S., Zhang, R.P., Takayama, H., 2010. Two new aspidosperma indole alkaloids from Yunnan *Kopsia arborea*. *Chem. Pharm. Bull.* 58, 961–963. <https://doi.org/10.1248/cpb.58.961>.
- Xiang, Q., Bi, R., Xu, M., Zhang, D.F., Tan, L.W., Zhang, C., Fang, Y.R., Yao, Y.G., 2017. Rare genetic variants of the transthyretin gene are associated with Alzheimer's disease in han Chinese. *Mol. Neurobiol.* 54, 5192–5200. <https://doi.org/10.1007/s12035-016-0065-2>.
- Yi, W.F., Ding, X., Chen, Y.Z., Adelakun, T.A., Zhang, Y., Hao, X.J., 2020. Tabernaesines A–I, cytotoxic aspidosperma–aspidosperma-type bisindole alkaloids from *Tabernaemontana pachysiphon*. *J. Nat. Prod.* 83, 3215–3222. <https://doi.org/10.1021/acs.jnatprod.9b00768>.
- Yuan, Y.X., Zhang, Y., Guo, L.L., Wang, Y.H., Goto, M., Morris-Natschke, S.L., Lee, K.H., Hao, X.J., 2017. Tabercorymines A and B, two vobasinylin–ibogan-type bisindole

- alkaloids from *Tabernaemontana corymbosa*. Org. Lett. 19, 4964–4967. <https://doi.org/10.1021/acs.orglett.7b02445>.
- Zhang, D.F., Li, J., Wu, H., Cui, Y., Bi, R., Zhou, H.J., Wang, H.Z., Zhang, C., Wang, D., Kong, Q.P., Li, T., Fang, Y.R., Jiang, T.Z., Yao, Y.G., 2016. CFH variants affect structural and functional brain changes and genetic risk of Alzheimer's disease. Neuropsychopharmacology 41, 1034–1045. <https://doi.org/10.1038/npp.2015.232>.
- Zhang, J., Cicero, S.A., Wang, L., Romito-Digiacomo, R.R., Yang, Y., Herrup, K., 2008. Nuclear localization of Cdk5 is a key determinant in the postmitotic state of neurons. Proc. Natl. Acad. Sci. U. S. A. 105, 8772–8777. <https://doi.org/10.1073/pnas.0711355105>.
- Zhang, Y., Ding, X., Yuan, Y.X., Guo, L.L., Hao, X.J., 2020. Cytotoxic monoterpenoid indole alkaloids from *Tabernaemontana corymbosa* as potent autophagy inhibitors by the attenuation of lysosomal acidification. J. Nat. Prod. 83, 1432–1439. <https://doi.org/10.1021/acs.jnatprod.9b00856>.
- Zhang, Y., Yuan, Y.X., Goto, M., Guo, L.L., Li, X.N., Morris-Natschke, S.L., Lee, K.H., Hao, X.J., 2018. Taburnaemines A–I, cytotoxic vobasinyl-iboga-type bisindole alkaloids from *Tabernaemontana corymbosa*. J. Nat. Prod. 81, 562–571. <https://doi.org/10.1021/acs.jnatprod.7b00949>.
- Zheng, Y.L., Kesavapany, S., Gravell, M., Hamilton, R.S., Schubert, M., Amin, N., Albers, W., Grant, P., Pant, H.C., 2005. A Cdk5 inhibitory peptide reduces tau hyperphosphorylation and apoptosis in neurons. EMBO (Eur. Mol. Biol. Organ.) J. 24, 209–220. <https://doi.org/10.1038/sj.emboj.7600441>.
- Zhou, J.C., Chow, H.M., Liu, Y., Wu, D., Shi, M., Li, J.Y., Wen, L., Gao, Y.H., Chen, G.M., Zhuang, K., Lin, H., Zhang, G.Y., Xie, W.T., Li, H.F., Leng, L.G., Wang, M.D., Zheng, N.Z., Sun, H., Zhao, Y.J., Zhang, Y.W., Xue, M.Q., Huang, T.Y., Bu, G.J., Xu, H.X., Yuan, Z.Q., Herrup, K., Zhang, J., 2020. Cyclin-Dependent Kinase 5-Dependent BAG3 Degradation Modulates Synaptic Protein Turnover. Biol. Psychiatry. 87, 756–769. <https://doi.org/10.1016/j.biopsych.2019.11.013>.

SUPPLEMENTARY MATERIAL

Monoterpenoid indole alkaloid dimers from *Kopsia arborea* inhibit cyclin-dependent kinase 5 and tau phosphorylation

Chen Chen^a, Jian-Wen Liu^a, Ling-Li Guo^a, Feng Xiong^a, Xiao-Qian Ran^{b,d}, Ya-Rong Guo^{b,e}, Yong-Gang Yao^{b,d}, Xiao-Jiang Hao^{a,c, ***}, Rong-Can Luo^{b,d, **}, Yu Zhang^{a,*}

^aState Key Laboratory of Phytochemistry and Plant Resources in West China, Kunming Institute of Botany, Chinese Academy of Sciences, Kunming 650201, Yunnan, China

^bKey Laboratory of Animal Models and Human Disease Mechanisms of the Chinese Academy of Sciences & Yunnan Province, and KIZ-CUHK Joint Laboratory of Bioresources and Molecular Research in Common Diseases, Kunming Institute of Zoology, Chinese Academy of Sciences, Kunming 650204, Yunnan, China

^cResearch Unit of Chemical Biology of Natural Anti-Virus Products, Chinese Academy of Medical Sciences, Beijing 100730, China

^dKunming College of Life Science, University of Chinese Academy of Sciences, Kunming 650201, Yunnan, China

^eSchool of Life Sciences, Division of Life Sciences and Medicine, University of Science and Technology of China, Hefei 230026, Anhui, China

Contents

Extraction and isolation procedures.

Computational methods for ECD calculation of compound 2.

Computational methods for ECD calculation of compound 3.

Figure S1.1 ^1H NMR (500 MHz, chloroform-*d*) of **1**.

Figure S1.2 ^{13}C NMR and DEPT spectra (125 MHz, chloroform-*d*) of **1**.

Figure S1.3 HSQC (500 MHz, chloroform-*d*) of **1**.

Figure S1.4 ^1H - ^1H COSY (500 MHz, chloroform-*d*) of **1**.

Figure S1.5 HMBC (500 MHz, chloroform-*d*) of **1**.

Figure S1.6 ROESY (500 MHz, chloroform-*d*) of **1**.

Figure S1.7 HRESIMS spectrum of **1**.

Figure S1.8 IR (KBr disk) spectrum of **1**.

Figure S1.9 ECD spectrum of compound **1** in MeOH.

Figure S1.10 X-ray crystal structure of compound **1**.

Figure S2.1 ^1H NMR (500 MHz, methanol-*d*₄) of **2**.

Figure S2.2 ^{13}C NMR and DEPT spectra (125 MHz, methanol-*d*₄) of **2**.

Figure S2.3 HSQC (500 MHz, methanol-*d*₄) of **2**.

Figure S2.4 ^1H - ^1H COSY (500 MHz, methanol-*d*₄) of **2**.

Figure S2.5 HMBC (500 MHz, methanol-*d*₄) of **2**.

Figure S2.6 ROESY (500 MHz, methanol-*d*₄) of **2**.

Figure S2.7 HRESIMS spectrum of **2**.

Figure S2.8 IR (KBr disk) spectrum of **2**.

Figure S2.9 ECD spectrum of compound **2** in MeOH.

Figure S2.10 The molecular docking results of compound **2** with CDK5. (A) Two-dimensional ligand interaction diagram of compound **2** with the residues in the active site of CDK5. (B) Site view of the interactions observed between the residues in the active cavity of CDK5 and compound **2**.

Figure S3.1 ^1H NMR (500 MHz, methanol- d_4) of **3**.

Figure S3.2 ^{13}C NMR and DEPT spectra (125 MHz, methanol- d_4) of **3**.

Figure S3.3 HSQC (500 MHz, methanol- d_4) of **3**.

Figure S3.4 ^1H - ^1H COSY (500 MHz, methanol- d_4) of **3**.

Figure S3.5 HMBC (500 MHz, methanol- d_4) of **3**.

Figure S3.6 ROESY (500 MHz, methanol- d_4) of **3**.

Figure S3.7 HRESIMS spectrum of **3**.

Figure S3.8 IR (KBr disk) spectrum of **3**.

Figure S3.9 ECD spectrum of compound **3** in MeOH.

Figure S3.10 Comparison of the experimental ECD and calculated ECD spectra of **3**.

Figure S3.11 Optical rotation analysis of compound **3**.

Figure S3.12 The chiral HPLC chromatogram of **3**.

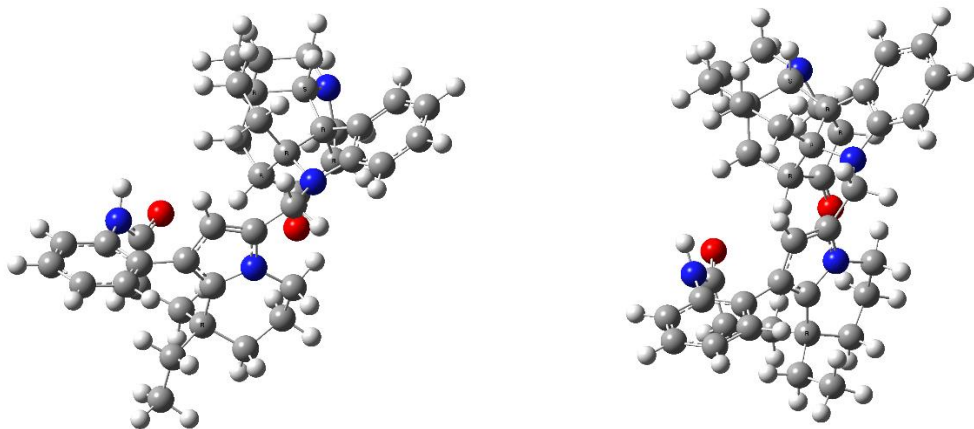
Figure S3.13 The molecular docking results of compound **3** with CDK5. (A) Two-dimensional ligand interaction diagram of compound **3** with the residues in the active site of CDK5. (B) Site view of the interactions observed between the residues in the active cavity of CDK5 and compound **3**.

Extraction and isolation procedures.

The dried fruits of *K. arborea* (3.5 kg) were extracted 3 times with 95% EtOH and then distill under reduced pressure to obtain the extract. Crude alkaloid (180 g) was obtained subsequently from the extract according to the methods described previously. Then the crude alkaloid was separated on silica gel column chromatography eluted with dichloromethane/methanol (100:1→1:1) gradient elution to obtain four major fractions (Fr. A-Fr. D). Fr. C (40 g) was divided into four subfractions (C_I-IV) by silica gel column chromatography (petroleum ether/acetone, 9:1–0:1). Fr. C_{III} (18.4 g) was further subjected to Sephadex LH-20 eluted with MeOH and followed by semi-preparative HPLC with MeOH/H₂O (54:46) (3.0 ml/min) to give compounds **5** (155.5 mg, *t_R*= 46.2 min), **6** (64.8 mg, *t_R*= 37.0 min), and **8** (24.9 mg, *t_R*= 21.1 min). Fr. C_{IV} (7.5 g) was separated on a RP C18 column and eluted with MeOH/H₂O (20:80 → 100:0, v/v) and subsequently by semi-preparative HPLC with CH₃CN/H₂O (41:59, 0.1% Et₂NH) (3.0 ml/min) to give compounds **9** (11.6 mg, *t_R*= 26.4 min), and **11** (4.3 mg, *t_R*= 32.8 min). Fr. D (38 g) was separated on a RP-C18 column and eluted with MeOH/H₂O (20:80 → 100:0, v/v) to obtain four subfractions (Fr. D1- Fr. D4). Fr. D1 (13 g) was separated on silica gel column chromatography (dichloromethane/methanol, 30:1→1:1) followed by semi-preparative HPLC with MeOH/H₂O (38:62, 0.1% Et₂NH) (3.0 ml/min) to give compounds **7** (33.3 mg, *t_R*= 20.2 min), and **10** (22.4 mg, *t_R*= 31.6 min). Fr. D2 (9.2 g) was subjected to Sephadex LH-20 (MeOH) and subsequently by semi-preparative HPLC (CH₃CN: H₂O=59:41) (3.0 ml/min) to give compounds **4** (10.8 mg, *t_R*= 19.6 min), and **12** (40.1 mg, *t_R*= 29.3 min).

Computational methods for ECD calculation of compound 2.

The CONFLEX^{1,2} searches based on molecular mechanics with MMFF94S force fields were performed for (*2R, 6R, 7R, 16R, 20R, 21S, 20'R*)-**2** and (*2R, 6R, 7R, 16R, 20R, 21S, 20'S*)-**2** which gave 2 and 4 stable conformers, respectively. Selected conformers (2 and 4) with distributions higher than 1% were further optimized by the density functional theory method at the B3LYP/6-31G* level in Gaussian 09 program package,³ leading to 2 and 4 stable geometries ($\Delta E < 2$ kcal/mol), respectively, which were in good agreement with the ROESY data. The optimized geometries were further checked by frequency calculation and resulted in no imaginary frequencies. The ECD was calculated using TD-DFT-B3LYP/6-31G+(d,p) of theory on B3LYP/6-31G(d) optimized geometries through the IEFPCM model (in MeOH). The overall calculated ECD curve was generated using SpecDis 1.60⁴ with $\sigma=0.30$ ev, UV shift -25 nm, respectively.



(*2R, 6R, 7R, 16R, 20R, 21S, 20'R*)-**2a** (51.05%)
(48.95%)

(*2R, 6R, 7R, 16R, 20R, 21S, 20'R*)-**2b**

Standard orientation of (*2R, 6R, 7R, 16R, 20R, 21S, 20'R*)-**2a** on B3LYP/6-31G(d) level in gas phase.

Center Number	Atomic Number	Atomic Type	Coordinates (Angstroms)		
			X	Y	Z
1	6	0	2.752999	2.187176	0.613121
2	7	0	3.129186	2.355530	-0.686311
3	6	0	3.768280	1.613863	1.584500
4	6	0	3.293940	0.341738	2.306685
5	6	0	3.500506	-1.021052	1.585936
6	6	0	2.668851	-1.071958	0.301084
7	6	0	2.883738	-0.540885	-0.946945
8	6	0	4.034875	0.226458	-1.504826
9	6	0	4.126901	1.612962	-1.378217
10	7	0	1.431742	-1.676365	0.283024
11	6	0	0.865121	-1.532903	-0.953897
12	6	0	1.732935	-0.842173	-1.731789

13	6	0	3.023286	-2.137545	2.546619
14	6	0	1.507770	-2.242598	2.661469
15	6	0	0.909971	-2.572558	1.308143
16	6	0	4.992766	-1.280200	1.251910
17	6	0	5.961446	-1.322963	2.438515
18	8	0	1.679070	2.570464	0.994216
19	6	0	-5.443470	-3.178060	-1.368170
20	6	0	-4.364571	-3.980023	-1.681190
21	6	0	-3.052858	-3.545018	-1.490867
22	6	0	-2.847711	-2.281131	-0.969292
23	6	0	-3.939493	-1.466891	-0.655920
24	6	0	-5.227562	-1.903194	-0.844126
25	7	0	-1.632071	-1.625947	-0.676720
26	6	0	-1.942949	-0.179791	-0.635406
27	6	0	-3.390201	-0.199058	-0.070051
28	6	0	-1.869742	0.480853	-2.024037
29	6	0	-2.463126	1.910597	-1.998798
30	6	0	-2.982151	2.221294	-0.589027
31	6	0	-4.070781	1.151435	-0.298246
32	6	0	-3.618502	3.615434	-0.495673
33	6	0	-4.396032	3.815389	0.812323
34	6	0	-5.426635	2.697145	1.009490
35	7	0	-4.868713	1.364561	0.891324
36	6	0	-3.243885	-0.266705	1.478836
37	6	0	-4.204946	0.798590	2.054671
38	6	0	-1.748313	2.101217	0.341955
39	6	0	-1.220055	0.631663	0.445400
40	6	0	-1.779756	0.055844	1.723575
41	8	0	-1.204958	-0.107611	2.754978
42	6	0	-0.447291	-2.139221	-1.355480
43	6	0	5.009962	-0.427308	-2.256376
44	6	0	6.046225	0.265921	-2.854837
45	6	0	6.128902	1.642153	-2.713942
46	6	0	5.170339	2.309071	-1.974468
47	1	0	2.395796	2.736992	-1.246855
48	1	0	4.735396	1.483064	1.121352
49	1	0	3.878902	2.391715	2.333201
50	1	0	3.816410	0.292924	3.255875
51	1	0	2.246186	0.473102	2.544935
52	1	0	1.582263	-0.565816	-2.756805
53	1	0	3.412049	-3.092434	2.197117
54	1	0	3.452129	-1.969244	3.527702
55	1	0	1.242933	-3.031859	3.358667
56	1	0	1.069313	-1.328324	3.037672

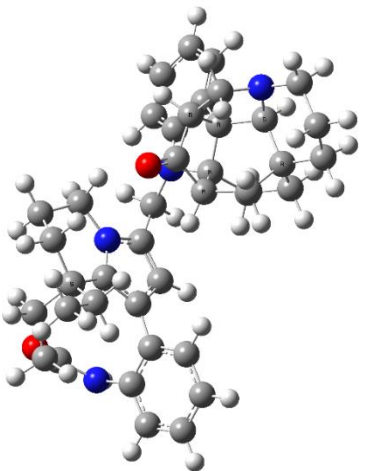
57	1	0	-0.164085	-2.480332	1.327081
58	1	0	1.155593	-3.596669	1.034644
59	1	0	5.049634	-2.227863	0.723427
60	1	0	5.352250	-0.536511	0.556505
61	1	0	6.966861	-1.510909	2.074423
62	1	0	5.988589	-0.384583	2.982309
63	1	0	5.722969	-2.110382	3.144408
64	1	0	-6.445489	-3.533312	-1.527582
65	1	0	-4.531324	-4.961527	-2.088949
66	1	0	-2.238795	-4.191801	-1.757650
67	1	0	-6.057127	-1.267869	-0.587721
68	1	0	-0.836475	0.504883	-2.347383
69	1	0	-2.406515	-0.139693	-2.733857
70	1	0	-1.712723	2.643087	-2.280636
71	1	0	-3.268908	1.998068	-2.721763
72	1	0	-4.738565	1.128293	-1.155687
73	1	0	-2.856096	4.383036	-0.604083
74	1	0	-4.305758	3.741976	-1.331551
75	1	0	-4.904797	4.775883	0.795442
76	1	0	-3.713132	3.846556	1.655969
77	1	0	-6.206139	2.801274	0.257350
78	1	0	-5.913252	2.786730	1.974885
79	1	0	-3.459096	-1.248613	1.876859
80	1	0	-4.937908	0.350909	2.716511
81	1	0	-3.661678	1.535575	2.643476
82	1	0	-0.955385	2.723089	-0.054247
83	1	0	-1.945303	2.489632	1.333298
84	1	0	-0.143856	0.608375	0.424880
85	1	0	-0.413729	-3.203209	-1.153582
86	1	0	-0.532343	-2.033720	-2.434918
87	1	0	4.943530	-1.494149	-2.368851
88	1	0	6.784374	-0.264825	-3.429203
89	1	0	6.931511	2.189909	-3.174027
90	1	0	5.215195	3.375889	-1.851315

Standard orientation of (2*R*, 6*R*, 7*R*, 16*R*, 20*R*, 21*S*, 20'(*R*))-2b on B3LYP/6-31G(d) level in gas phase.

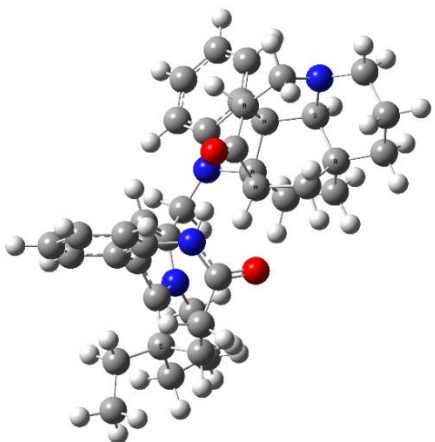
Center Number	Atomic Number	Atomic Type	Coordinates (Angstroms)		
			X	Y	Z
1	6	0	-2.702778	-2.273459	0.686960
2	7	0	-3.102856	-2.426762	-0.607178
3	6	0	-3.716585	-1.754243	1.688938

4	6	0	-3.276034	-0.479215	2.426448
5	6	0	-3.504879	0.896993	1.733515
6	6	0	-2.704180	0.985168	0.433784
7	6	0	-2.935592	0.473863	-0.819402
8	6	0	-4.085231	-0.307699	-1.360785
9	6	0	-4.139464	-1.698841	-1.256512
10	7	0	-1.477586	1.609330	0.404062
11	6	0	-0.933597	1.499418	-0.846245
12	6	0	-1.806466	0.810006	-1.620737
13	6	0	-3.012086	1.984711	2.718166
14	6	0	-1.494038	2.084015	2.806659
15	6	0	-0.935022	2.469805	1.449970
16	6	0	-5.024392	1.097200	1.502151
17	6	0	-5.467055	2.447813	0.929912
18	8	0	-1.608852	-2.628467	1.037235
19	6	0	5.327694	3.274695	-1.418800
20	6	0	4.224060	4.061848	-1.678712
21	6	0	2.927921	3.597995	-1.453153
22	6	0	2.764121	2.320273	-0.950987
23	6	0	3.880870	1.521201	-0.691322
24	6	0	5.153477	1.985821	-0.913915
25	7	0	1.571071	1.636158	-0.631863
26	6	0	1.910390	0.195800	-0.629075
27	6	0	3.375581	0.232033	-0.112652
28	6	0	1.802630	-0.439932	-2.027079
29	6	0	2.421989	-1.858608	-2.049408
30	6	0	2.994402	-2.185550	-0.664254
31	6	0	4.072624	-1.100762	-0.390155
32	6	0	3.658938	-3.568908	-0.619331
33	6	0	4.484692	-3.778322	0.657236
34	6	0	5.500943	-2.644665	0.840298
35	7	0	4.914955	-1.320937	0.767072
36	6	0	3.281531	0.267549	1.441258
37	6	0	4.281406	-0.789700	1.963171
38	6	0	1.790964	-2.106220	0.310007
39	6	0	1.239923	-0.649083	0.459846
40	6	0	1.833002	-0.087394	1.729374
41	8	0	1.291384	0.045596	2.782846
42	6	0	0.357169	2.140115	-1.265159
43	6	0	-5.095293	0.332643	-2.076155
44	6	0	-6.132085	-0.377042	-2.655629
45	6	0	-6.178192	-1.756226	-2.534056
46	6	0	-5.181738	-2.411039	-1.834055
47	1	0	-2.369519	-2.767182	-1.193645

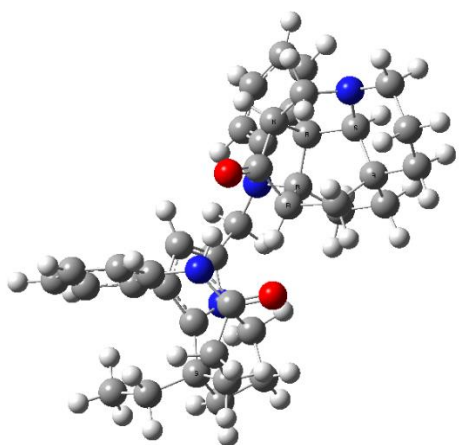
48	1	0	-4.697704	-1.655194	1.249274
49	1	0	-3.780956	-2.546408	2.428023
50	1	0	-3.818349	-0.450341	3.367314
51	1	0	-2.229779	-0.597200	2.676966
52	1	0	-1.672741	0.558662	-2.654513
53	1	0	-3.388816	2.953419	2.408210
54	1	0	-3.439538	1.785662	3.696516
55	1	0	-1.212844	2.847692	3.525546
56	1	0	-1.041556	1.158735	3.135470
57	1	0	0.139609	2.385622	1.436363
58	1	0	-1.194960	3.501607	1.222938
59	1	0	-5.397769	0.320617	0.850429
60	1	0	-5.518409	0.947368	2.460009
61	1	0	-6.507969	2.393071	0.626394
62	1	0	-5.387923	3.250184	1.654298
63	1	0	-4.884071	2.725905	0.059182
64	1	0	6.316936	3.652227	-1.604637
65	1	0	4.358554	5.054294	-2.071626
66	1	0	2.093411	4.234256	-1.678863
67	1	0	6.002931	1.361612	-0.698631
68	1	0	0.759838	-0.477002	-2.316573
69	1	0	2.304307	0.203767	-2.741951
70	1	0	3.203949	-1.917758	-2.800846
71	1	0	1.675584	-2.599547	-2.319572
72	1	0	4.709852	-1.048863	-1.269321
73	1	0	2.907365	-4.348632	-0.716327
74	1	0	4.319138	-3.666977	-1.480459
75	1	0	5.009939	-4.728597	0.604620
76	1	0	3.832047	-3.837879	1.523022
77	1	0	6.255607	-2.720026	0.059922
78	1	0	6.022370	-2.742950	1.786482
79	1	0	3.492029	1.245730	1.850813
80	1	0	5.028359	-0.340546	2.608156
81	1	0	3.772484	-1.547856	2.555782
82	1	0	0.996306	-2.735142	-0.071291
83	1	0	2.028800	-2.509454	1.286394
84	1	0	0.163330	-0.645904	0.476526
85	1	0	0.307780	3.198010	-1.036198
86	1	0	0.415513	2.062595	-2.348722
87	1	0	-5.056000	1.401135	-2.181261
88	1	0	-6.897788	0.144323	-3.201818
89	1	0	-6.980291	-2.316354	-2.979903
90	1	0	-5.196116	-3.480562	-1.728481



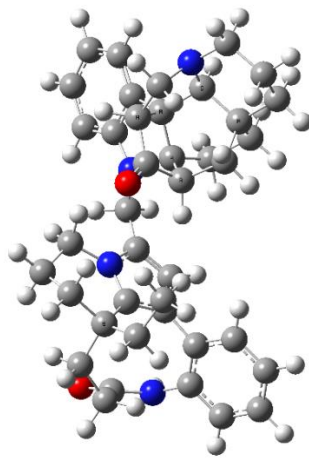
(2*R*, 6*R*, 7*R*, 16*R*, 20*R*, 21*S*, 20'*S*)-**2a** (46.89%)



(2*R*, 6*R*, 7*R*, 16*R*, 20*R*, 21*S*, 20'*S*)-**2b** (35.68%)



(2*R*, 6*R*, 7*R*, 16*R*, 20*R*, 21*S*, 20'*S*)-**2c** (9.92%)



(2*R*, 6*R*, 7*R*, 16*R*, 20*R*, 21*S*, 20'*S*)-**2d** (7.52%)

Standard orientation of (2*R*, 6*R*, 7*R*, 16*R*, 20*R*, 21*S*, 20'*S*)-**2a** on B3LYP/6-31G(d) level in gas phase.

Center Number	Atomic Number	Atomic Type	Coordinates (Angstroms)		
			X	Y	Z
1	6	0	5.357762	-1.317678	-0.928681
2	7	0	5.224464	-0.342714	-1.873790
3	6	0	5.674046	-0.888317	0.492901
4	6	0	4.671303	-1.428971	1.521029
5	6	0	3.352175	-0.638651	1.747441
6	6	0	2.522384	-0.542336	0.462251
7	6	0	2.647137	0.261484	-0.647191
8	6	0	3.638383	1.317385	-1.006285
9	6	0	4.851593	1.007185	-1.622802
10	7	0	1.424580	-1.347367	0.261328
11	6	0	0.847779	-1.052274	-0.943185
12	6	0	1.584618	-0.079196	-1.530878

13	6	0	2.533939	-1.405802	2.812941
14	6	0	1.892022	-2.675970	2.269231
15	6	0	0.875752	-2.318906	1.202001
16	6	0	3.623559	0.794191	2.278138
17	6	0	4.369717	0.904079	3.611982
18	8	0	5.310848	-2.479189	-1.227299
19	6	0	-5.185464	-3.513188	-1.256194
20	6	0	-4.019000	-4.151011	-1.628739
21	6	0	-2.775981	-3.531248	-1.504305
22	6	0	-2.727861	-2.249213	-0.988190
23	6	0	-3.908673	-1.601766	-0.614325
24	6	0	-5.128754	-2.219971	-0.737393
25	7	0	-1.607560	-1.424978	-0.747109
26	6	0	-2.122342	-0.040785	-0.686557
27	6	0	-3.521945	-0.265049	-0.051235
28	6	0	-2.207903	0.617603	-2.076855
29	6	0	-3.014100	1.938256	-2.029502
30	6	0	-3.500049	2.185207	-0.595876
31	6	0	-4.403054	0.969744	-0.245983
32	6	0	-4.327859	3.472108	-0.470381
33	6	0	-5.059696	3.566973	0.875437
34	6	0	-5.905437	2.312310	1.124899
35	7	0	-5.164538	1.075172	0.980288
36	6	0	-3.293285	-0.297800	1.489416
37	6	0	-4.376106	0.614122	2.111170
38	6	0	-2.213080	2.256572	0.267334
39	6	0	-1.475313	0.878243	0.356573
40	6	0	-1.889142	0.252141	1.666586
41	8	0	-1.253665	0.217048	2.674458
42	6	0	-0.377717	-1.736142	-1.468707
43	6	0	3.319441	2.663259	-0.832857
44	6	0	4.172333	3.668618	-1.250913
45	6	0	5.373845	3.345283	-1.860744
46	6	0	5.709324	2.016375	-2.040437
47	1	0	4.991578	-0.711429	-2.772492
48	1	0	5.809267	0.179975	0.575938
49	1	0	6.636343	-1.346086	0.699875
50	1	0	4.443665	-2.446595	1.233908
51	1	0	5.179049	-1.491487	2.477167
52	1	0	1.404809	0.358311	-2.493180
53	1	0	3.178469	-1.650635	3.649353
54	1	0	1.747773	-0.759799	3.195543
55	1	0	1.380409	-3.207202	3.065591
56	1	0	2.637720	-3.352247	1.867505

57	1	0	0.578221	-3.200742	0.650050
58	1	0	-0.007874	-1.903506	1.663407
59	1	0	4.173790	1.360515	1.540171
60	1	0	2.662527	1.290220	2.378284
61	1	0	4.483835	1.951825	3.872774
62	1	0	3.837694	0.426949	4.427138
63	1	0	5.365715	0.476369	3.565961
64	1	0	-6.132333	-4.010131	-1.365575
65	1	0	-4.062762	-5.147173	-2.032451
66	1	0	-1.893221	-4.055978	-1.816264
67	1	0	-6.026858	-1.710671	-0.434611
68	1	0	-1.204499	0.801739	-2.441273
69	1	0	-2.667008	-0.082390	-2.766330
70	1	0	-2.403521	2.773564	-2.359143
71	1	0	-3.861517	1.888431	-2.706469
72	1	0	-5.100748	0.842422	-1.069427
73	1	0	-3.693752	4.342915	-0.619888
74	1	0	-5.067061	3.488952	-1.270116
75	1	0	-5.702358	4.443446	0.883904
76	1	0	-4.347765	3.703102	1.684377
77	1	0	-6.727680	2.295778	0.412513
78	1	0	-6.351670	2.338187	2.113152
79	1	0	-3.335228	-1.298011	1.897708
80	1	0	-5.005650	0.064152	2.801474
81	1	0	-3.922448	1.424001	2.680425
82	1	0	-1.549447	2.982452	-0.190863
83	1	0	-2.411033	2.632240	1.263975
84	1	0	-0.405690	0.995078	0.285018
85	1	0	-0.237938	-2.806487	-1.406543
86	1	0	-0.462394	-1.499523	-2.526423
87	1	0	2.385264	2.914716	-0.364276
88	1	0	3.899705	4.698427	-1.103387
89	1	0	6.043941	4.119165	-2.189466
90	1	0	6.638482	1.742303	-2.506016

Standard orientation of (*2R, 6R, 7R, 16R, 20R, 21S, 20'S*)-**2b** on B3LYP/6-31G(d) level in gas phase.

Center Number	Atomic Number	Atomic Type	Coordinates (Angstroms)		
			X	Y	Z
1	6	0	-2.515645	-2.140260	-0.650119
2	7	0	-2.356292	-2.255744	0.692980
3	6	0	-3.908377	-1.866328	-1.193322

4	6	0	-3.963114	-0.615441	-2.082894
5	6	0	-4.090412	0.770569	-1.388371
6	6	0	-2.909306	1.030180	-0.447247
7	6	0	-2.658909	0.605230	0.832280
8	6	0	-3.415210	-0.307252	1.736866
9	6	0	-3.229170	-1.688875	1.664716
10	7	0	-1.815054	1.771947	-0.852926
11	6	0	-0.894709	1.824178	0.165646
12	6	0	-1.388268	1.121129	1.209597
13	6	0	-4.096301	1.847331	-2.498826
14	6	0	-2.722028	2.094112	-3.106624
15	6	0	-1.763544	2.602164	-2.046184
16	6	0	-5.415977	0.889190	-0.590863
17	6	0	-6.716235	0.754184	-1.390686
18	8	0	-1.597436	-2.315816	-1.411086
19	6	0	5.202652	3.112524	1.944736
20	6	0	4.127391	3.976190	2.001517
21	6	0	2.868268	3.608261	1.527824
22	6	0	2.707806	2.341810	0.995933
23	6	0	3.797307	1.466984	0.936830
24	6	0	5.032859	1.836399	1.407715
25	7	0	1.551280	1.723491	0.480817
26	6	0	2.018782	0.623907	-0.389369
27	6	0	3.296723	0.172182	0.364720
28	6	0	2.314953	1.096414	-1.825989
29	6	0	3.092998	0.022814	-2.626152
30	6	0	3.329346	-1.202598	-1.734043
31	6	0	4.178835	-0.689968	-0.538667
32	6	0	4.107904	-2.311696	-2.455530
33	6	0	4.599016	-3.399564	-1.490402
34	6	0	5.407593	-2.785082	-0.341316
35	7	0	4.722135	-1.704605	0.339326
36	6	0	2.810676	-0.832640	1.451747
37	6	0	3.765931	-2.046648	1.379981
38	6	0	1.917638	-1.685196	-1.315176
39	6	0	1.193291	-0.666189	-0.371878
40	6	0	1.393191	-1.181996	1.030214
41	8	0	0.617826	-1.806886	1.689389
42	6	0	0.421523	2.557108	0.100413
43	6	0	-4.233201	0.196977	2.744073
44	6	0	-4.859733	-0.642943	3.648013
45	6	0	-4.671045	-2.012735	3.563110
46	6	0	-3.856947	-2.530347	2.571700
47	1	0	-1.396366	-2.343332	0.973992

48	1	0	-4.656454	-1.846832	-0.414781
49	1	0	-4.126177	-2.724343	-1.821609
50	1	0	-3.077179	-0.632495	-2.703547
51	1	0	-4.806684	-0.722826	-2.756367
52	1	0	-0.888217	0.935923	2.138154
53	1	0	-4.791779	1.557144	-3.277871
54	1	0	-4.464115	2.784326	-2.084933
55	1	0	-2.788693	2.835901	-3.896819
56	1	0	-2.326697	1.190269	-3.555693
57	1	0	-0.754838	2.603503	-2.433134
58	1	0	-2.014890	3.627230	-1.784099
59	1	0	-5.433921	0.154261	0.200180
60	1	0	-5.413651	1.855885	-0.095115
61	1	0	-7.561937	0.862327	-0.718590
62	1	0	-6.817072	1.514399	-2.157389
63	1	0	-6.810079	-0.215609	-1.867461
64	1	0	6.164550	3.420472	2.312789
65	1	0	4.257355	4.961384	2.413831
66	1	0	2.060493	4.312842	1.583305
67	1	0	5.856753	1.145778	1.363793
68	1	0	1.376953	1.322946	-2.321655
69	1	0	2.877569	2.022830	-1.783688
70	1	0	2.539655	-0.271147	-3.512776
71	1	0	4.041955	0.423259	-2.970407
72	1	0	5.007380	-0.121943	-0.953888
73	1	0	3.496089	-2.749816	-3.240338
74	1	0	4.972086	-1.867761	-2.948602
75	1	0	5.218999	-4.114190	-2.025687
76	1	0	3.757548	-3.961010	-1.095556
77	1	0	6.340404	-2.391236	-0.740129
78	1	0	5.677155	-3.541362	0.388085
79	1	0	2.788517	-0.400975	2.442806
80	1	0	4.282401	-2.197799	2.321322
81	1	0	3.214204	-2.962543	1.175603
82	1	0	1.318434	-1.811654	-2.208837
83	1	0	1.940919	-2.661845	-0.848274
84	1	0	0.154253	-0.576359	-0.635048
85	1	0	0.376824	3.370371	0.810311
86	1	0	0.574227	3.016059	-0.870888
87	1	0	-4.370990	1.260764	2.815524
88	1	0	-5.487209	-0.229552	4.417466
89	1	0	-5.151322	-2.672360	4.263383
90	1	0	-3.693353	-3.589385	2.491007

Standard orientation of ($2R$, $6R$, $7R$, $16R$, $20R$, $21S$, $20'S$)-**2c** on B3LYP/6-31G(d) level in gas phase.

Center Number	Atomic Number	Atomic Type	Coordinates (Angstroms)		
			X	Y	Z
1	6	0	-2.473771	-2.240970	-0.710852
2	7	0	-2.337410	-2.329400	0.636914
3	6	0	-3.865872	-2.025753	-1.279975
4	6	0	-3.954850	-0.793194	-2.191121
5	6	0	-4.107442	0.611396	-1.534036
6	6	0	-2.953292	0.913682	-0.576497
7	6	0	-2.716969	0.519859	0.715559
8	6	0	-3.473739	-0.392853	1.619905
9	6	0	-3.248878	-1.770744	1.577591
10	7	0	-1.867632	1.668251	-0.979556
11	6	0	-0.966004	1.759838	0.052382
12	6	0	-1.464008	1.069275	1.103353
13	6	0	-4.101397	1.644958	-2.684102
14	6	0	-2.715926	1.876076	-3.273027
15	6	0	-1.793888	2.443961	-2.208606
16	6	0	-5.483499	0.674025	-0.822431
17	6	0	-5.881513	2.012417	-0.192552
18	8	0	-1.536220	-2.396347	-1.452363
19	6	0	5.037434	3.253822	1.975307
20	6	0	3.938293	4.088850	1.977051
21	6	0	2.705234	3.675521	1.473281
22	6	0	2.595601	2.393000	0.967613
23	6	0	3.709240	1.547046	0.964622
24	6	0	4.918817	1.961135	1.464929
25	7	0	1.473096	1.731072	0.431690
26	6	0	1.997356	0.623709	-0.395172
27	6	0	3.261778	0.225459	0.409959
28	6	0	2.327477	1.068852	-1.833203
29	6	0	3.158622	-0.002650	-2.581057
30	6	0	3.398025	-1.199031	-1.651233
31	6	0	4.194835	-0.634423	-0.443027
32	6	0	4.228194	-2.304109	-2.319369
33	6	0	4.716463	-3.354211	-1.311892
34	6	0	5.471357	-2.689965	-0.154008
35	7	0	4.736198	-1.612085	0.477082
36	6	0	2.767690	-0.765270	1.506241
37	6	0	3.756470	-1.954249	1.495562
38	6	0	1.986560	-1.709066	-1.265118

39	6	0	1.205786	-0.687300	-0.371080
40	6	0	1.374360	-1.163301	1.049090
41	8	0	0.594888	-1.792709	1.699105
42	6	0	0.333737	2.522472	-0.005395
43	6	0	-4.327999	0.105545	2.599098
44	6	0	-4.955686	-0.736482	3.501208
45	6	0	-4.729616	-2.101483	3.444366
46	6	0	-3.876257	-2.613385	2.482887
47	1	0	-1.381390	-2.380022	0.939633
48	1	0	-4.626085	-2.025110	-0.513793
49	1	0	-4.042220	-2.899155	-1.900148
50	1	0	-3.078919	-0.811732	-2.825351
51	1	0	-4.812733	-0.928517	-2.844289
52	1	0	-0.977379	0.916248	2.044764
53	1	0	-4.792346	1.316517	-3.454876
54	1	0	-4.469727	2.599224	-2.323426
55	1	0	-2.769446	2.582815	-4.095681
56	1	0	-2.296371	0.959793	-3.671062
57	1	0	-0.774689	2.441258	-2.566827
58	1	0	-2.064915	3.476302	-2.000703
59	1	0	-6.238426	0.398801	-1.556103
60	1	0	-5.524464	-0.084888	-0.054113
61	1	0	-6.765689	1.877737	0.422812
62	1	0	-5.095907	2.408359	0.440352
63	1	0	-6.122919	2.764049	-0.935842
64	1	0	5.978511	3.596589	2.365710
65	1	0	4.028687	5.086697	2.368981
66	1	0	1.877658	4.358856	1.486443
67	1	0	5.761642	1.292310	1.464147
68	1	0	1.400673	1.258043	-2.364247
69	1	0	2.864111	2.010774	-1.796352
70	1	0	2.641954	-0.332943	-3.476965
71	1	0	4.107388	0.414614	-2.905240
72	1	0	5.021040	-0.054536	-0.846300
73	1	0	3.653658	-2.777777	-3.111666
74	1	0	5.095808	-1.849217	-2.796127
75	1	0	5.371831	-4.064775	-1.809054
76	1	0	3.877804	-3.928336	-0.929481
77	1	0	6.405768	-2.280881	-0.533235
78	1	0	5.737221	-3.420480	0.602494
79	1	0	2.702146	-0.310198	2.484822
80	1	0	4.246237	-2.068068	2.456222
81	1	0	3.235941	-2.889557	1.297376
82	1	0	1.420093	-1.873148	-2.173945

83	1	0	2.020479	-2.673112	-0.773276
84	1	0	0.173590	-0.632214	-0.668802
85	1	0	0.250928	3.358697	0.673705
86	1	0	0.500040	2.951432	-0.988037
87	1	0	-4.491371	1.166153	2.655843
88	1	0	-5.611776	-0.326945	4.248531
89	1	0	-5.209898	-2.762093	4.143699
90	1	0	-3.681972	-3.668710	2.425064

Standard orientation of ($2R, 6R, 7R, 16R, 20R, 21S, 20'S$)-**2d** on B3LYP/6-31G(d) level in gas phase.

Center Number	Atomic Number	Atomic Type	Coordinates (Angstroms)		
			X	Y	Z
1	6	0	5.564745	-1.318677	-0.626674
2	7	0	5.450752	-0.372648	-1.609799
3	6	0	5.641510	-0.849168	0.818713
4	6	0	4.557962	-1.430046	1.721377
5	6	0	3.239036	-0.601836	1.879062
6	6	0	2.519588	-0.551797	0.534127
7	6	0	2.724694	0.193159	-0.622884
8	6	0	3.725649	1.223590	-0.862848
9	6	0	4.964669	0.934113	-1.464454
10	7	0	1.454104	-1.404350	0.266215
11	6	0	0.932906	-1.148248	-0.984073
12	6	0	1.732942	-0.190674	-1.564902
13	6	0	2.348560	-1.341112	2.932740
14	6	0	1.772687	-2.648631	2.405900
15	6	0	0.894156	-2.373421	1.198521
16	6	0	3.558253	0.815775	2.449584
17	6	0	2.354969	1.711357	2.743272
18	8	0	5.753293	-2.498603	-0.929144
19	6	0	-5.184310	-3.512466	-1.191700
20	6	0	-4.024369	-4.200321	-1.576270
21	6	0	-2.765497	-3.592109	-1.490894
22	6	0	-2.677145	-2.290752	-1.027837
23	6	0	-3.850941	-1.619928	-0.636596
24	6	0	-5.102945	-2.208290	-0.709673
25	7	0	-1.531158	-1.486789	-0.874443
26	6	0	-2.056235	-0.106974	-0.753093
27	6	0	-3.469531	-0.278484	-0.103464
28	6	0	-2.122418	0.573980	-2.151114
29	6	0	-2.877406	1.908666	-2.112313

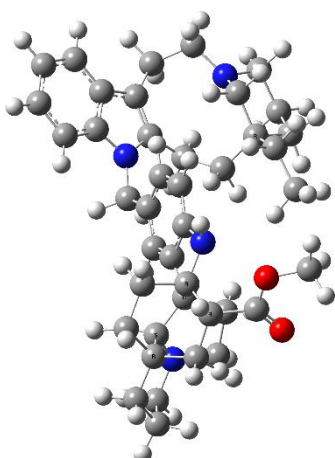
30	6	0	-3.376802	2.168390	-0.676788
31	6	0	-4.320168	0.963075	-0.340399
32	6	0	-4.162347	3.481846	-0.576829
33	6	0	-4.883494	3.592736	0.769130
34	6	0	-5.768293	2.374006	1.045113
35	7	0	-5.104399	1.085374	0.886873
36	6	0	-3.276592	-0.333562	1.428579
37	6	0	-4.288338	0.645963	2.016975
38	6	0	-2.072083	2.219362	0.192724
39	6	0	-1.409500	0.824030	0.276923
40	6	0	-1.888021	0.221490	1.569672
41	8	0	-1.276187	0.283332	2.629756
42	6	0	-0.277506	-1.831760	-1.533459
43	6	0	3.324811	2.563923	-0.741146
44	6	0	4.135633	3.595092	-1.217505
45	6	0	5.333614	3.295993	-1.861999
46	6	0	5.738349	1.967924	-2.002840
47	1	0	5.782700	-0.669454	-2.529014
48	1	0	5.742362	0.232733	0.904555
49	1	0	6.608742	-1.233885	1.174133
50	1	0	4.331098	-2.443831	1.371891
51	1	0	4.999720	-1.546654	2.720924
52	1	0	1.605723	0.216941	-2.559785
53	1	0	2.924387	-1.535310	3.846188
54	1	0	1.498120	-0.717728	3.231397
55	1	0	1.177579	-3.137861	3.185759
56	1	0	2.568645	-3.352502	2.143531
57	1	0	0.718793	-3.307272	0.654855
58	1	0	-0.070596	-1.973408	1.523829
59	1	0	4.127226	0.704797	3.382490
60	1	0	4.214101	1.372770	1.776908
61	1	0	2.697677	2.729622	2.956385
62	1	0	1.661955	1.762453	1.899687
63	1	0	1.804485	1.371941	3.625127
64	1	0	-6.151126	-4.005306	-1.259544
65	1	0	-4.103197	-5.221426	-1.942132
66	1	0	-1.888738	-4.153119	-1.791875
67	1	0	-5.993272	-1.677825	-0.386321
68	1	0	-1.108719	0.752469	-2.529621
69	1	0	-2.603620	-0.084127	-2.885856
70	1	0	-2.220663	2.719226	-2.452519
71	1	0	-3.714733	1.879925	-2.821080
72	1	0	-5.019798	0.808240	-1.172748
73	1	0	-3.497903	4.343349	-0.713004

74	1	0	-4.908874	3.530734	-1.380159
75	1	0	-5.504912	4.496163	0.769444
76	1	0	-4.158140	3.718776	1.580189
77	1	0	-6.614082	2.400850	0.345712
78	1	0	-6.212627	2.454458	2.044621
79	1	0	-3.330728	-1.335738	1.864825
80	1	0	-4.928078	0.135752	2.745386
81	1	0	-3.805441	1.480668	2.537490
82	1	0	-1.360314	2.917236	-0.269294
83	1	0	-2.266509	2.623585	1.191581
84	1	0	-0.323327	0.881587	0.257447
85	1	0	-0.091096	-2.910142	-1.463250
86	1	0	-0.361224	-1.617923	-2.606767
87	1	0	2.357437	2.806204	-0.305971
88	1	0	3.814561	4.628621	-1.115604
89	1	0	5.953943	4.097433	-2.255424
90	1	0	6.681769	1.750742	-2.497169

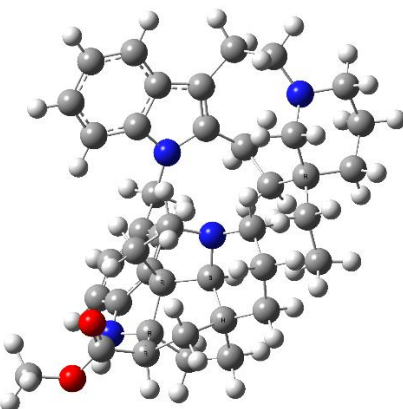
-
- (1) Goto, H.; Osawa, E. *J. Am. Chem. Soc.* **1989**, *111*, 8950–8951.
- (2) Goto, H.; Osawa, E. *J. Chem. Soc., Perkin Trans.* **1993**, *2*, 187–198.
- (3) Frisch, M. J.; Trucks, G. W.; Schlegel, H. B.; Scuseria, G. E.; Robb, M.A.; Cheeseman, J. R.; Scalmani, G.; Barone, V.; Mennucci, B.; Petersson, G. A.; Nakatsuji, H.; Caricato, M.; Li, X.; Hratchian, H. P.; Izmaylov, A. F.; Bloino, J.; Zheng, G.; Sonnenberg, J. L.; Hada, M.; Ehara,M.; Toyota, K.; Fukuda, R.;Hasegawa, J.; Ishida, M.;Nakajima, T.; Honda, Y.; Kitao, O.; Nakai, H.; Vreven, T.; Montgomery, Jr., J. A.; Peralta, J. E.; Ogliaro, F.; Bearpark,M.; Heyd, J. J.; Brothers, E.; Kudin, K. N.; Staroverov, V. N.; Keith, T.; Kobayashi, R.; Normand, J.; Raghavachari, K.; Rendell, A.; Burant, J. C.; Iyengar, S. S.; Tomasi, J.; Cossi, M.; Rega, N.; Millam, J. M.; Klene, M.; Knox, J. E.; Cross, J. B.; Bakken, V.; Adamo, C.; Jaramillo, J.; Gomperts, R.; Stratmann, R. E.; Yazyev,O.; Austin,A. J.; Cammi, R.; Pomelli,C.; Ochterski, J.W.; Martin,R. L.;Morokuma, K.; Zakrzewski,V. G.;Voth, G. A.; Salvador, P.; Dannenberg, J. J.; Dapprich, S.;Daniels, A. D.; Farkas, O.; Foresman, J. B.; Ortiz, J. V.; Cioslowski, J.; Fox, D. J. Gaussian 09, revision C.01; Gaussian, Inc.: Wallingford, CT, 2010.
- (4) Bruhn, T.; Schaumlöffel, A.; Hemberger, Y.; Bringmann, G. *SpecDis*, version 1.60, University of Wuerzburg, Germany, 2012.

Computational methods for ECD calculation of compound 3.

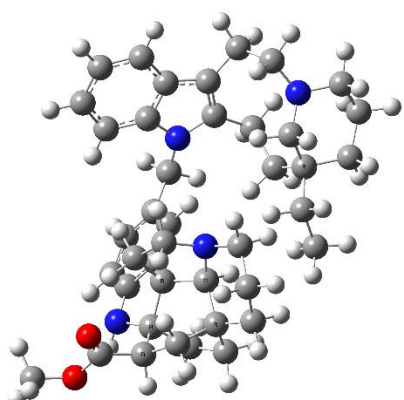
The CONFLEX^{1,2} searches based on molecular mechanics with MMFF94S force fields were performed for (20*R*, 2'*R*, 7'*R*, 16'*R*, 20'*R*, 21'S)-3 and (20*S*, 2'*R*, 7'*R*, 16'*R*, 20'*R*, 21'S)-3 which gave 2 and 4 stable conformers, respectively. Selected conformers (4 and 2) with distributions higher than 1% were further optimized by the density functional theory method at the B3LYP/6-31G* level in Gaussian 09 program package,³ leading to 4 and 2 stable geometries ($\Delta E < 2$ kcal/mol), respectively, which were in good agreement with the ROESY data. The optimized geometries were further checked by frequency calculation and resulted in no imaginary frequencies. The ECD was calculated using TD-DFT-B3LYP/6-31G+(d,p) of theory on B3LYP/6-31G(d) optimized geometries through the IEFPCM model (in MeOH). The overall calculated ECD curve was generated using SpecDis 1.60⁴ with $\sigma=0.30$ ev, UV shift -30 nm, respectively.



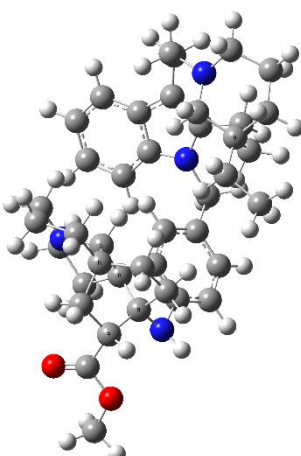
(20*R*, 2'*R*, 7'*R*, 16'*R*, 20'*R*, 21'S)-3a (48.61%)
(20.60%)



(20*R*, 2'*R*, 7'*R*, 16'*R*, 20'*R*, 21'S)-3b



(20*R*, 2'*R*, 7'*R*, 16'*R*, 20'*R*, 21'S)-3c (20.60%)
(10.20%)



(20*R*, 2'*R*, 7'*R*, 16'*R*, 20'*R*, 21'S)-3d

Standard orientation of (20*R*, 2'*R*, 7'*R*, 16'*R*, 20'*R*, 21'S)-3a on B3LYP/6-31G(d) level

in gas phase.

Center Number	Atomic Number	Atomic Type	Coordinates (Angstroms)		
			X	Y	Z
1	6	0	-1.616300	1.522765	1.182793
2	6	0	-4.414673	4.575107	-1.910724
3	6	0	-3.045522	4.639684	-1.620430
4	6	0	-2.446071	3.711197	-0.798947
5	6	0	-3.249656	2.706112	-0.261355
6	6	0	-4.617977	2.627704	-0.534267
7	6	0	-5.200419	3.579075	-1.376716
8	7	0	-2.921032	1.669267	0.579072
9	6	0	-4.078552	0.943013	0.858080
10	6	0	-5.130800	1.493015	0.198481
11	6	0	-4.057581	-0.232252	1.802862
12	6	0	-3.314965	-1.502995	1.310948
13	6	0	-3.976786	-2.512015	0.318981
14	6	0	-4.929446	-1.826211	-0.677032
15	6	0	-4.780914	-3.618059	1.043894
16	6	0	-6.138681	-3.164909	1.585744
17	6	0	-6.936869	-2.422262	0.518210
18	7	0	-6.128944	-1.355885	-0.023373
19	6	0	-6.570960	1.045606	0.182763
20	6	0	-6.815546	-0.232924	-0.628810
21	6	0	-2.850296	-3.175415	-0.513017
22	6	0	-1.782576	-3.951978	0.263028
23	6	0	-0.525039	0.968457	0.275960
24	6	0	-0.761103	0.532937	-1.014504
25	6	0	0.264326	0.025080	-1.815439
26	6	0	1.535060	-0.036638	-1.293926
27	6	0	1.792098	0.398334	0.007711
28	6	0	0.777851	0.891115	0.787279
29	7	0	2.718041	-0.504366	-1.893417
30	6	0	3.807671	0.120177	-1.148902
31	6	0	3.252476	0.113471	0.309285
32	6	0	4.020062	1.599642	-1.566051
33	6	0	5.180406	2.218404	-0.753374
34	6	0	5.453931	1.326322	0.469540
35	6	0	4.070367	1.108711	1.151256
36	6	0	6.412069	1.996084	1.464951
37	6	0	6.453422	1.273158	2.815181
38	6	0	5.038841	1.163199	3.393805
39	7	0	4.091686	0.548600	2.486879

40	6	0	4.076330	-0.901523	2.423691
41	6	0	3.338320	-1.227910	1.116900
42	6	0	6.039311	-0.003495	-0.077943
43	6	0	5.214468	-0.504572	-1.286725
44	6	0	5.284303	-2.003647	-1.503036
45	8	0	5.609317	-2.818555	-0.698650
46	8	0	4.988280	-2.311491	-2.756934
47	6	0	4.974071	-3.686518	-3.096155
48	1	0	-1.306114	2.493956	1.556772
49	1	0	-1.712244	0.886184	2.050195
50	1	0	-4.852425	5.313445	-2.558915
51	1	0	-2.450894	5.426299	-2.050316
52	1	0	-1.392385	3.758030	-0.594126
53	1	0	-6.250736	3.540558	-1.605939
54	1	0	-3.562118	0.082643	2.718881
55	1	0	-5.074799	-0.456128	2.072855
56	1	0	-3.030153	-2.060529	2.199051
57	1	0	-2.382111	-1.174873	0.867382
58	1	0	-4.430273	-0.987617	-1.143097
59	1	0	-5.170694	-2.536214	-1.477263
60	1	0	-4.957132	-4.422224	0.330585
61	1	0	-4.192902	-4.047466	1.848936
62	1	0	-6.005818	-2.511719	2.442470
63	1	0	-6.697660	-4.030347	1.933382
64	1	0	-7.833200	-1.999652	0.958711
65	1	0	-7.261889	-3.124978	-0.259002
66	1	0	-6.927345	0.871840	1.194471
67	1	0	-7.182505	1.848818	-0.219625
68	1	0	-7.883368	-0.430718	-0.669141
69	1	0	-6.491339	-0.086430	-1.656365
70	1	0	-3.307607	-3.851882	-1.231322
71	1	0	-2.355466	-2.402598	-1.096624
72	1	0	-1.050427	-4.360356	-0.426779
73	1	0	-1.246413	-3.322435	0.964454
74	1	0	-2.205417	-4.784379	0.815600
75	1	0	-1.752430	0.596553	-1.421755
76	1	0	0.055396	-0.299073	-2.819875
77	1	0	0.984700	1.216122	1.794105
78	1	0	2.768519	-0.404412	-2.886354
79	1	0	4.227368	1.634363	-2.632155
80	1	0	3.105368	2.156818	-1.408613
81	1	0	6.080839	2.301638	-1.356272
82	1	0	4.925156	3.225533	-0.439131
83	1	0	3.587139	2.081826	1.203680

84	1	0	7.408488	2.066661	1.035442
85	1	0	6.077217	3.018564	1.634241
86	1	0	6.892329	0.285673	2.704021
87	1	0	7.089709	1.818279	3.507783
88	1	0	4.681133	2.162584	3.634916
89	1	0	5.041993	0.601597	4.321913
90	1	0	3.555316	-1.297940	3.289515
91	1	0	5.071418	-1.342831	2.431005
92	1	0	3.833613	-2.017201	0.578954
93	1	0	2.336851	-1.573720	1.330213
94	1	0	7.066255	0.164751	-0.388838
95	1	0	6.072939	-0.771005	0.678627
96	1	0	5.638683	-0.099403	-2.198962
97	1	0	4.243223	-4.214034	-2.500697
98	1	0	4.706834	-3.729713	-4.140509
99	1	0	5.948417	-4.126077	-2.939882

Standard orientation of (20*R*, 2'(*R*, 7'(*R*, 16'*R*, 20'*R*, 21'*S*)-3**b** on B3LYP/6-31G(d) level in gas phase.

Center Number	Atomic Number	Atomic Type	Coordinates (Angstroms)		
			X	Y	Z
1	6	0	1.768125	2.136499	-2.116321
2	6	0	2.467468	4.469641	2.448539
3	6	0	1.449609	4.675792	1.508875
4	6	0	1.372137	3.918290	0.361064
5	6	0	2.343516	2.936643	0.164279
6	6	0	3.376647	2.728803	1.081887
7	6	0	3.427543	3.505113	2.242822
8	7	0	2.509736	2.050013	-0.875886
9	6	0	3.668627	1.308381	-0.638756
10	6	0	4.218874	1.685201	0.543436
11	6	0	4.162084	0.286555	-1.632247
12	6	0	3.298956	-0.994644	-1.785943
13	6	0	3.421617	-2.190604	-0.790354
14	6	0	3.705013	-1.731043	0.651436
15	6	0	4.532282	-3.192028	-1.190829
16	6	0	5.956523	-2.728138	-0.875185
17	6	0	6.064373	-2.219875	0.559615
18	7	0	5.048758	-1.220467	0.787100
19	6	0	5.457545	1.155130	1.221425
20	6	0	5.286157	-0.242484	1.829179
21	6	0	2.063429	-2.935398	-0.767820

22	6	0	1.560717	-3.503236	-2.098405
23	6	0	0.279061	1.842658	-2.002240
24	6	0	-0.586195	2.416004	-2.921481
25	6	0	-1.955566	2.168767	-2.900434
26	6	0	-2.449552	1.330916	-1.923970
27	6	0	-1.596778	0.744996	-0.991069
28	6	0	-0.245267	0.999031	-1.019228
29	7	0	-3.781857	0.960466	-1.674116
30	6	0	-3.707324	-0.268700	-0.890898
31	6	0	-2.457492	-0.010553	0.007360
32	6	0	-3.402659	-1.501475	-1.782584
33	6	0	-3.338665	-2.779574	-0.916123
34	6	0	-3.167778	-2.365342	0.555299
35	6	0	-1.978697	-1.358866	0.574745
36	6	0	-2.834223	-3.565827	1.452644
37	6	0	-2.355784	-3.142352	2.845097
38	6	0	-1.159498	-2.192952	2.720404
39	7	0	-1.420338	-1.047849	1.873580
40	6	0	-2.125702	0.072253	2.470009
41	6	0	-2.640288	0.891625	1.277213
42	6	0	-4.498715	-1.688146	0.979870
43	6	0	-4.968838	-0.688976	-0.103140
44	6	0	-5.854577	0.422491	0.424892
45	8	0	-5.948723	0.772092	1.558572
46	8	0	-6.588160	0.941501	-0.548914
47	6	0	-7.438477	2.021378	-0.207762
48	1	0	1.897021	3.129887	-2.537147
49	1	0	2.213943	1.448490	-2.818695
50	1	0	2.497186	5.074961	3.337186
51	1	0	0.712318	5.438485	1.687378
52	1	0	0.582605	4.078526	-0.348348
53	1	0	4.208719	3.359213	2.967850
54	1	0	4.202598	0.758167	-2.611552
55	1	0	5.177506	0.041439	-1.375298
56	1	0	3.487000	-1.383082	-2.783165
57	1	0	2.260097	-0.681584	-1.791085
58	1	0	3.002906	-0.958073	0.933464
59	1	0	3.534799	-2.576347	1.329155
60	1	0	4.355367	-4.117726	-0.644797
61	1	0	4.455883	-3.440325	-2.244934
62	1	0	6.256204	-1.934740	-1.552378
63	1	0	6.648099	-3.552552	-1.031263
64	1	0	7.041079	-1.776295	0.718398
65	1	0	5.976076	-3.060098	1.259444

66	1	0	6.287454	1.114760	0.520976
67	1	0	5.753830	1.851885	2.000897
68	1	0	6.183294	-0.503300	2.384543
69	1	0	4.470691	-0.235624	2.547925
70	1	0	2.133559	-3.753364	-0.054793
71	1	0	1.310942	-2.256345	-0.373726
72	1	0	0.608206	-4.003647	-1.949851
73	1	0	1.406118	-2.730352	-2.843249
74	1	0	2.246043	-4.234469	-2.513563
75	1	0	-0.193045	3.077421	-3.675319
76	1	0	-2.604895	2.631295	-3.622927
77	1	0	0.399809	0.572853	-0.272525
78	1	0	-4.379411	0.921497	-2.473949
79	1	0	-4.176441	-1.581830	-2.541437
80	1	0	-2.467323	-1.348897	-2.305998
81	1	0	-4.240594	-3.375579	-1.028510
82	1	0	-2.512001	-3.408045	-1.232288
83	1	0	-1.190092	-1.792401	-0.035353
84	1	0	-3.693392	-4.228434	1.525320
85	1	0	-2.040592	-4.142394	0.979235
86	1	0	-3.161333	-2.662760	3.393945
87	1	0	-2.068470	-4.018966	3.420296
88	1	0	-0.318492	-2.743079	2.302288
89	1	0	-0.843976	-1.836012	3.694875
90	1	0	-1.441274	0.646591	3.085535
91	1	0	-2.946513	-0.233709	3.116732
92	1	0	-3.657916	1.205036	1.432852
93	1	0	-2.048487	1.788015	1.159553
94	1	0	-5.257204	-2.453513	1.116224
95	1	0	-4.407440	-1.178527	1.925746
96	1	0	-5.609828	-1.205850	-0.809216
97	1	0	-6.860785	2.849108	0.177119
98	1	0	-7.935458	2.305661	-1.122246
99	1	0	-8.162776	1.715031	0.532889

Standard orientation of (*20R, 2'R, 7'R, 16'R, 20'R, 21'S*)-**3c** on B3LYP/6-31G(d) level in gas phase.

Center Number	Atomic Number	Atomic Type	Coordinates (Angstroms)		
			X	Y	Z
1	6	0	1.768155	2.136214	-2.116210
2	6	0	2.467839	4.469703	2.448430
3	6	0	1.449786	4.675640	1.508932

4	6	0	1.372196	3.918018	0.361204
5	6	0	2.343661	2.936471	0.164328
6	6	0	3.376980	2.728848	1.081768
7	6	0	3.427992	3.505266	2.242629
8	7	0	2.509771	2.049730	-0.875772
9	6	0	3.668836	1.308306	-0.638802
10	6	0	4.219253	1.685316	0.543244
11	6	0	4.162180	0.286379	-1.632239
12	6	0	3.299005	-0.994808	-1.785666
13	6	0	3.421858	-2.190671	-0.789985
14	6	0	3.705515	-1.730948	0.651703
15	6	0	4.532482	-3.192089	-1.190574
16	6	0	5.956762	-2.728090	-0.875269
17	6	0	6.064888	-2.219663	0.559452
18	7	0	5.049265	-1.220292	0.787050
19	6	0	5.458052	1.155370	1.221091
20	6	0	5.286819	-0.242202	1.828983
21	6	0	2.063696	-2.935510	-0.767112
22	6	0	1.560752	-3.503524	-2.097533
23	6	0	0.279042	1.842709	-2.002000
24	6	0	-0.586193	2.416500	-2.920971
25	6	0	-1.955618	2.169481	-2.899889
26	6	0	-2.449651	1.331406	-1.923661
27	6	0	-1.596890	0.745071	-0.990983
28	6	0	-0.245354	0.998886	-1.019174
29	7	0	-3.781976	0.961057	-1.673817
30	6	0	-3.707589	-0.268348	-0.890967
31	6	0	-2.457672	-0.010623	0.007298
32	6	0	-3.403094	-1.500919	-1.783021
33	6	0	-3.339284	-2.779283	-0.916943
34	6	0	-3.168301	-2.365493	0.554582
35	6	0	-1.979086	-1.359163	0.574327
36	6	0	-2.834879	-3.566275	1.451579
37	6	0	-2.356418	-3.143263	2.844167
38	6	0	-1.160033	-2.193943	2.719765
39	7	0	-1.420748	-1.048582	1.873274
40	6	0	-2.125948	0.071452	2.469987
41	6	0	-2.640219	0.891293	1.277386
42	6	0	-4.499158	-1.688270	0.979361
43	6	0	-4.969143	-0.688654	-0.103299
44	6	0	-5.854629	0.422829	0.425140
45	8	0	-5.948538	0.772203	1.558907
46	8	0	-6.588322	0.942169	-0.548399
47	6	0	-7.438369	2.022125	-0.206816

48	1	0	1.897232	3.129499	-2.537225
49	1	0	2.213785	1.447966	-2.818469
50	1	0	2.497648	5.075112	3.337014
51	1	0	0.712431	5.438257	1.687502
52	1	0	0.582517	4.078091	-0.348079
53	1	0	4.209323	3.359534	2.967523
54	1	0	4.202586	0.757875	-2.611607
55	1	0	5.177634	0.041277	-1.375386
56	1	0	3.486876	-1.383324	-2.782888
57	1	0	2.260147	-0.681734	-1.790652
58	1	0	3.003424	-0.957986	0.933796
59	1	0	3.535485	-2.576189	1.329547
60	1	0	4.355712	-4.117740	-0.644418
61	1	0	4.455883	-3.440488	-2.244641
62	1	0	6.256267	-1.934751	-1.552612
63	1	0	6.648347	-3.552488	-1.031393
64	1	0	7.041606	-1.776014	0.717969
65	1	0	5.976793	-3.059817	1.259388
66	1	0	6.287854	1.114991	0.520515
67	1	0	5.754425	1.852203	2.000462
68	1	0	6.184078	-0.502931	2.384192
69	1	0	4.471498	-0.235309	2.547896
70	1	0	2.133984	-3.753395	-0.054010
71	1	0	1.311253	-2.256448	-0.372949
72	1	0	0.608257	-4.003898	-1.948743
73	1	0	1.406038	-2.730745	-2.842461
74	1	0	2.245995	-4.234829	-2.512703
75	1	0	-0.193011	3.078095	-3.674634
76	1	0	-2.604926	2.632363	-3.622173
77	1	0	0.399728	0.572406	-0.272643
78	1	0	-4.379664	0.922513	-2.473565
79	1	0	-4.176886	-1.580956	-2.541896
80	1	0	-2.467736	-1.348332	-2.306392
81	1	0	-4.241324	-3.375100	-1.029471
82	1	0	-2.512746	-3.407805	-1.233328
83	1	0	-1.190522	-1.792647	-0.035863
84	1	0	-3.694114	-4.228823	1.524034
85	1	0	-2.041294	-4.142767	0.978008
86	1	0	-3.161923	-2.663730	3.393130
87	1	0	-2.069226	-4.020076	3.419120
88	1	0	-0.319078	-2.744036	2.301499
89	1	0	-0.844474	-1.837318	3.694341
90	1	0	-2.946898	-0.234525	3.116532
91	1	0	-1.441490	0.645487	3.085770

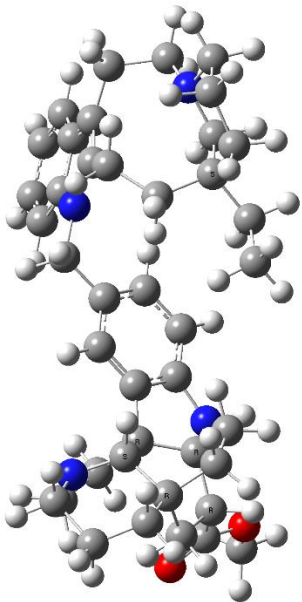
92	1	0	-3.657740	1.205045	1.433049
93	1	0	-2.048063	1.787478	1.159978
94	1	0	-5.257754	-2.453578	1.115456
95	1	0	-4.407816	-1.178979	1.925405
96	1	0	-5.610250	-1.205176	-0.809521
97	1	0	-6.860433	2.849653	0.178129
98	1	0	-7.935506	2.306713	-1.121121
99	1	0	-8.162555	1.715725	0.533924

Standard orientation of (20R, 2'R, 7'R, 16'R, 20'R, 21'S)-3d on B3LYP/6-31G(d) level in gas phase.

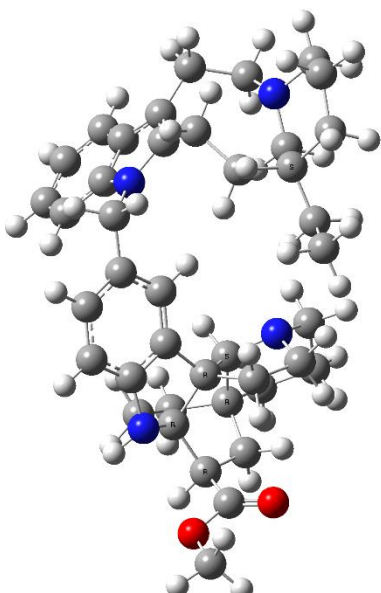
Center Number	Atomic Number	Atomic Type	Coordinates (Angstroms)		
			X	Y	Z
1	6	0	1.839499	1.885705	-2.398746
2	6	0	2.479915	4.622851	1.941448
3	6	0	1.520587	4.789271	0.933896
4	6	0	1.465750	3.937181	-0.146800
5	6	0	2.400797	2.903678	-0.205670
6	6	0	3.369672	2.725570	0.785311
7	6	0	3.399579	3.601021	1.874751
8	7	0	2.574294	1.924031	-1.154587
9	6	0	3.667508	1.140337	-0.784911
10	6	0	4.175101	1.592669	0.390757
11	6	0	4.158851	0.018714	-1.665021
12	6	0	3.241139	-1.227730	-1.774813
13	6	0	3.231479	-2.338603	-0.678221
14	6	0	3.454629	-1.772968	0.736377
15	6	0	4.303528	-3.428758	-0.920395
16	6	0	5.730884	-3.013519	-0.555773
17	6	0	5.783838	-2.389383	0.835486
18	7	0	4.815019	-1.322608	0.915502
19	6	0	5.339472	1.055648	1.184768
20	6	0	5.047617	-0.275298	1.889196
21	6	0	1.832568	-3.004510	-0.686880
22	6	0	1.391043	-3.670177	-1.993711
23	6	0	0.390891	1.419260	-2.298057
24	6	0	-0.390794	1.455841	-3.442540
25	6	0	-1.720223	1.046354	-3.440959
26	6	0	-2.265127	0.605358	-2.254179
27	6	0	-1.500235	0.571175	-1.087999
28	6	0	-0.182427	0.968408	-1.106029
29	7	0	-3.574370	0.159390	-2.000676

30	6	0	-3.474892	-0.635994	-0.778724
31	6	0	-2.444132	0.186493	0.043503
32	6	0	-2.852789	-2.031437	-1.067263
33	6	0	-2.683796	-2.839524	0.238618
34	6	0	-2.889486	-1.898640	1.432767
35	6	0	-1.977737	-0.671225	1.240155
36	6	0	-2.489651	-2.567084	2.761972
37	6	0	-2.390473	-1.598570	3.953315
38	6	0	-1.574849	-0.346075	3.609986
39	7	0	-2.104583	0.188040	2.388429
40	6	0	-2.022534	1.564177	1.976140
41	6	0	-2.900194	1.518683	0.722863
42	6	0	-4.365655	-1.429929	1.409429
43	6	0	-4.776662	-0.967700	-0.014786
44	6	0	-5.860006	0.094058	-0.029210
45	8	0	-6.167365	0.806397	0.872488
46	8	0	-6.493711	0.100046	-1.194299
47	6	0	-7.507777	1.072193	-1.368441
48	1	0	1.858605	2.880268	-2.834406
49	1	0	2.372258	1.246566	-3.086701
50	1	0	2.494351	5.303367	2.774209
51	1	0	0.812291	5.595486	1.006600
52	1	0	0.718932	4.064124	-0.908650
53	1	0	4.132729	3.484856	2.653284
54	1	0	4.275907	0.411153	-2.672887
55	1	0	5.145251	-0.252748	-1.332365
56	1	0	3.477020	-1.707927	-2.720513
57	1	0	2.223794	-0.867310	-1.881427
58	1	0	2.782915	-0.942538	0.907996
59	1	0	3.196254	-2.546976	1.469134
60	1	0	4.041394	-4.292236	-0.310346
61	1	0	4.275147	-3.764310	-1.952331
62	1	0	6.113682	-2.298131	-1.276631
63	1	0	6.382694	-3.882697	-0.598880
64	1	0	6.773162	-1.984592	1.017839
65	1	0	5.607417	-3.160064	1.595951
66	1	0	6.205295	0.911960	0.543983
67	1	0	5.630218	1.797090	1.924055
68	1	0	5.891688	-0.538091	2.521417
69	1	0	4.191975	-0.163068	2.550328
70	1	0	1.803431	-3.752273	0.102151
71	1	0	1.095578	-2.250918	-0.418123
72	1	0	0.400228	-4.098111	-1.873738
73	1	0	1.340276	-2.965497	-2.816391

74	1	0	2.056012	-4.476316	-2.284522
75	1	0	0.040460	1.806324	-4.365914
76	1	0	-2.301696	1.077605	-4.345688
77	1	0	0.405695	0.944584	-0.208155
78	1	0	-4.034116	-0.287548	-2.767211
79	1	0	-3.498639	-2.552437	-1.768936
80	1	0	-1.897376	-1.908157	-1.559307
81	1	0	-3.397432	-3.657546	0.289556
82	1	0	-1.696246	-3.288998	0.276423
83	1	0	-0.946999	-1.016002	1.102623
84	1	0	-3.180414	-3.372797	2.999636
85	1	0	-1.515880	-3.032521	2.617067
86	1	0	-3.383672	-1.281535	4.255321
87	1	0	-1.949116	-2.116898	4.801004
88	1	0	-0.509506	-0.591893	3.531447
89	1	0	-1.675366	0.390902	4.399313
90	1	0	-1.007622	1.902733	1.751402
91	1	0	-2.427178	2.218860	2.740303
92	1	0	-3.930874	1.485168	1.035031
93	1	0	-2.768124	2.370801	0.069716
94	1	0	-5.011573	-2.245650	1.721441
95	1	0	-4.510718	-0.621510	2.108603
96	1	0	-5.231725	-1.799250	-0.542174
97	1	0	-7.098659	2.066902	-1.267054
98	1	0	-7.889369	0.925253	-2.367003
99	1	0	-8.295703	0.933899	-0.642314



(20*S*, 2'*R*, 7'*R*, 16'*R*, 20'*R*, 21'*S*)-3a (61.89%)



(20*S*, 2'*R*, 7'*R*, 16'*R*, 20'*R*, 21'*S*)-3b

(38.11%)

Standard orientation of (20S, 2'R, 7'R, 16'R, 20'R, 21'S)-**3a** on B3LYP/6-31G(d) level in gas phase.

Center Number	Atomic Number	Atomic Type	Coordinates (Angstroms)		
			X	Y	Z
1	6	0	-1.644301	1.033965	-1.653820
2	6	0	-4.549245	4.934733	0.097677
3	6	0	-3.182059	4.928676	-0.209142
4	6	0	-2.550203	3.779361	-0.628398
5	6	0	-3.319163	2.621336	-0.742022
6	6	0	-4.684624	2.607857	-0.445427
7	6	0	-5.300389	3.787016	-0.015626
8	7	0	-2.954213	1.355577	-1.135132
9	6	0	-4.086214	0.541453	-1.108342
10	6	0	-5.157652	1.265290	-0.692817
11	6	0	-4.024556	-0.901591	-1.541825
12	6	0	-3.239938	-1.869276	-0.616765
13	6	0	-3.866412	-2.447479	0.692311
14	6	0	-4.843939	-1.467301	1.366000
15	6	0	-4.629950	-3.772005	0.451423
16	6	0	-6.001993	-3.603296	-0.205430
17	6	0	-6.827381	-2.538449	0.510909
18	7	0	-6.058477	-1.320125	0.597772
19	6	0	-6.581820	0.810548	-0.494574
20	6	0	-6.785055	-0.074740	0.741569
21	6	0	-2.717976	-2.707207	1.699735
22	6	0	-1.622301	-3.683874	1.262525
23	6	0	-0.539941	0.874727	-0.616648
24	6	0	-0.757505	0.976998	0.744517
25	6	0	0.279062	0.813191	1.666464
26	6	0	1.541303	0.541946	1.193596
27	6	0	1.780480	0.438743	-0.178235
28	6	0	0.758212	0.610510	-1.075183
29	7	0	2.733811	0.343043	1.911603
30	6	0	3.612935	-0.399017	1.012858
31	6	0	3.272177	0.233345	-0.372324
32	6	0	3.238949	-1.903778	0.949726
33	6	0	4.193501	-2.647640	-0.012084
34	6	0	4.906415	-1.610160	-0.896090
35	6	0	3.779431	-0.707122	-1.479909
36	6	0	5.676913	-2.271239	-2.047956
37	6	0	6.129653	-1.260214	-3.106388

38	6	0	4.923618	-0.470433	-3.625747
39	7	0	4.154499	0.163369	-2.575063
40	6	0	4.644649	1.430632	-2.064235
41	6	0	3.920772	1.617400	-0.722594
42	6	0	5.854349	-0.812010	0.039436
43	6	0	5.122875	-0.410643	1.341911
44	6	0	5.691047	0.824254	2.013630
45	8	0	6.376455	1.652905	1.503496
46	8	0	5.374999	0.846725	3.299764
47	6	0	5.805404	1.969052	4.049023
48	1	0	-1.720612	0.124064	-2.231088
49	1	0	-1.360275	1.811314	-2.356777
50	1	0	-5.012575	5.848195	0.426015
51	1	0	-2.614530	5.837133	-0.111045
52	1	0	-1.497876	3.779196	-0.845277
53	1	0	-6.349409	3.804175	0.222047
54	1	0	-3.538766	-0.939445	-2.514626
55	1	0	-5.033283	-1.243018	-1.695820
56	1	0	-2.938479	-2.712567	-1.232334
57	1	0	-2.317951	-1.369579	-0.343436
58	1	0	-5.060797	-1.828862	2.378437
59	1	0	-4.375336	-0.498637	1.473539
60	1	0	-4.026238	-4.455297	-0.137689
61	1	0	-4.778838	-4.250510	1.418615
62	1	0	-5.890777	-3.319166	-1.247154
63	1	0	-6.529539	-4.553981	-0.192807
64	1	0	-7.737602	-2.344644	-0.045777
65	1	0	-7.128116	-2.904520	1.500387
66	1	0	-6.929702	0.256694	-1.362327
67	1	0	-7.221260	1.685906	-0.418096
68	1	0	-7.845530	-0.278069	0.863812
69	1	0	-6.469703	0.459088	1.634905
70	1	0	-2.252013	-1.754466	1.940128
71	1	0	-3.151197	-3.075813	2.626581
72	1	0	-0.876821	-3.776016	2.046775
73	1	0	-2.014171	-4.677381	1.072033
74	1	0	-1.109009	-3.349698	0.367534
75	1	0	-1.744612	1.190494	1.108683
76	1	0	0.082907	0.898326	2.720922
77	1	0	0.955623	0.542624	-2.132807
78	1	0	2.629399	-0.047860	2.825193
79	1	0	3.293612	-2.318228	1.952751
80	1	0	2.211787	-2.010178	0.624768
81	1	0	4.928836	-3.229573	0.537321

82	1	0	3.638300	-3.351055	-0.624622
83	1	0	2.993617	-1.371020	-1.833497
84	1	0	6.526212	-2.827836	-1.659093
85	1	0	5.025272	-3.000314	-2.527664
86	1	0	6.872330	-0.583983	-2.692577
87	1	0	6.609651	-1.778777	-3.932473
88	1	0	4.267392	-1.149993	-4.166569
89	1	0	5.234107	0.291026	-4.333229
90	1	0	4.403090	2.223406	-2.765187
91	1	0	5.724905	1.451763	-1.931490
92	1	0	4.595661	1.974773	0.035355
93	1	0	3.138541	2.356621	-0.820416
94	1	0	6.711503	-1.432037	0.285278
95	1	0	6.245673	0.070519	-0.440763
96	1	0	5.266046	-1.188359	2.084208
97	1	0	5.384253	2.877171	3.642957
98	1	0	5.447189	1.807618	5.053789
99	1	0	6.883363	2.039321	4.041898

Standard orientation of (20'S, 2'R, 7'R, 16'R, 20'R, 21'S)-**3b** on B3LYP/6-31G(d) level in gas phase.

Center Number	Atomic Number	Atomic Type	Coordinates (Angstroms)		
			X	Y	Z
1	6	0	-1.822165	1.755956	-2.414084
2	6	0	-2.726027	4.564906	1.838060
3	6	0	-1.708375	4.719442	0.888330
4	6	0	-1.572432	3.840159	-0.163213
5	6	0	-2.484388	2.788331	-0.252753
6	6	0	-3.517234	2.628856	0.675252
7	6	0	-3.627565	3.529624	1.738070
8	7	0	-2.587306	1.780760	-1.184743
9	6	0	-3.706025	1.006428	-0.872472
10	6	0	-4.292800	1.484640	0.254580
11	6	0	-4.130373	-0.145853	-1.748364
12	6	0	-3.201926	-1.390259	-1.747881
13	6	0	-3.282534	-2.474389	-0.628019
14	6	0	-3.607744	-1.873066	0.751172
15	6	0	-4.340191	-3.565164	-0.925955
16	6	0	-5.789051	-3.139021	-0.675944
17	6	0	-5.940749	-2.481412	0.692605
18	7	0	-4.976007	-1.415575	0.817239
19	6	0	-5.510931	0.968592	0.979132

20	6	0	-5.274947	-0.341195	1.741293
21	6	0	-1.891609	-3.147059	-0.511924
22	6	0	-1.345808	-3.828164	-1.770667
23	6	0	-0.323212	1.563836	-2.234410
24	6	0	0.540446	2.103474	-3.173725
25	6	0	1.921989	1.953030	-3.079291
26	6	0	2.426774	1.250590	-2.007538
27	6	0	1.573662	0.691691	-1.057147
28	6	0	0.211822	0.838639	-1.165106
29	7	0	3.767832	0.993833	-1.672314
30	6	0	3.761578	0.726556	-0.235995
31	6	0	2.432330	-0.070956	-0.062139
32	6	0	3.638827	2.032489	0.594402
33	6	0	3.621772	1.703557	2.104895
34	6	0	3.329427	0.203828	2.278133
35	6	0	2.054033	-0.082132	1.430257
36	6	0	3.054359	-0.161695	3.743776
37	6	0	2.475428	-1.572224	3.896162
38	6	0	1.213017	-1.716959	3.039588
39	7	0	1.415192	-1.364991	1.649267
40	6	0	2.008260	-2.368192	0.784550
41	6	0	2.432161	-1.586494	-0.465641
42	6	0	4.570853	-0.549496	1.729470
43	6	0	5.003145	0.027895	0.360966
44	6	0	5.724191	-0.968249	-0.525878
45	8	0	5.688802	-2.154043	-0.429388
46	8	0	6.475439	-0.343715	-1.420991
47	6	0	7.179066	-1.151873	-2.346804
48	1	0	-2.212584	0.962077	-3.032592
49	1	0	-1.994429	2.680836	-2.957537
50	1	0	-2.802843	5.266402	2.649894
51	1	0	-1.018564	5.539686	0.981944
52	1	0	-0.784083	3.962972	-0.881334
53	1	0	-4.409842	3.424108	2.468870
54	1	0	-4.178909	0.210798	-2.774811
55	1	0	-5.136198	-0.412606	-1.475793
56	1	0	-3.352839	-1.894945	-2.698130
57	1	0	-2.179677	-1.027963	-1.775187
58	1	0	-3.407562	-2.628831	1.520044
59	1	0	-2.946623	-1.040748	0.951763
60	1	0	-4.237452	-3.923226	-1.945610
61	1	0	-4.127828	-4.416110	-0.280209
62	1	0	-6.116914	-2.440843	-1.439474
63	1	0	-6.438687	-4.008219	-0.745355

64	1	0	-6.939226	-2.070209	0.792718
65	1	0	-5.823244	-3.234080	1.482024
66	1	0	-6.328406	0.806011	0.281787
67	1	0	-5.853265	1.731647	1.673026
68	1	0	-6.163517	-0.584201	2.318253
69	1	0	-4.468775	-0.211050	2.458830
70	1	0	-1.174994	-2.399235	-0.180803
71	1	0	-1.937410	-3.889026	0.281736
72	1	0	-0.375340	-4.267981	-1.561527
73	1	0	-1.993460	-4.627783	-2.114371
74	1	0	-1.212741	-3.131332	-2.590977
75	1	0	0.138654	2.670635	-3.996575
76	1	0	2.570276	2.395435	-3.815216
77	1	0	-0.437974	0.421986	-0.417211
78	1	0	4.426563	1.682344	-1.973340
79	1	0	4.473287	2.682500	0.345059
80	1	0	2.737198	2.560288	0.312030
81	1	0	4.573331	1.947486	2.570081
82	1	0	2.868213	2.298536	2.610825
83	1	0	1.333748	0.696853	1.668334
84	1	0	3.961631	-0.052691	4.333260
85	1	0	2.336348	0.549536	4.149440
86	1	0	3.211927	-2.317912	3.610309
87	1	0	2.232137	-1.761884	4.938570
88	1	0	0.438986	-1.068232	3.444891
89	1	0	0.826975	-2.729726	3.086182
90	1	0	1.271679	-3.129637	0.551285
91	1	0	2.855062	-2.883303	1.233225
92	1	0	3.380403	-1.929035	-0.842403
93	1	0	1.707601	-1.734383	-1.254113
94	1	0	5.387174	-0.442150	2.437856
95	1	0	4.391274	-1.607410	1.631668
96	1	0	5.741866	0.806021	0.519326
97	1	0	6.489615	-1.744914	-2.929925
98	1	0	7.716968	-0.468633	-2.985477
99	1	0	7.868246	-1.806005	-1.832846

-
- (1) Goto, H.; Osawa, E. *J. Am. Chem. Soc.* **1989**, *111*, 8950–8951.
- (2) Goto, H.; Osawa, E. *J. Chem. Soc., Perkin Trans.* **1993**, *2*, 187–198.
- (3) Frisch, M. J.; Trucks, G. W.; Schlegel, H. B.; Scuseria, G. E.; Robb, M.A.; Cheeseman, J. R.; Scalmani, G.; Barone, V.; Mennucci, B.; Petersson, G. A.; Nakatsuji, H.; Caricato, M.; Li, X.; Hratchian, H. P.; Izmaylov, A. F.; Bloino, J.; Zheng, G.;

Sonnenberg, J. L.; Hada, M.; Ehara,M.; Toyota, K.; Fukuda, R.;Hasegawa, J.; Ishida, M.;Nakajima, T; Honda, Y.; Kitao, O.; Nakai, H.; Vreven, T.; Montgomery, Jr., J. A.; Peralta, J. E.; Ogliaro, F.; Bearpark,M.; Heyd, J. J.; Brothers, E.; Kudin, K. N.; Staroverov, V. N.; Keith, T.; Kobayashi, R.; Normand, J.; Raghavachari, K.; Rendell, A.; Burant, J. C.; Iyengar, S. S.; Tomasi, J.; Cossi, M.; Rega, N.; Millam, J. M.; Klene, M.; Knox, J. E.; Cross, J. B.; Bakken, V.; Adamo, C.; Jaramillo, J.; Gomperts, R.; Stratmann, R. E.; Yazyev,O.; Austin,A. J.; Cammi, R.; Pomelli,C.; Ochterski, J.W.; Martin,R. L.;Morokuma, K.; Zakrzewski,V. G.;Voth, G. A.; Salvador, P.; Dannenberg, J. J.; Dapprich, S.;Daniels, A. D.; Farkas, O.; Foresman, J. B.; Ortiz, J. V.; Cioslowski, J.; Fox, D. J. Gaussian 09, revision C.01; Gaussian, Inc.: Wallingford, CT, 2010.

(4) Bruhn, T.; Schaumlöffel, A.; Hemberger, Y.; Bringmann, G. *SpecDis*, version 1.60, University of Wuerzburg, Germany, 2012.

7.29
7.28
7.27
7.26
7.24
7.23
7.15
7.14
7.13
7.11
7.11
7.10
7.02
7.00
7.00
6.70
6.69
6.67
6.46
6.33
6.31
5.55
4.41
4.38
3.73
3.70
3.58
3.57
3.41
3.35
3.34
3.31
3.11
3.10
2.98
2.96
2.95
2.94
2.93
2.92
2.54
2.41
2.38
2.36
2.17
1.95
1.94
1.92
1.76
1.74
1.73
1.72
1.71
1.70
1.57
1.56
1.55
1.53
1.52
1.51
1.50
1.49
1.48
1.47
1.46
1.45
1.44
1.42
1.39
1.37
1.36
1.35
1.30
1.28
1.27
1.25
1.23
1.21
1.22
0.74
0.73
0.71

Figure S1.1 ^1H NMR (500 MHz, chloroform-*d*) of 1.

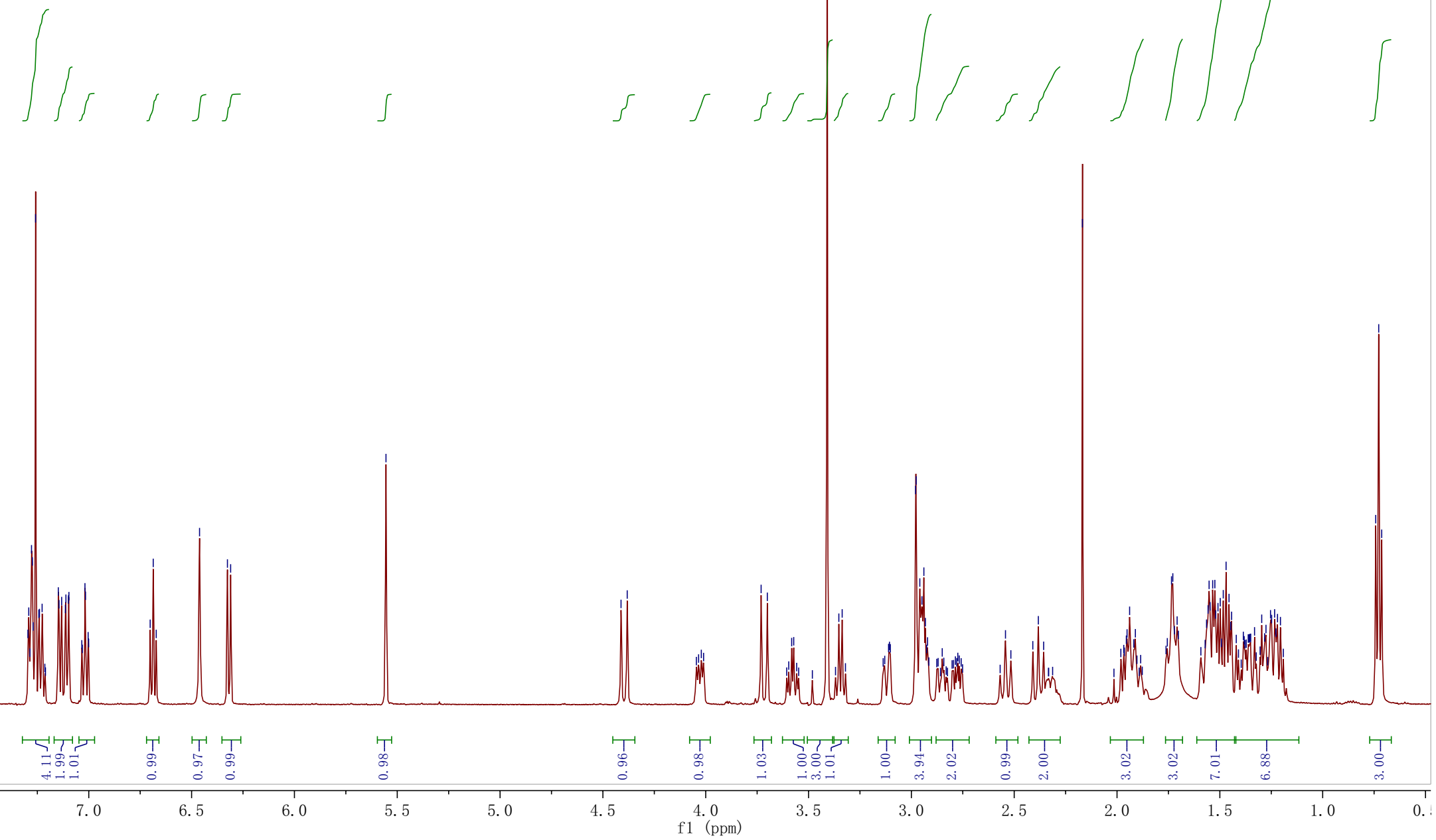


Figure S1.2 ^{13}C NMR and DEPT spectra (125 MHz, chloroform-*d*) of **1**.

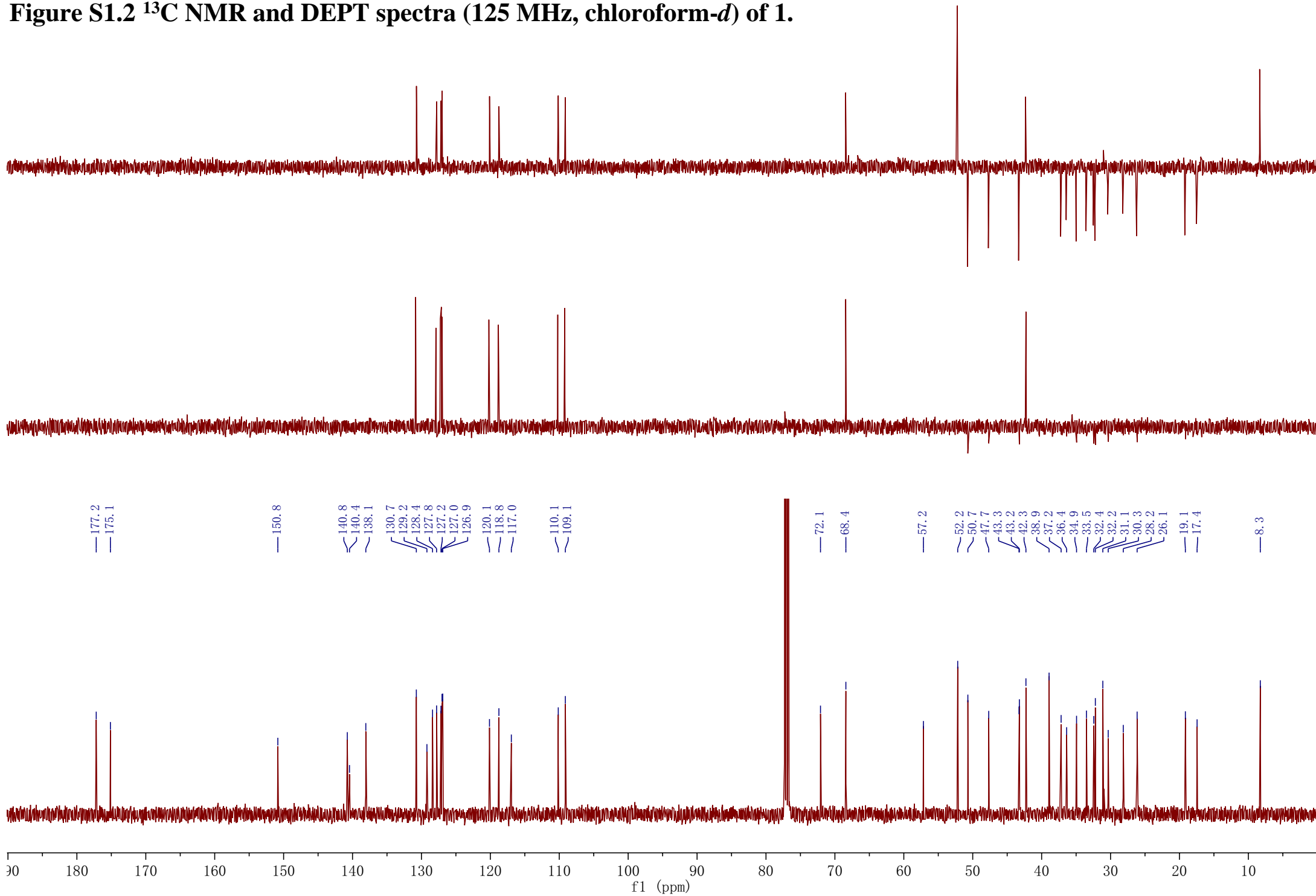


Figure S1.3 HSQC (500 MHz, chloroform-*d*) of **1**.

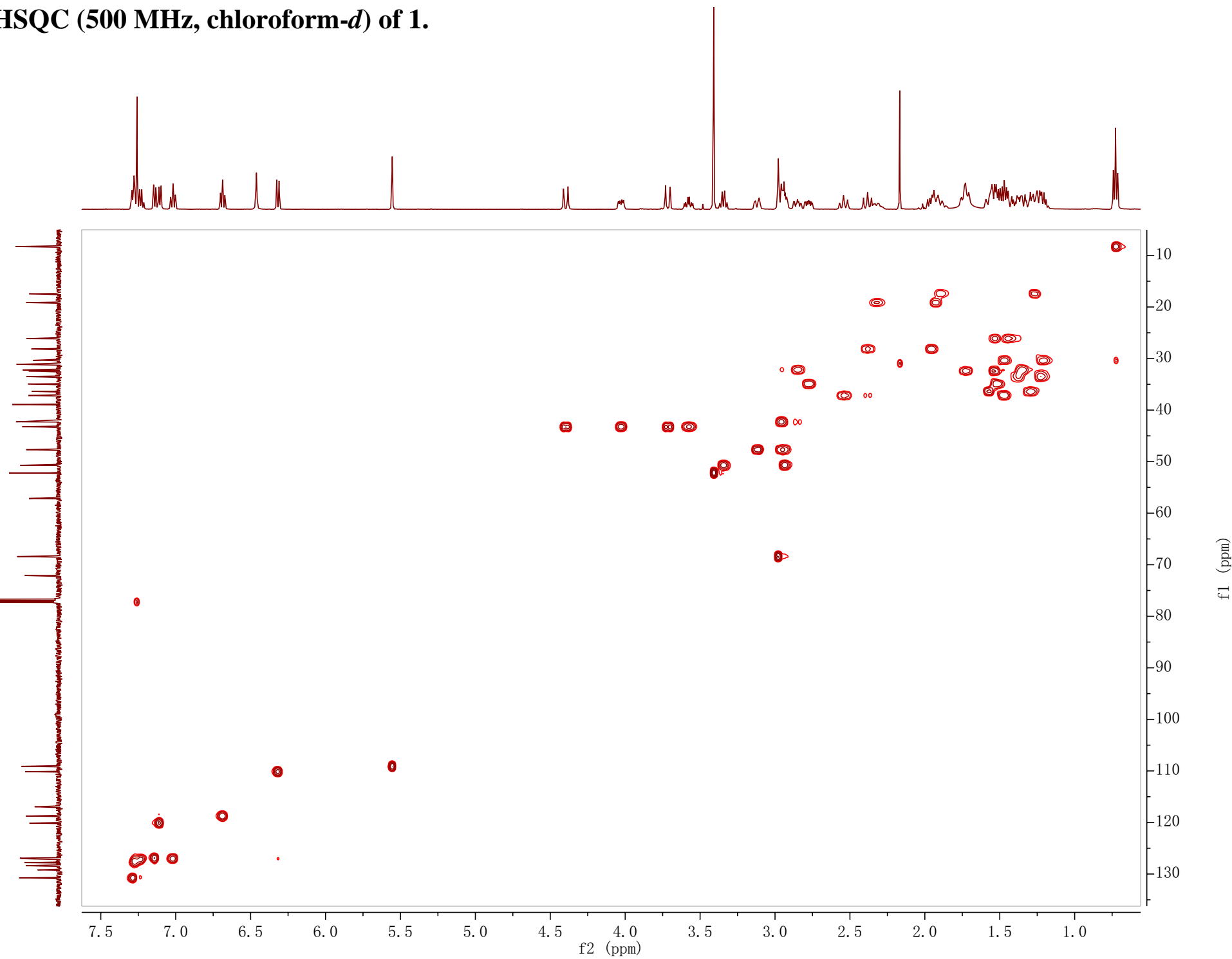


Figure S1.4 ^1H - ^1H COSY (500 MHz, chloroform-*d*) of **1**.

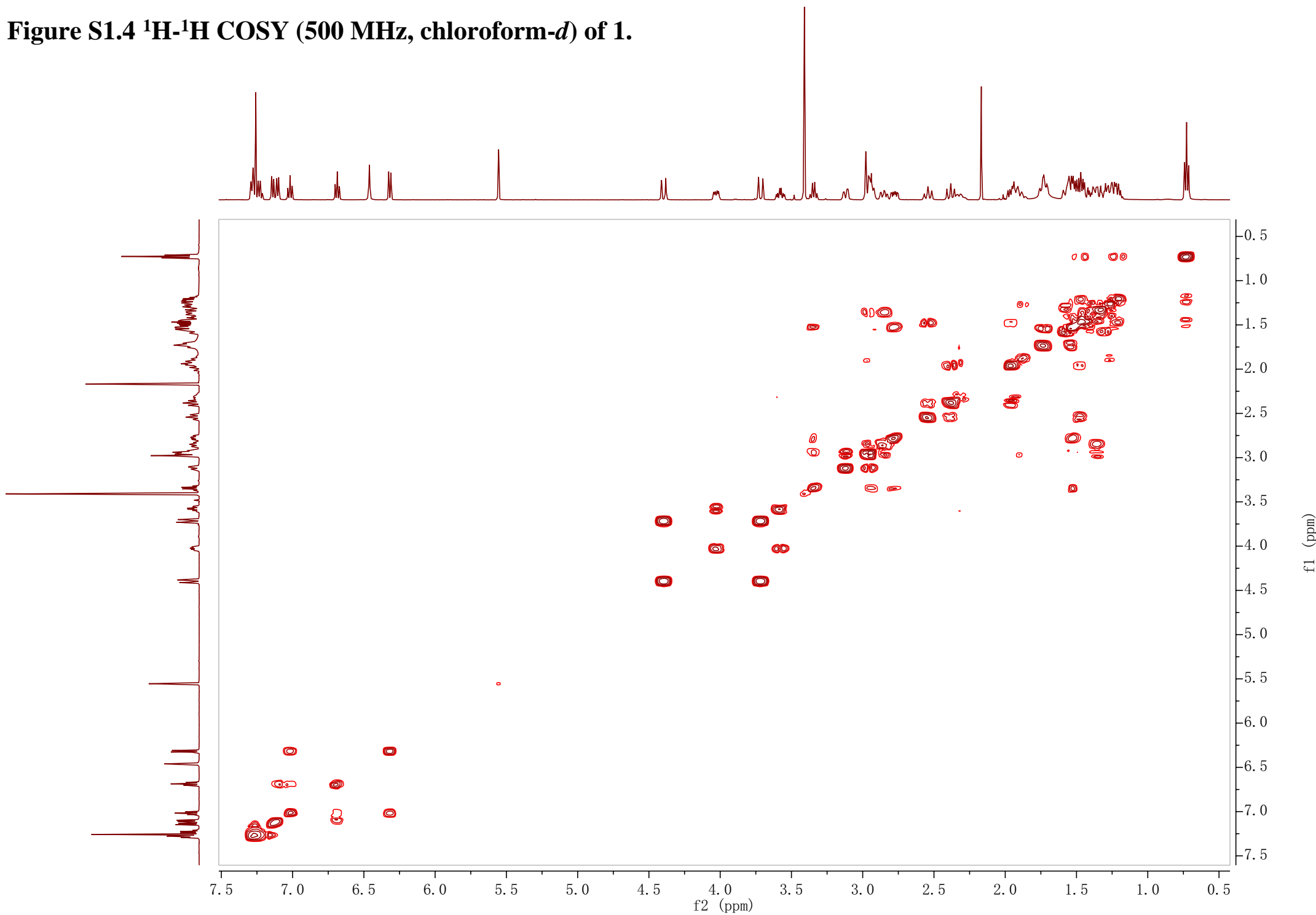


Figure S1.5 HMBC (500 MHz, chloroform-*d*) of 1.

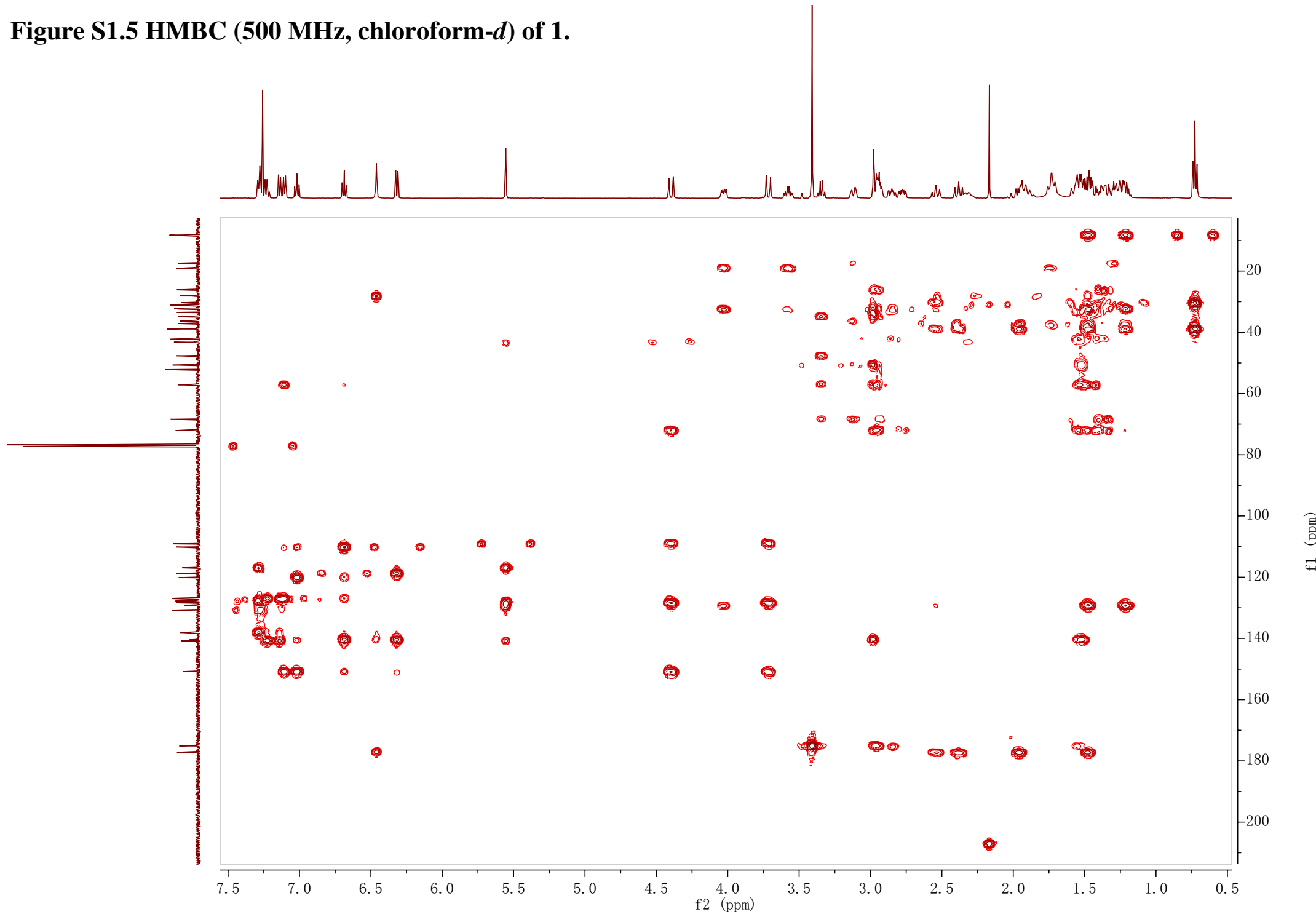


Figure S1.6 ROESY (500 MHz, chloroform-*d*) of 1.

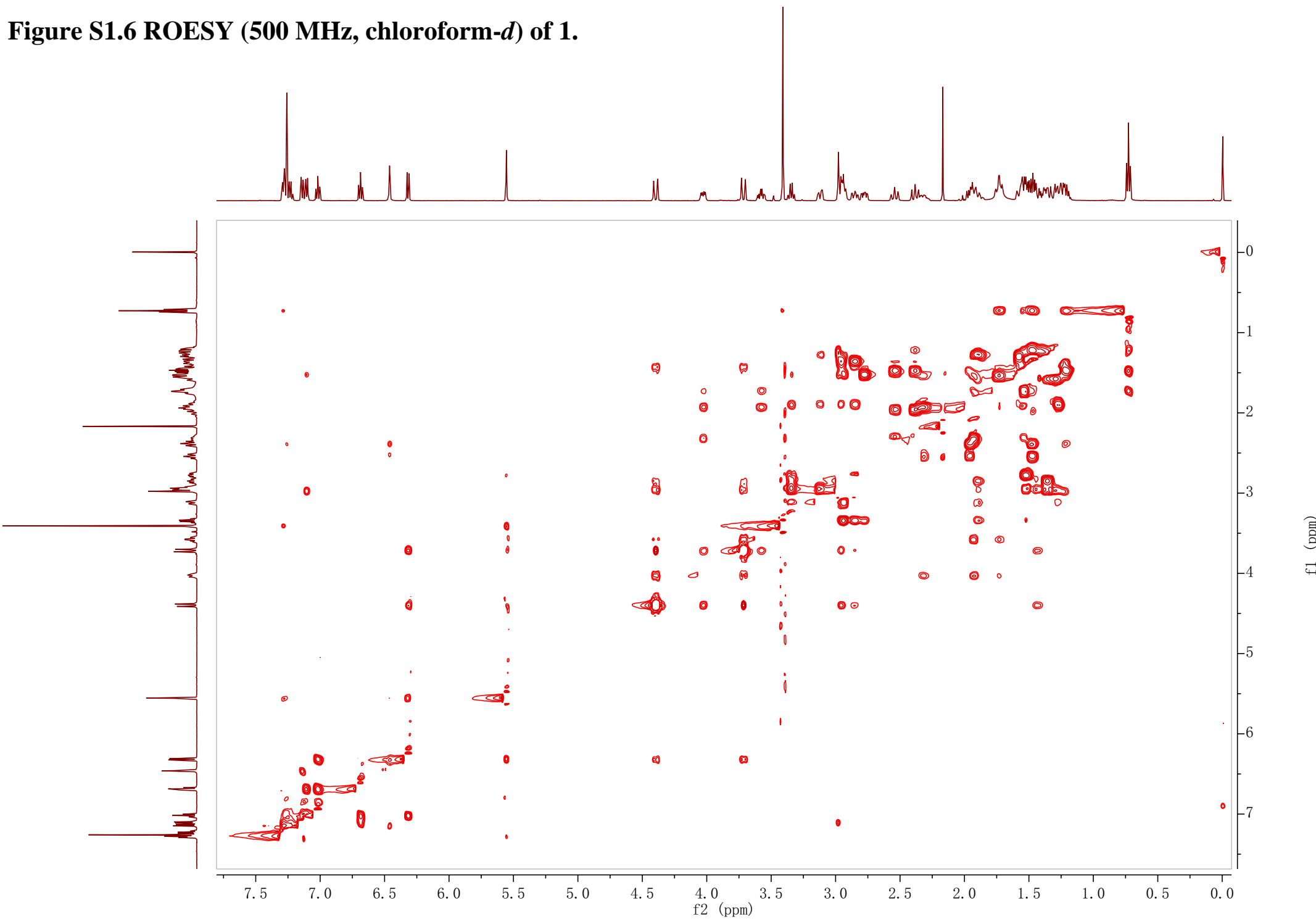


Figure S1.7 HRESIMS spectrum of 1.

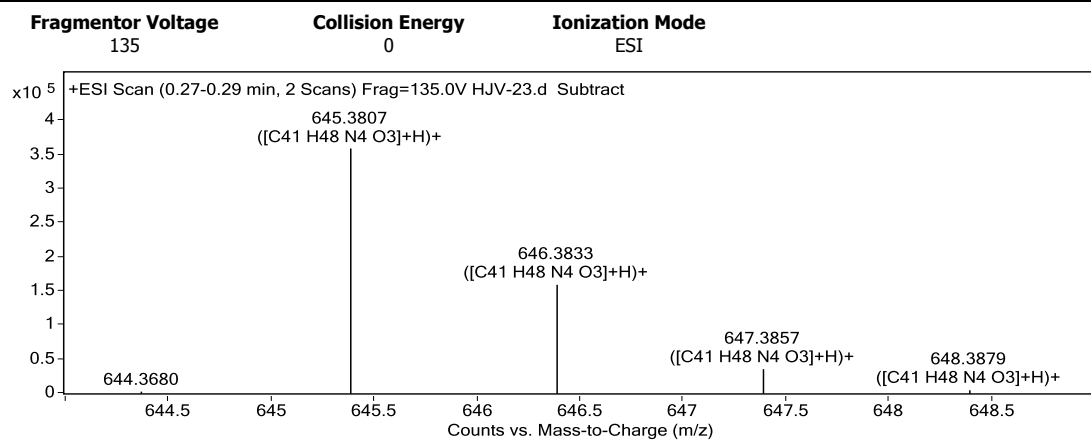
Qualitative Analysis Report

Data Filename	HJV-23.d	Sample Name	HJV-23
Sample Type	Sample	Position	P1-A2
Instrument Name	Instrument 1	User Name	
Acq Method	s.m	Acquired Time	9/26/2019 3:02:00 PM
IRM Calibration Status	Success	DA Method	Default.m

Comment

Sample Group Info.
Acquisition SW 6200 series TOF/6500 series
Version Q-TOF B.05.01 (B5125.2)

User Spectra



Peak List

m/z	z	Abund	Formula	Ion
74.0969	1	6977.53		
307.1808	1	39020.12		
308.1836	1	8186.93		
339.2071	1	51117.36		
340.2103	1	12114.92		
388.2067	2	4867.96		
645.3807	1	359329.5	C ₄₁ H ₄₈ N ₄ O ₃	(M+H) ⁺
646.3833	1	160601.97	C ₄₁ H ₄₈ N ₄ O ₃	(M+H) ⁺
647.3857	1	36542.01	C ₄₁ H ₄₈ N ₄ O ₃	(M+H) ⁺
648.3879	1	6258.97	C ₄₁ H ₄₈ N ₄ O ₃	(M+H) ⁺

Formula Calculator Element Limits

Element	Min	Max
C	3	60
H	0	120
O	0	30
N	0	8

Formula Calculator Results

Formula	CalculatedMass	CalculatedMz	Mz	Diff. (mDa)	Diff. (ppm)	DBE
C ₄₁ H ₄₈ N ₄ O ₃	644.3726	645.3799	645.3807	-0.80	-1.24	20.0000

--- End Of Report ---

Figure S1.8 IR (KBr disk) spectrum of 1.

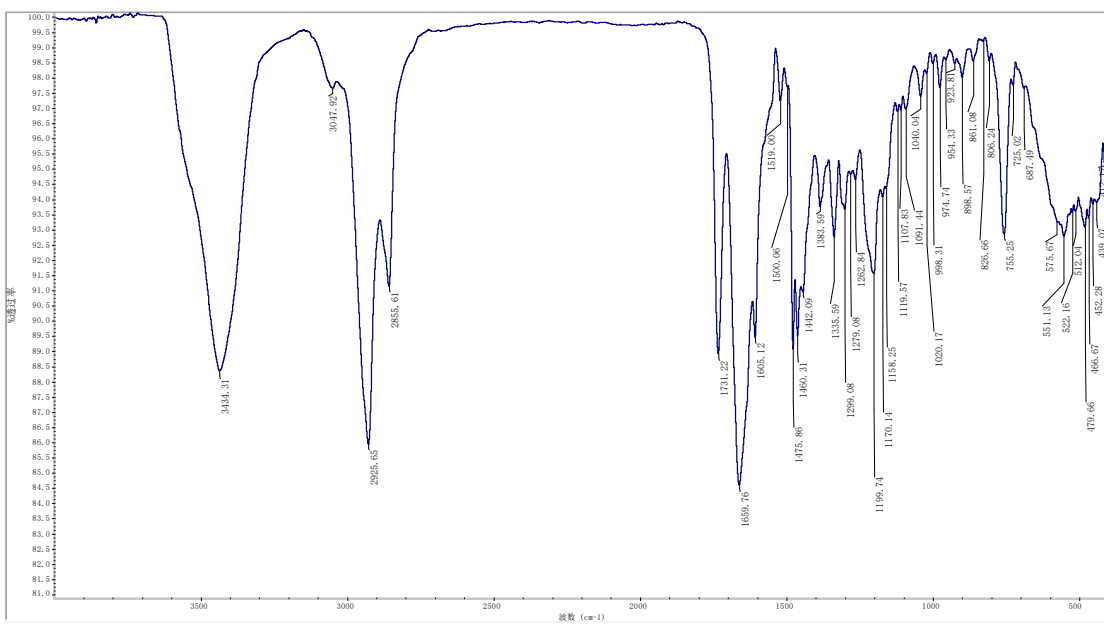
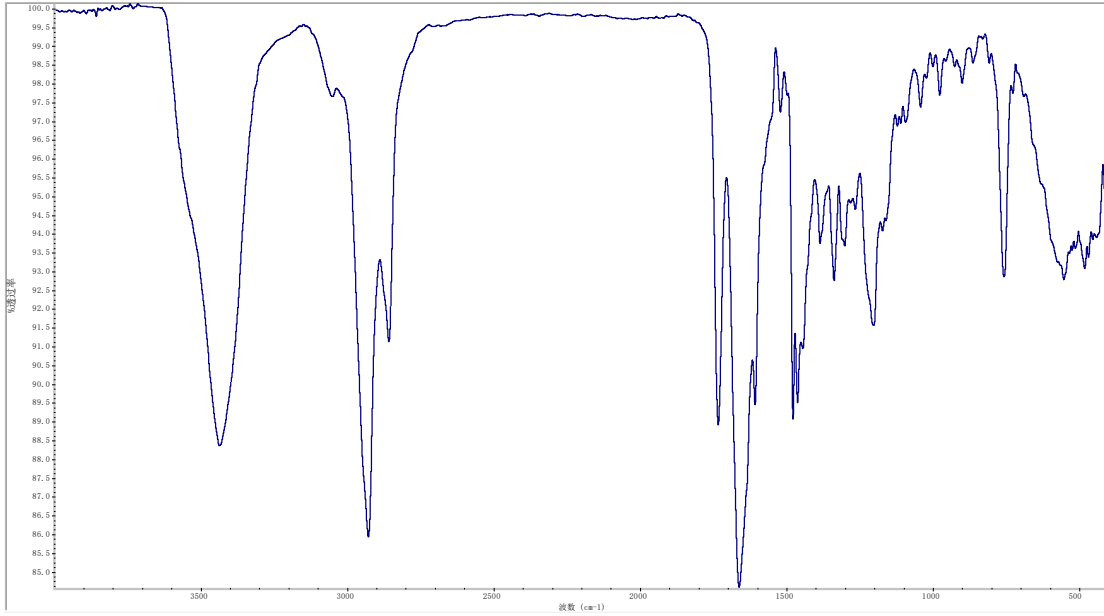


Figure S1.9 ECD spectrum of compound 1 in MeOH.

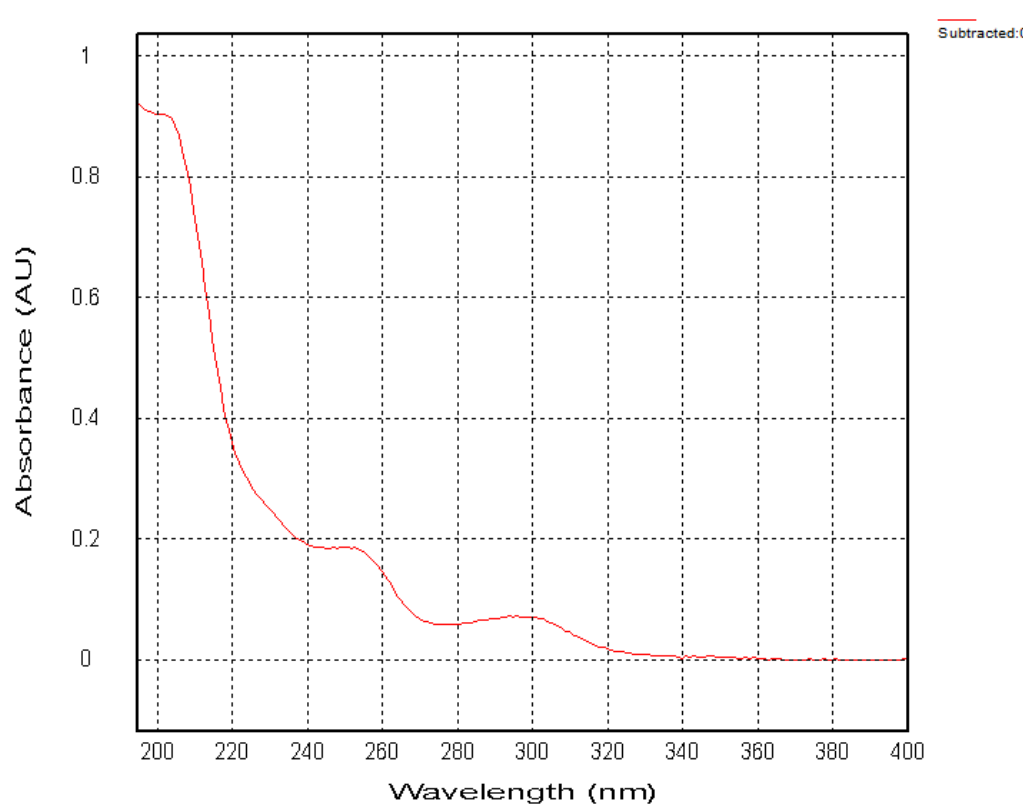
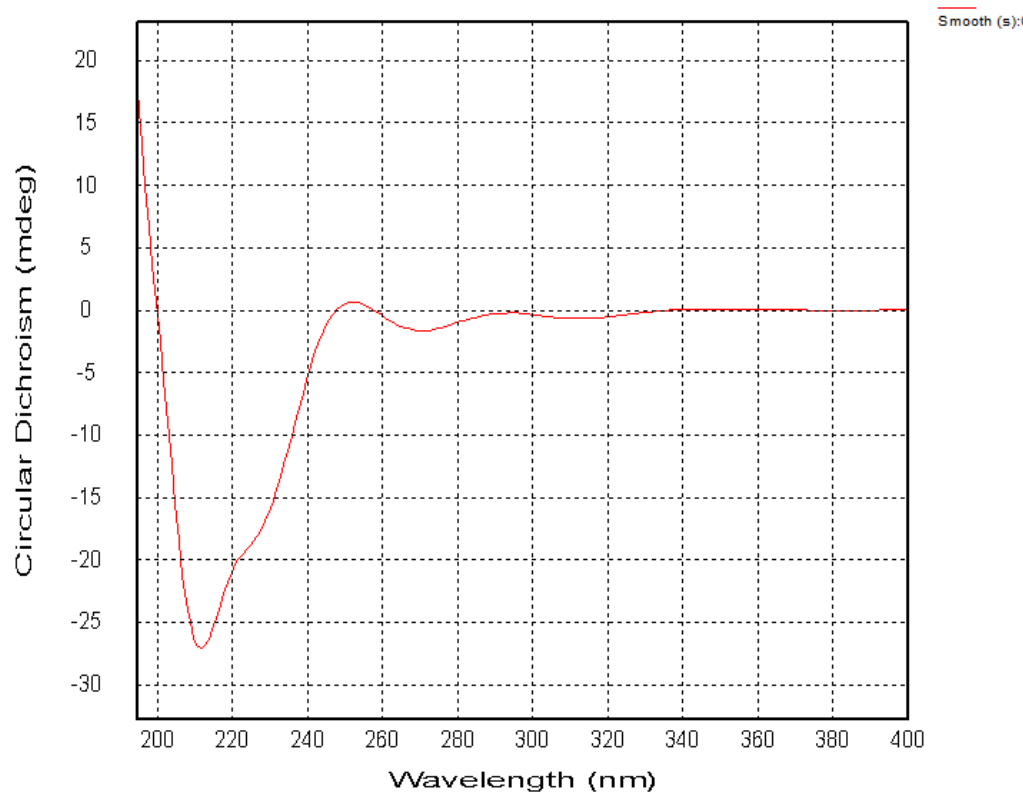
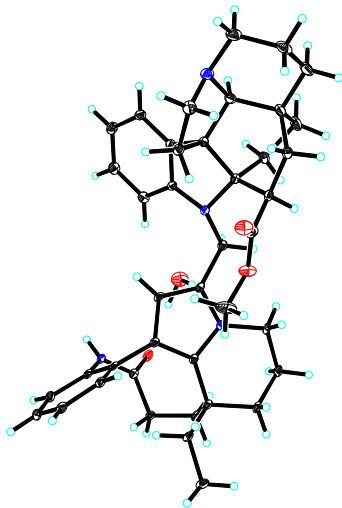


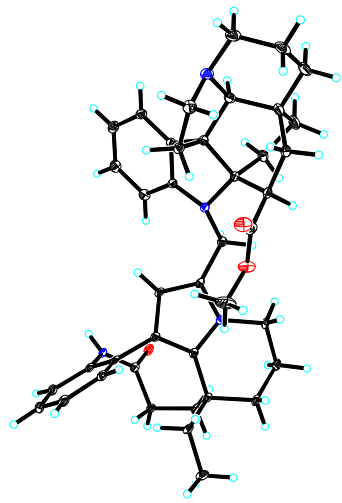
Figure S1.10 X-ray crystal structure of compound 1.

Crystal data for h23b: $C_{41}H_{48}N_4O_3 \cdot H_2O$, $M = 662.85$, $a = 8.3245(2)$ Å, $b = 16.4573(5)$ Å, $c = 25.0171(8)$ Å, $\alpha = 90^\circ$, $\beta = 90^\circ$, $\gamma = 90^\circ$, $V = 3427.31(17)$ Å 3 , $T = 100.2$ K, space group $P212121$, $Z = 4$, $\mu(\text{Cu K}\alpha) = 0.657$ mm $^{-1}$, 31679 reflections measured, 6722 independent reflections ($R_{int} = 0.0859$). The final R_I values were 0.0406 ($I > 2\sigma(I)$). The final $wR(F^2)$ values were 0.1014 ($I > 2\sigma(I)$). The final R_I values were 0.0492 (all data). The final $wR(F^2)$ values were 0.1050 (all data). The goodness of fit on F^2 was 1.058. Flack parameter = 0.01(12).



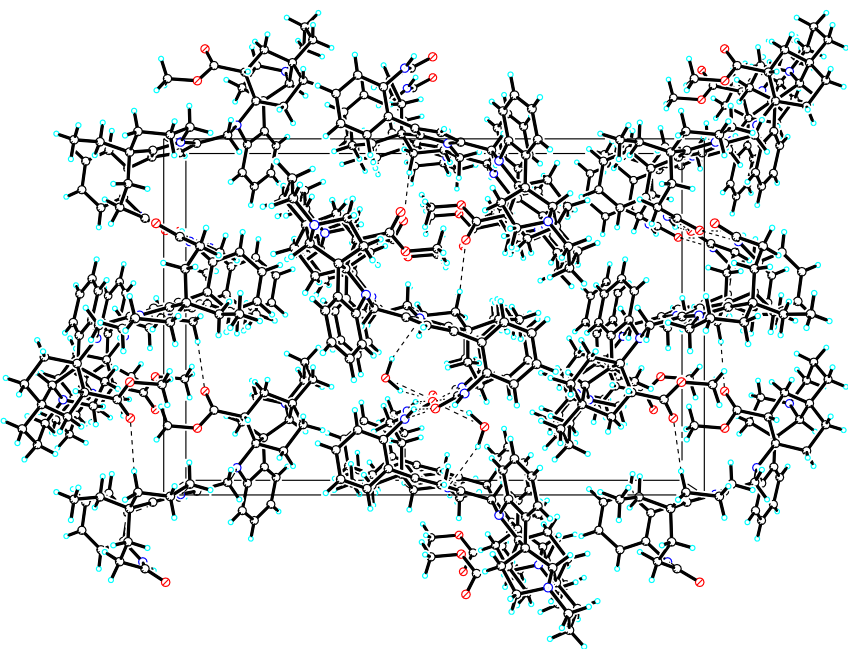
View of the molecules in an asymmetric unit.

Displacement ellipsoids are drawn at the 30% probability level.



View of a molecule of h23b with the atom-labelling scheme.

Displacement ellipsoids are drawn at the 30% probability level.



View of the pack drawing of h23b.

Hydrogen-bonds are shown as dashed lines.

Table 1. Crystal data and structure refinement for h23b_0m.

Identification code	global	
Empirical formula	C41 H50 N4 O4	
Formula weight	662.85	
Temperature	100(2) K	
Wavelength	1.54178 Å	
Crystal system	Orthorhombic	
Space group	P2 ₁ 2 ₁ 2 ₁	
Unit cell dimensions	a = 8.3245(2) Å b = 16.4573(5) Å c = 25.0171(8) Å	α= 90 ° β= 90 ° γ= 90 °
Volume	3427.31(17) Å ³	
Z	4	
Density (calculated)	1.285 Mg/m ³	
Absorption coefficient	0.657 mm ⁻¹	

F(000)	1424
Crystal size	0.540 x 0.150 x 0.090 mm ³
Theta range for data collection	3.21 to 72.11 °
Index ranges	-10<=h<=7, -20<=k<=20, -30<=l<=30
Reflections collected	31679
Independent reflections	6722 [R(int) = 0.0859]
Completeness to theta = 72.11 °	99.9 %
Absorption correction	Semi-empirical from equivalents
Max. and min. transmission	0.94 and 0.64
Refinement method	Full-matrix least-squares on F ²
Data / restraints / parameters	6722 / 0 / 444
Goodness-of-fit on F ²	1.058
Final R indices [I>2sigma(I)]	R1 = 0.0406, wR2 = 0.1014
R indices (all data)	R1 = 0.0492, wR2 = 0.1050
Absolute structure parameter	0.01(12)
Largest diff. peak and hole	0.274 and -0.342 e.Å ⁻³



Figure S2.1 ^1H NMR (500 MHz, methanol- d_4) of 2.

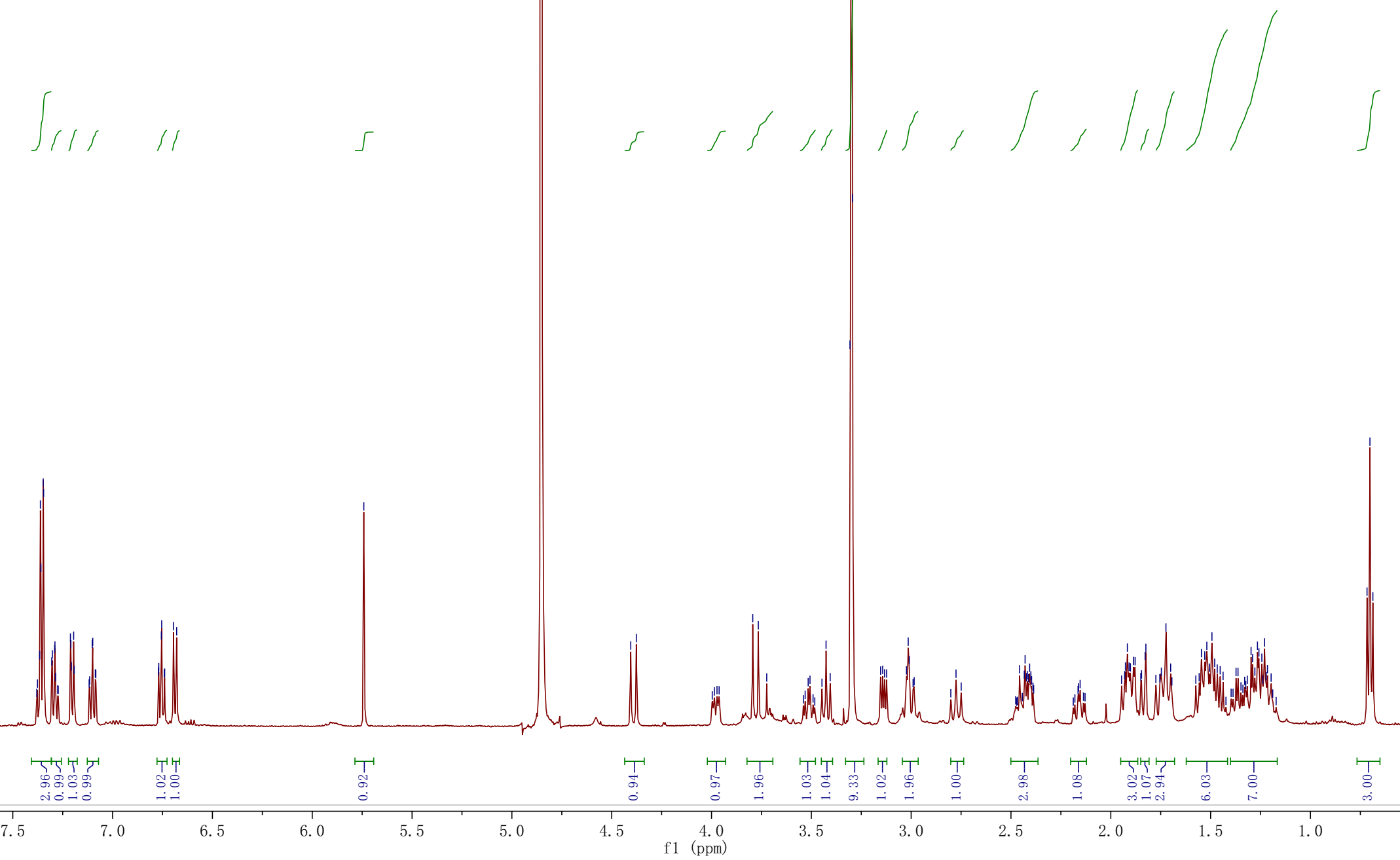


Figure S2.2 ^{13}C NMR and DEPT spectra (125 MHz, methanol- d_4) of 2.

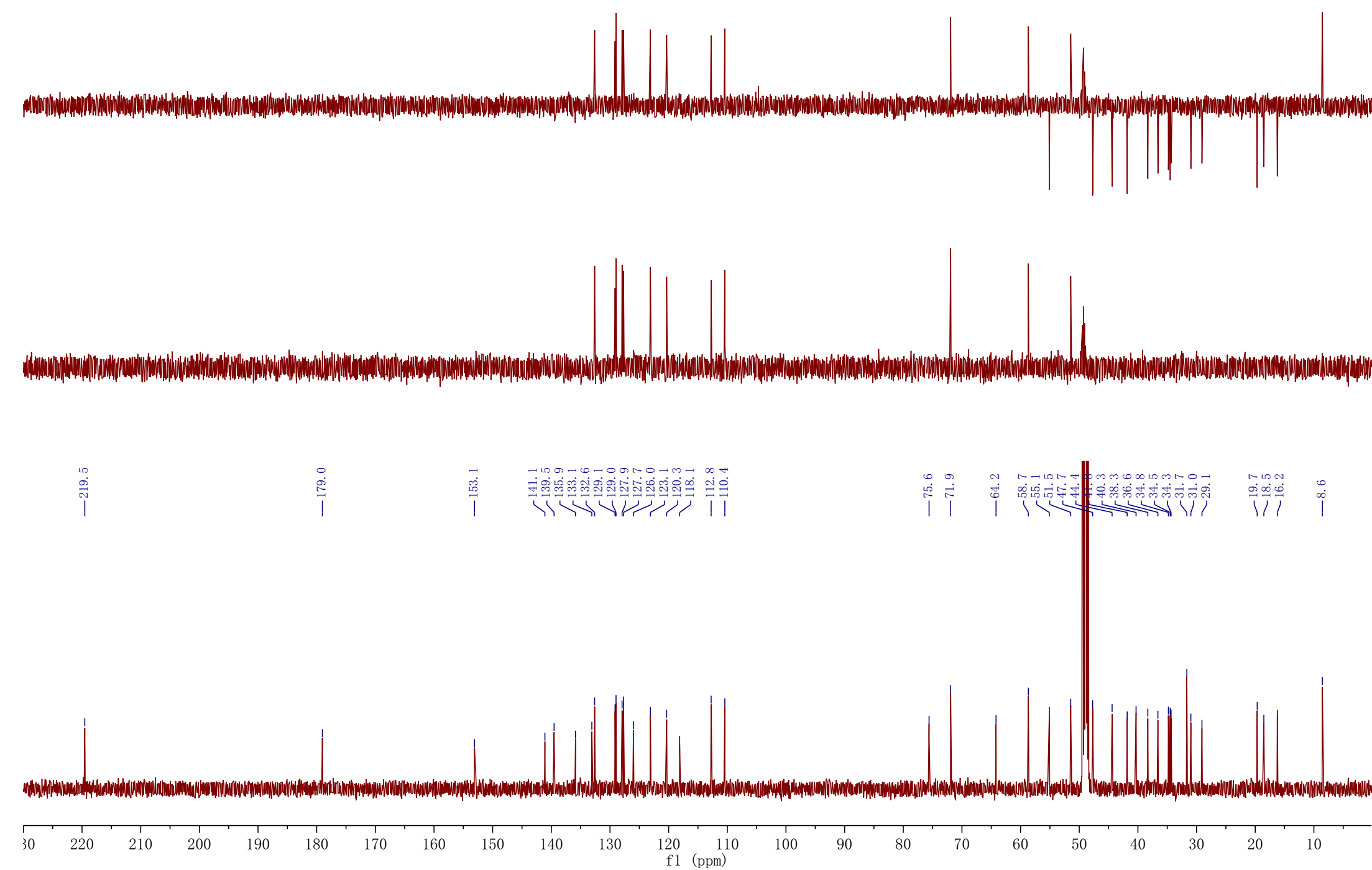


Figure S2.3 HSQC (500 MHz, methanol-*d*₄) of **2**.

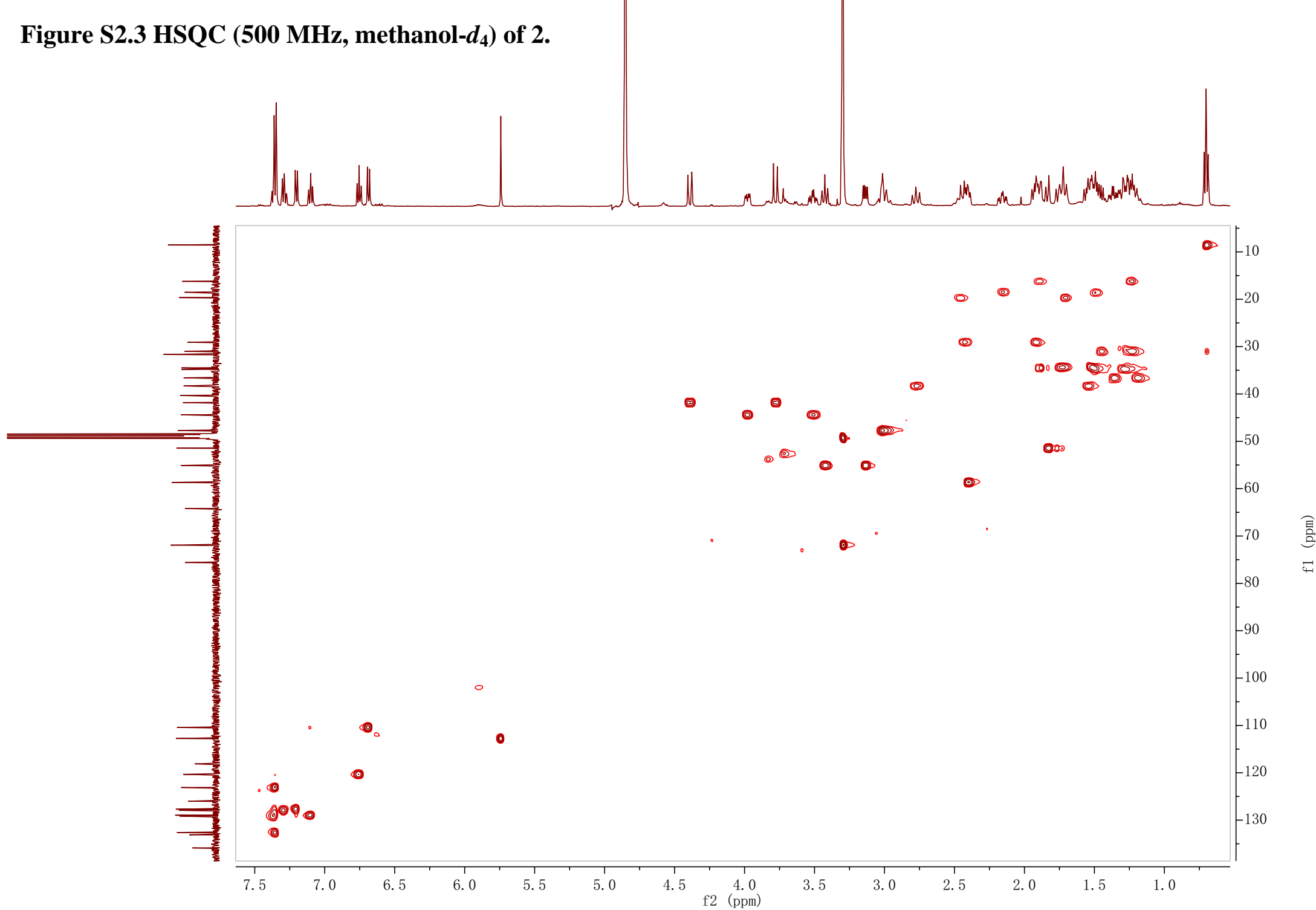


Figure S2.4 ^1H - ^1H COSY (500 MHz, methanol- d_4) of 2.

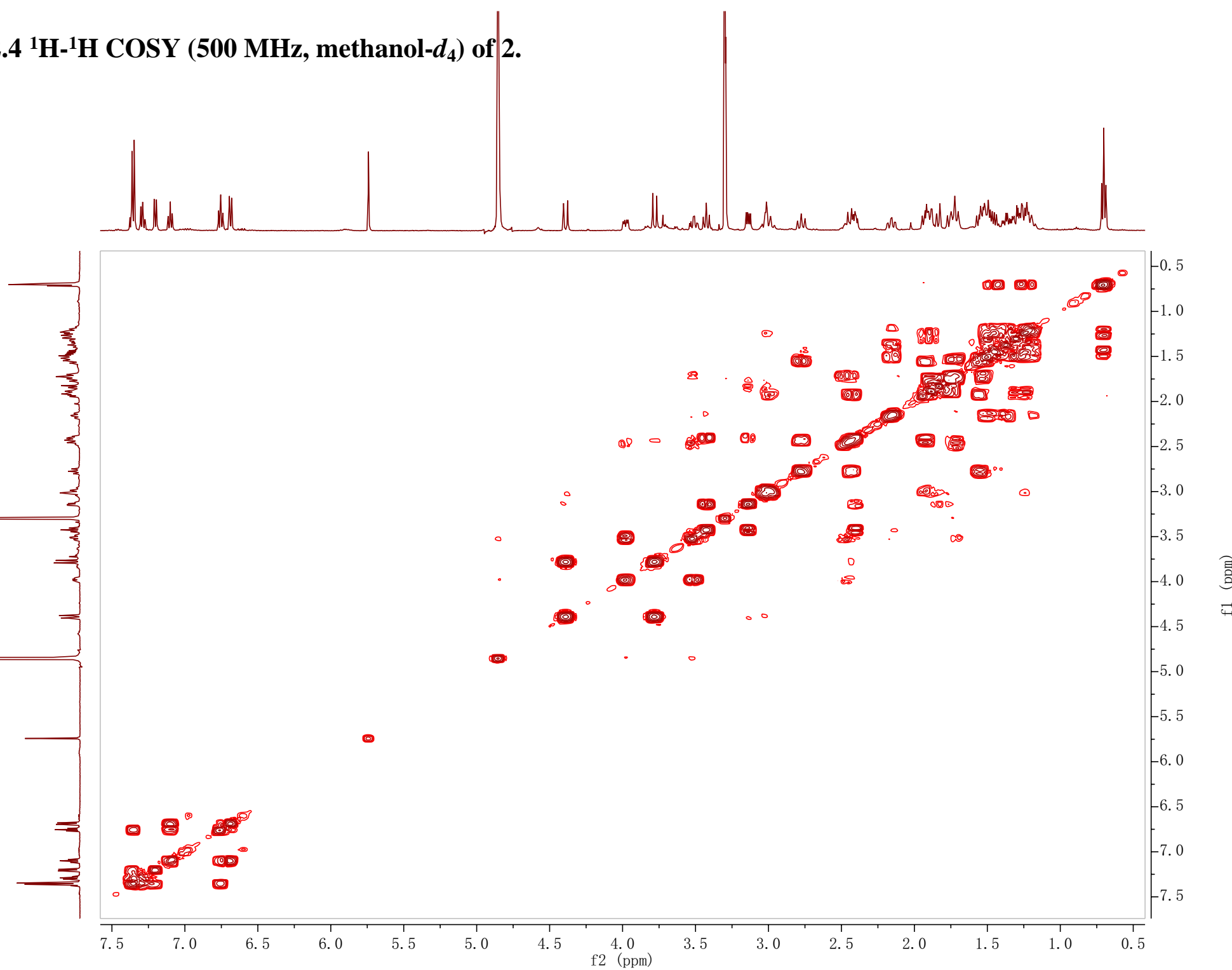


Figure S2.5 HMBC (500 MHz, methanol-*d*₄) of 2.

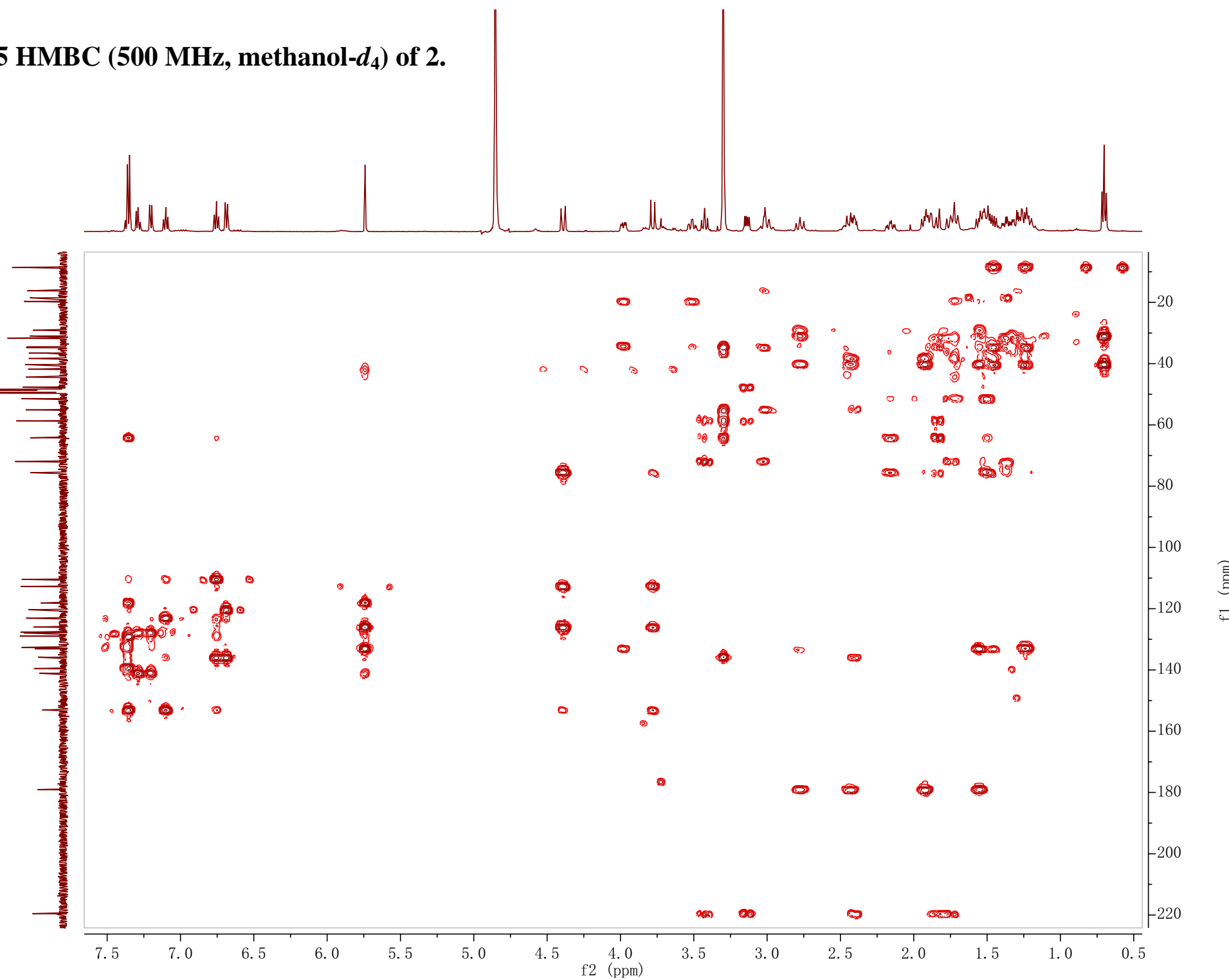


Figure S2.6 ROESY (500 MHz, methanol-*d*₄) of 2.

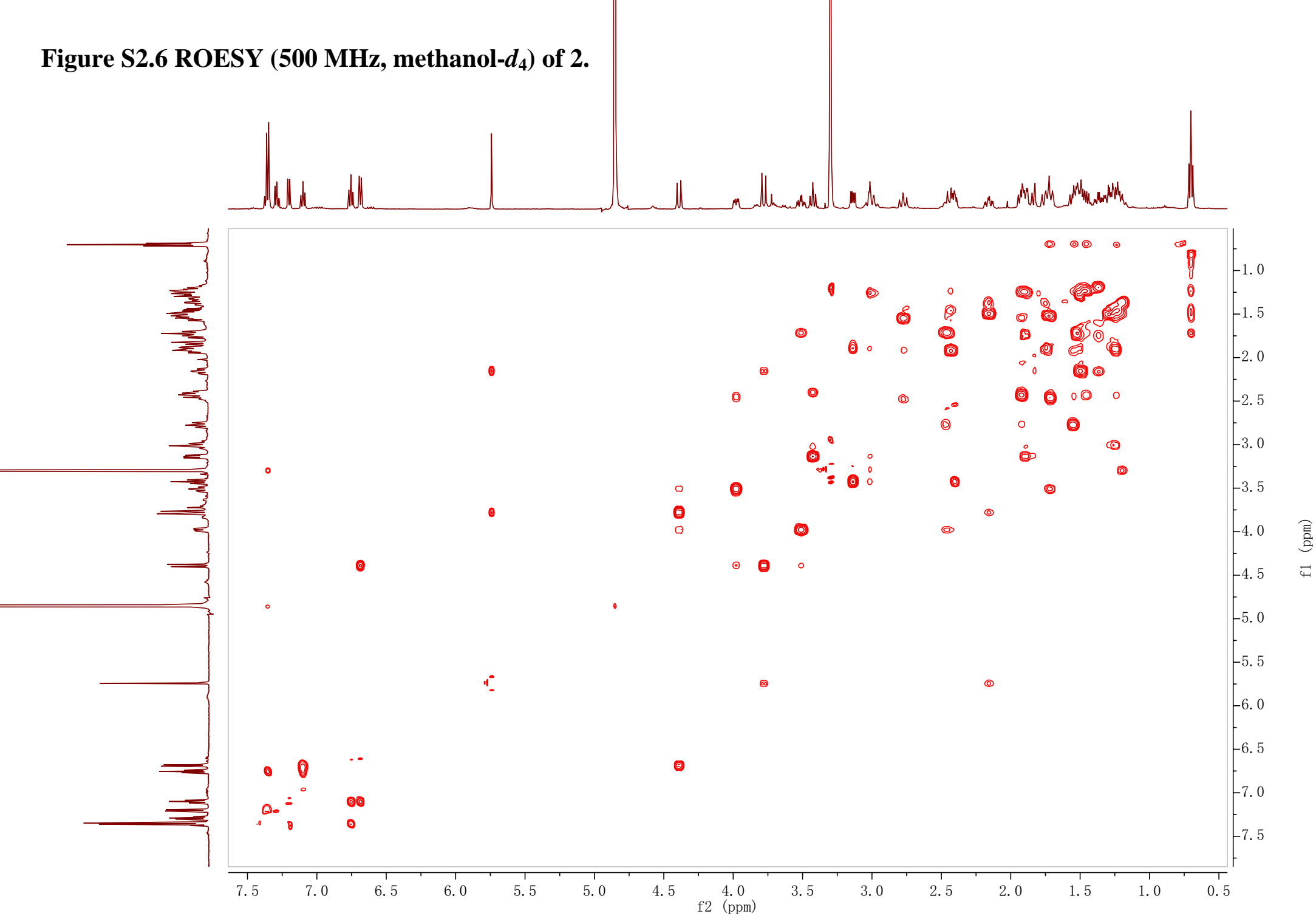


Figure S2.7 HRESIMS spectrum of 2.

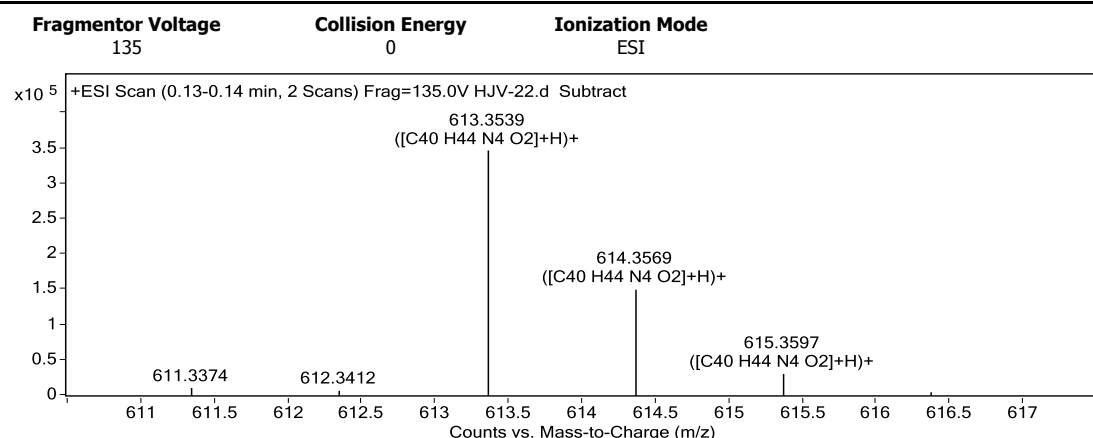
Qualitative Analysis Report

Data Filename	HJV-22.d	Sample Name	HJV-22
Sample Type	Sample	Position	P1-A1
Instrument Name	Instrument 1	User Name	
Acq Method	s.m	Acquired Time	9/26/2019 3:00:50 PM
IRM Calibration Status	Success	DA Method	Default.m

Comment

Sample Group Info.
Acquisition SW 6200 series TOF/6500 series
Version Q-TOF B.05.01 (B5125.2)

User Spectra



Peak List

m/z	z	Abund	Formula	Ion
307.1806	2	153839.06		
308.1836	2	32317.3		
613.3539	1	347138.31	C ₄₀ H ₄₄ N ₄ O ₂	(M+H) ⁺
614.3569	1	151580.75	C ₄₀ H ₄₄ N ₄ O ₂	(M+H) ⁺
615.3597	1	31622.09	C ₄₀ H ₄₄ N ₄ O ₂	(M+H) ⁺
635.335	1	50859.85		
636.3382	1	20327.78		
643.3641	1	34938.95		
1247.6805	1	32784.74		
1248.6834	1	26855.86		

Formula Calculator Element Limits

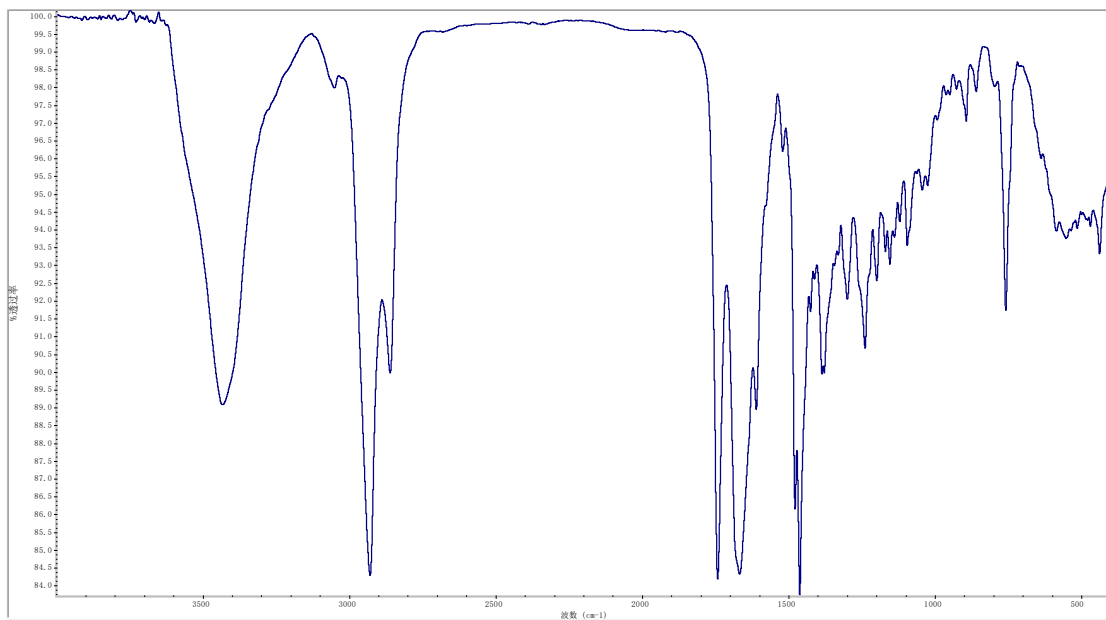
Element	Min	Max
C	3	60
H	0	120
O	0	30
N	0	8

Formula Calculator Results

Formula	CalculatedMass	CalculatedMz	Mz	Diff. (mDa)	Diff. (ppm)	DBE
C ₄₀ H ₄₄ N ₄ O ₂	612.3464	613.3537	613.3539	-0.20	-0.33	21.0000

--- End Of Report ---

Figure S2.8 IR (KBr disk) spectrum of 2.



Sample Name: HJV-22

KBr压片

采集时间: 星期五 6月 25 13:21:22 2021 (GMT+08:00)

仪器型号: NICOLET iS10

Software version: OMNIC 9.8.372

样品扫描次数: 16

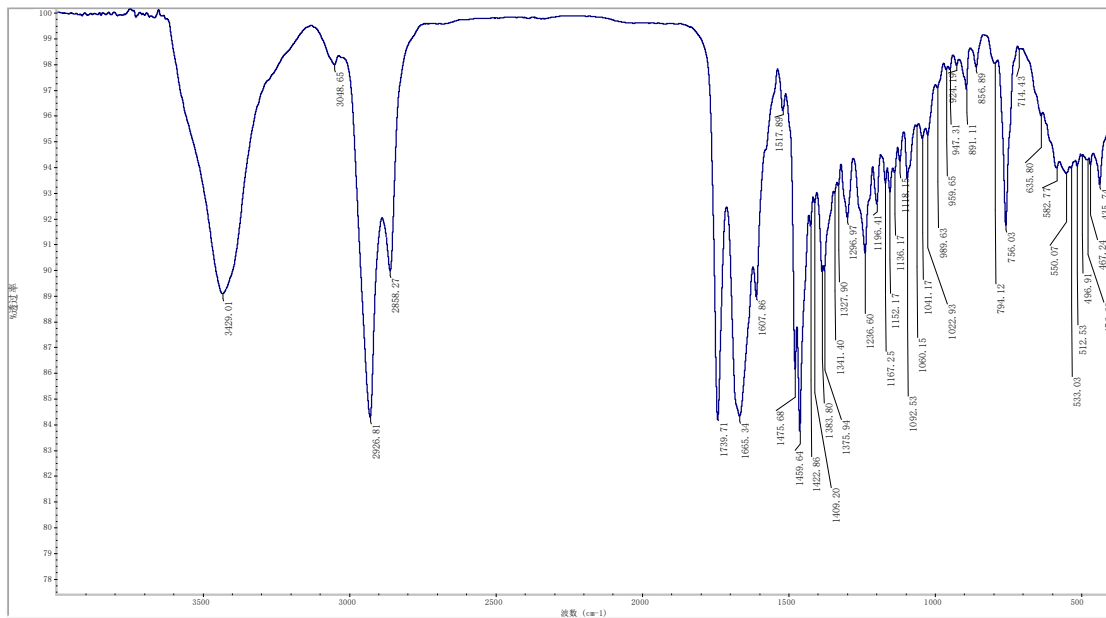
背景扫描次数: 16

分辨率: 4.000

采样增益: 1.0

动镜速度: 0.4747

光阑: 80.00



Sample Name: HJV-22

KBr压片

采集时间: 星期五 6月 25 13:21:22 2021 (GMT+08:00)

仪器型号: NICOLET iS10

Software version: OMNIC 9.8.372

样品扫描次数: 16

背景扫描次数: 16

分辨率: 4.000

采样增益: 1.0

动镜速度: 0.4747

光阑: 80.00

Figure S2.9 ECD spectrum of compound 2 in MeOH.

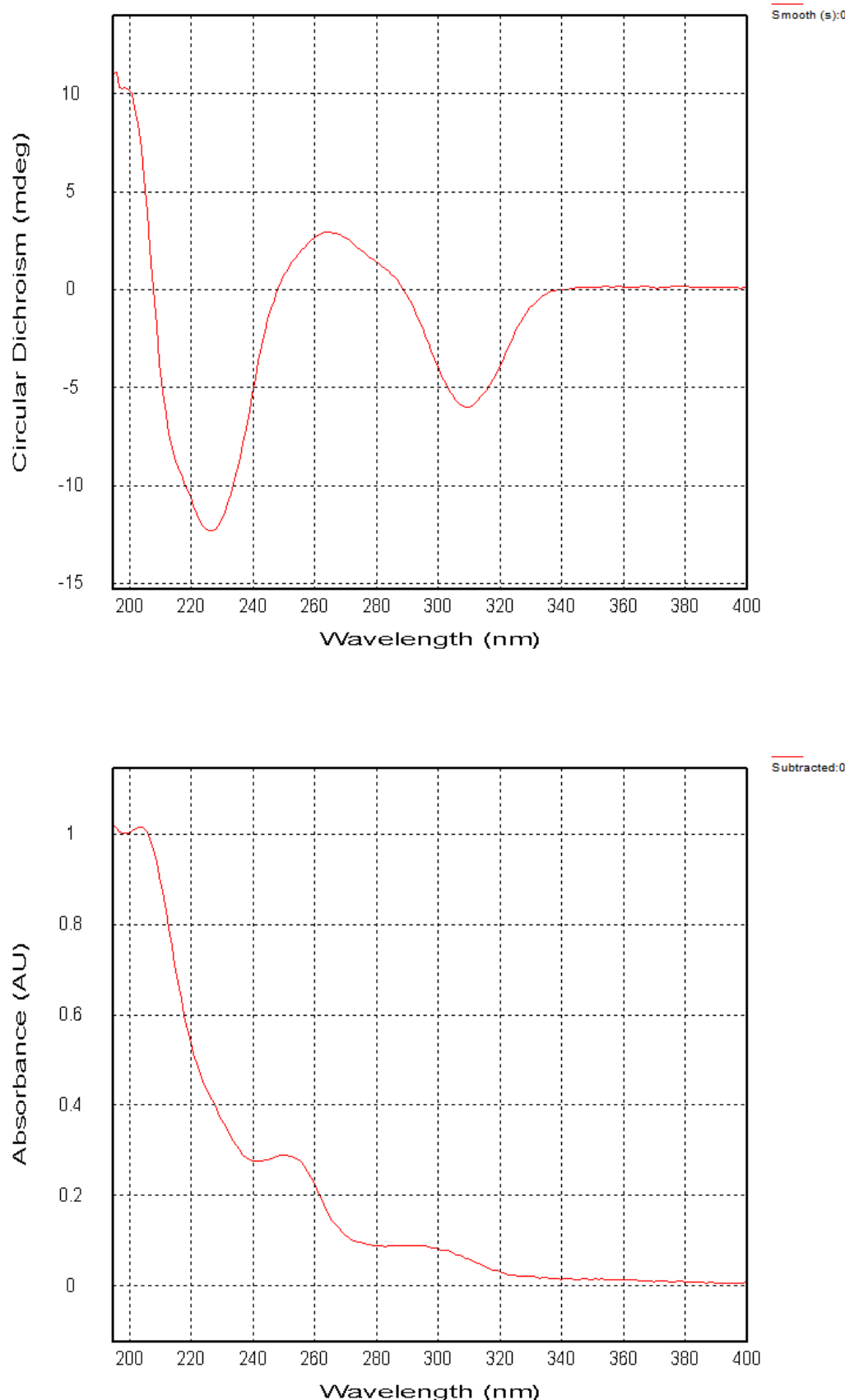
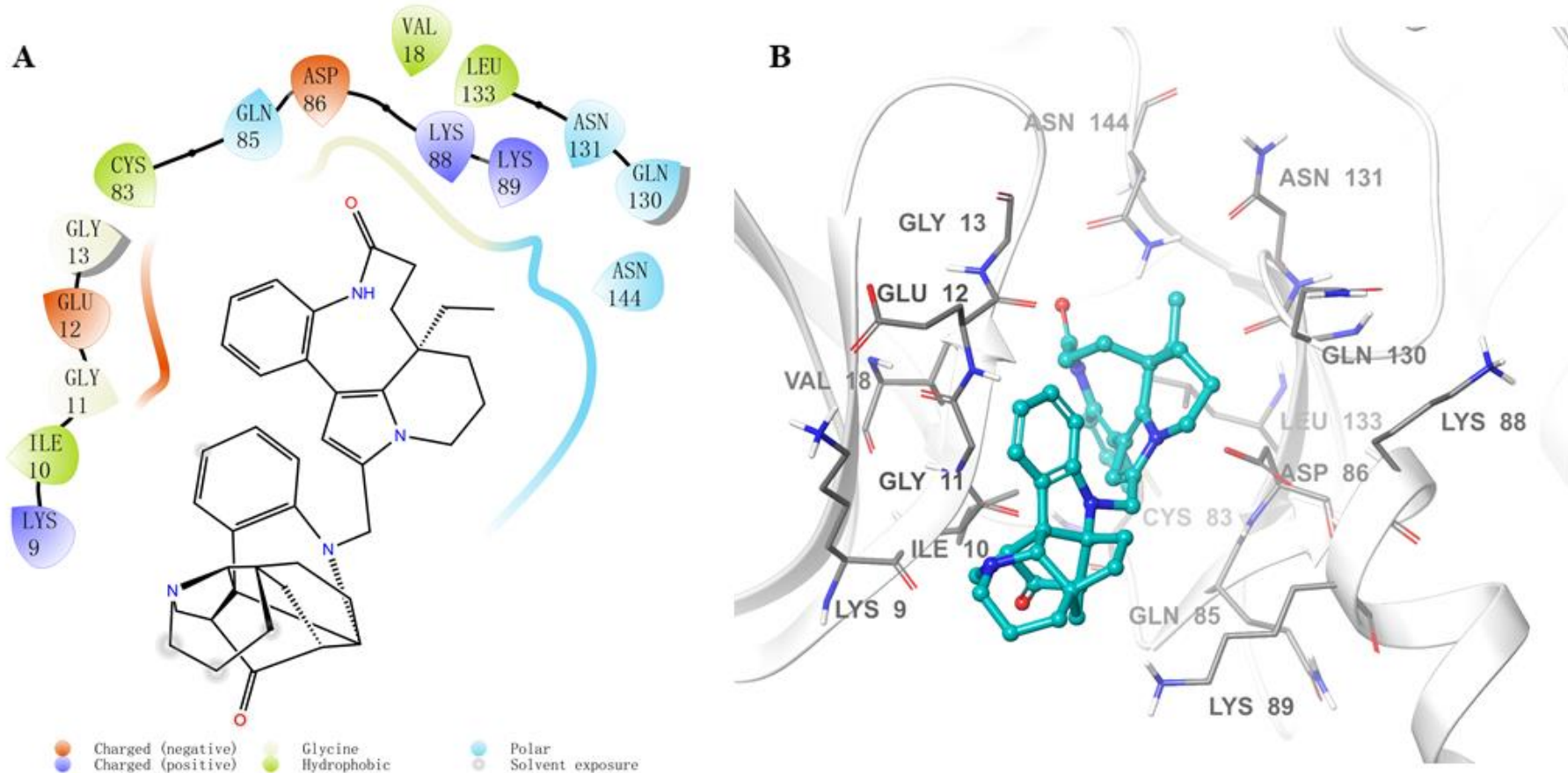


Figure S2.10 The molecular docking results of compound **2** with CDK5. (A) Two-dimensional ligand interaction diagram of compound **2** with the residues in the active site of CDK5. (B) Site view of the interactions observed between the residues in the active cavity of CDK5 and compound **2**.



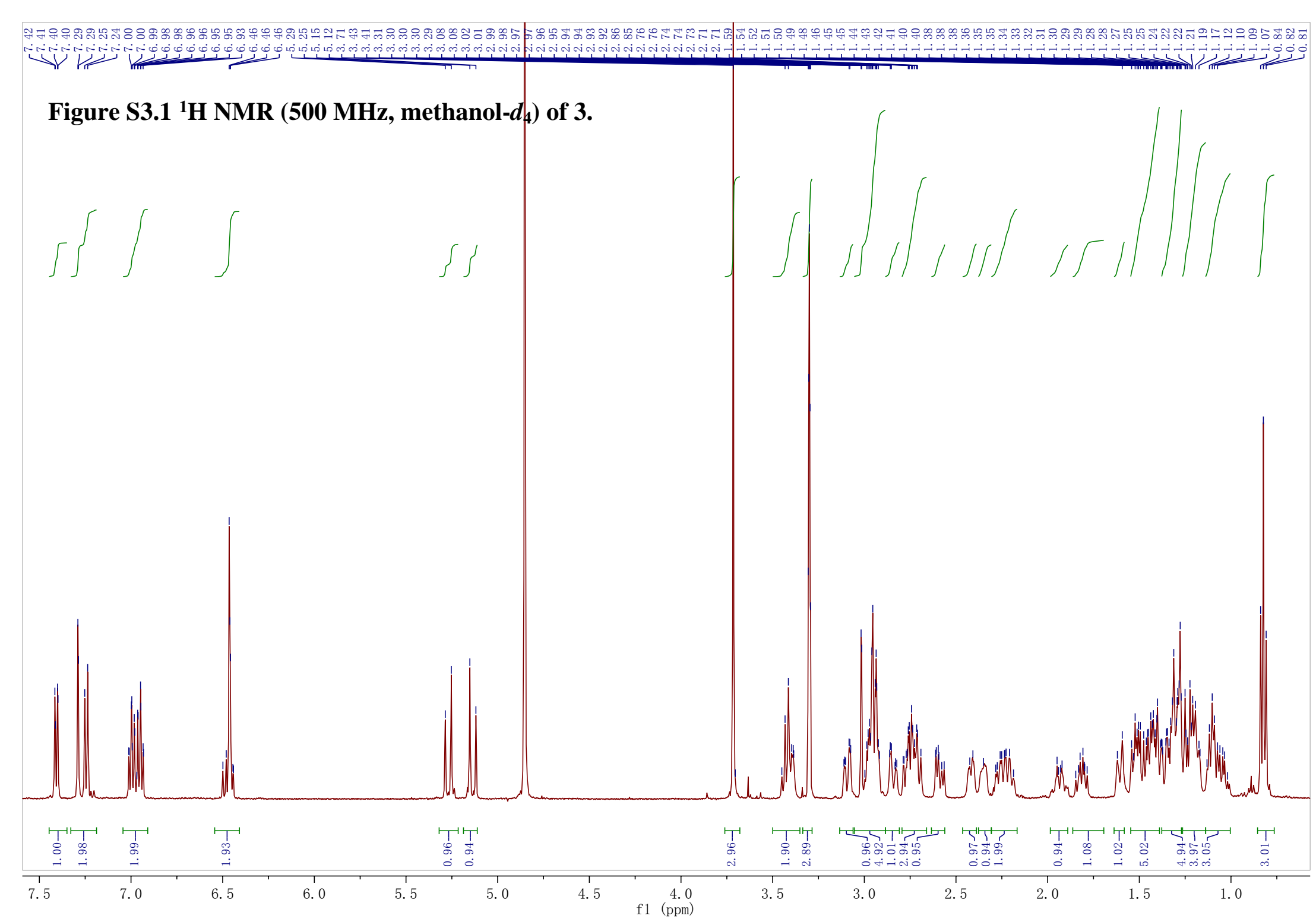


Figure S3.2 ^{13}C NMR and DEPT spectra (125 MHz, methanol- d_4) of 3.

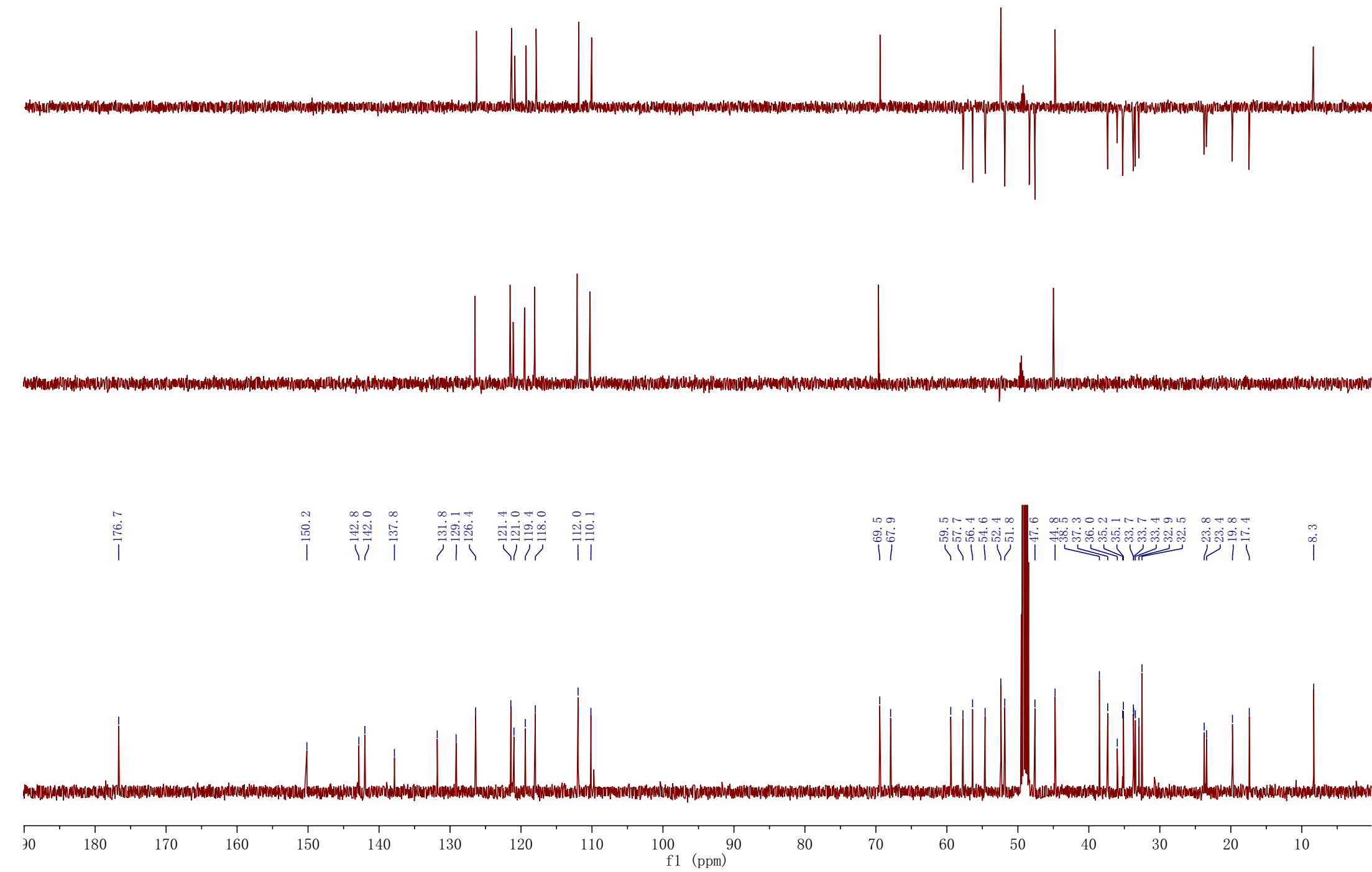


Figure S3.3. HSQC (500 MHz, methanol-*d*₄) of 3.

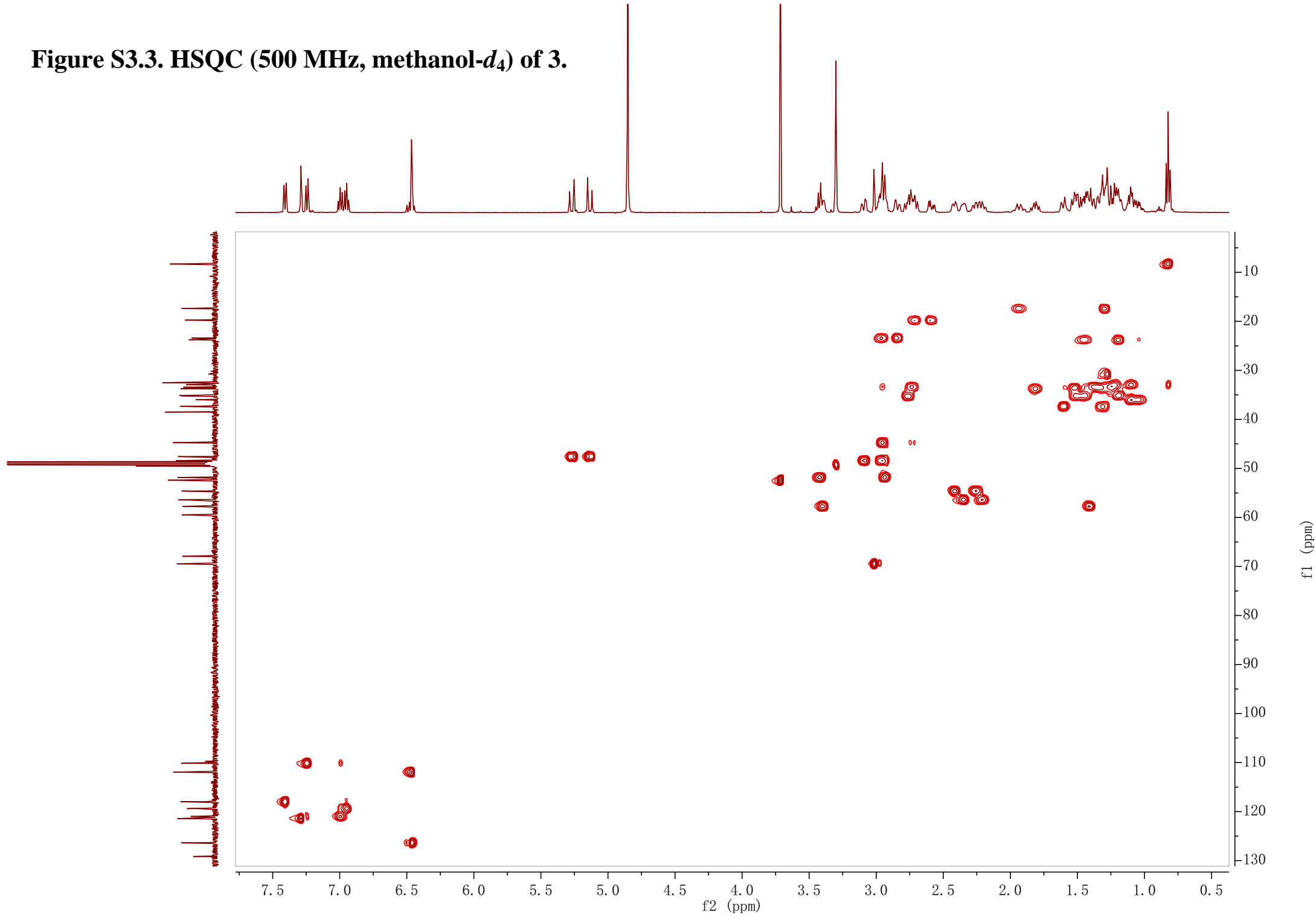


Figure S3.4 ^1H - ^1H COSY (500 MHz, methanol- d_4) of **3**.

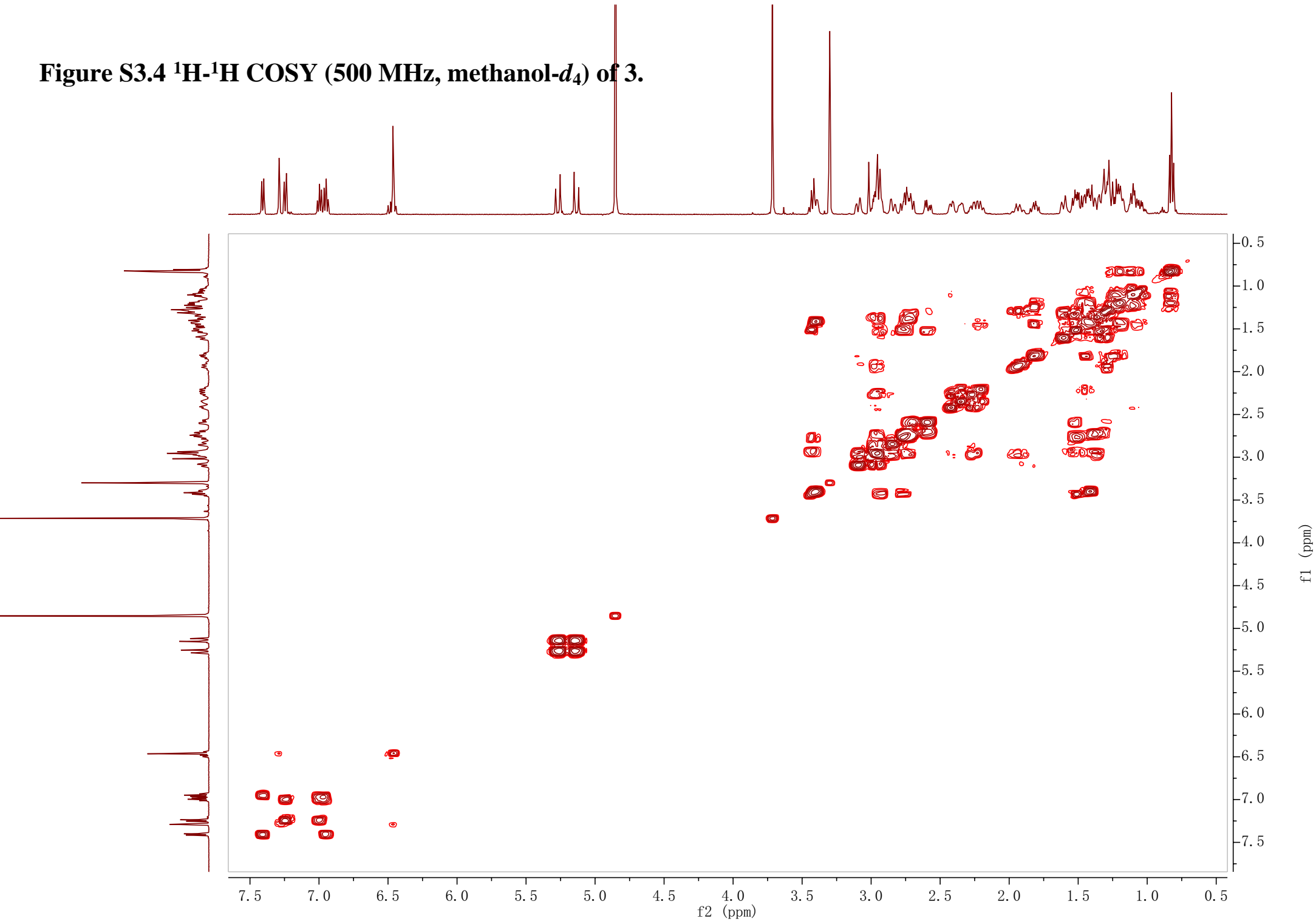


Figure S3.5 HMBC (500 MHz, methanol-*d*₄) of 3.

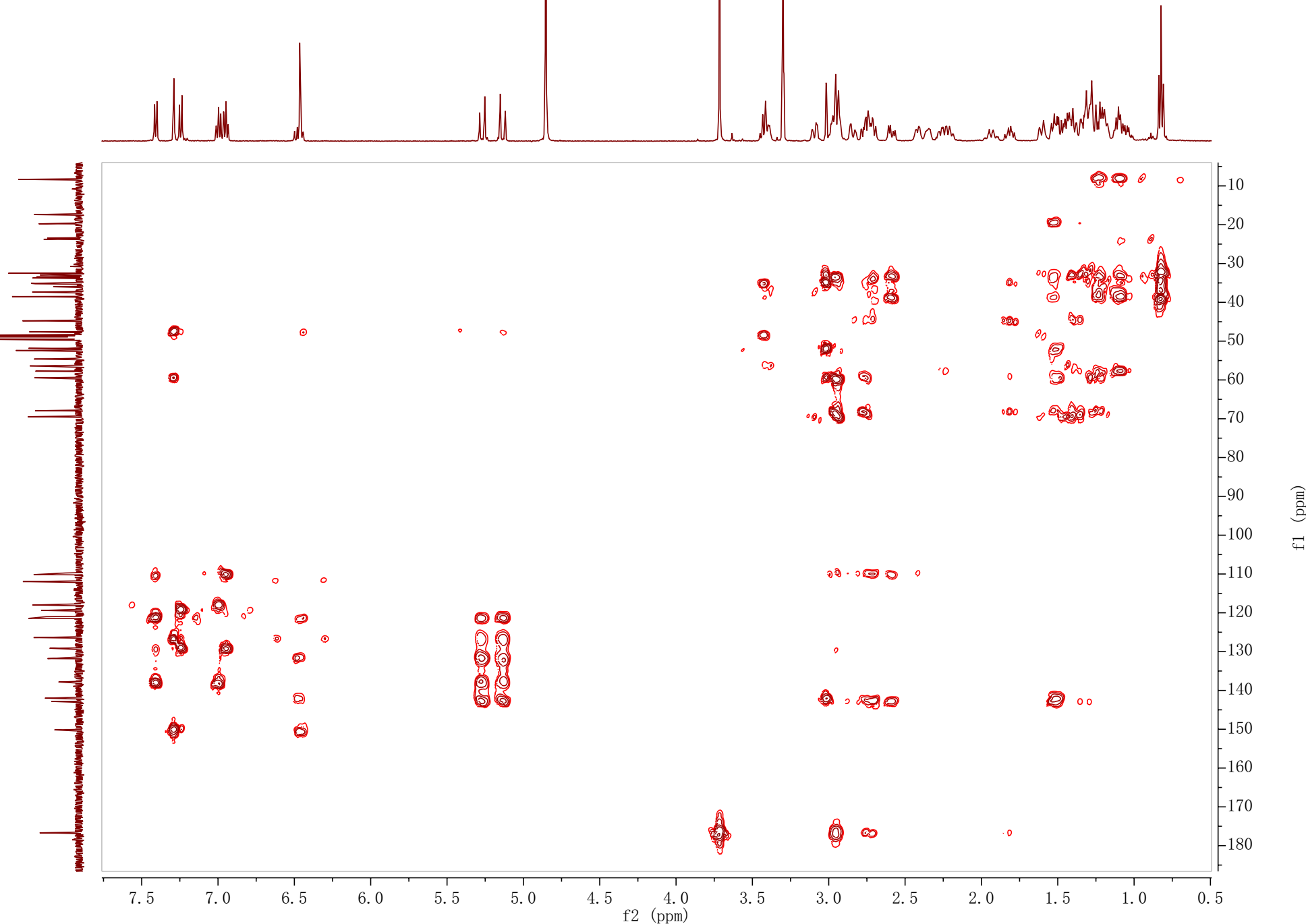


Figure S3.6 ROESY (500 MHz, methanol-*d*₄) of 3.

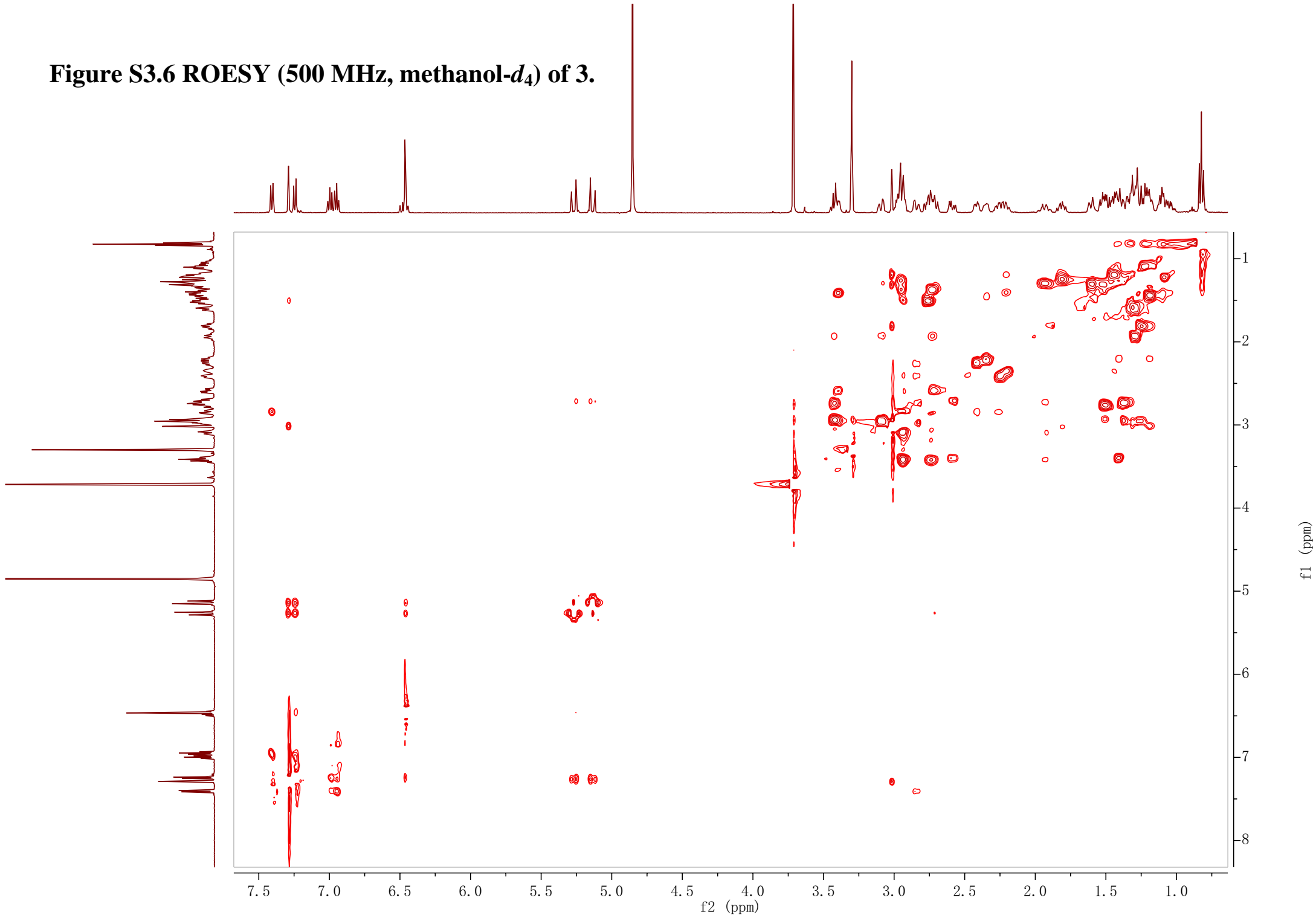


Figure S3.7 HRESIMS spectrum of 3.

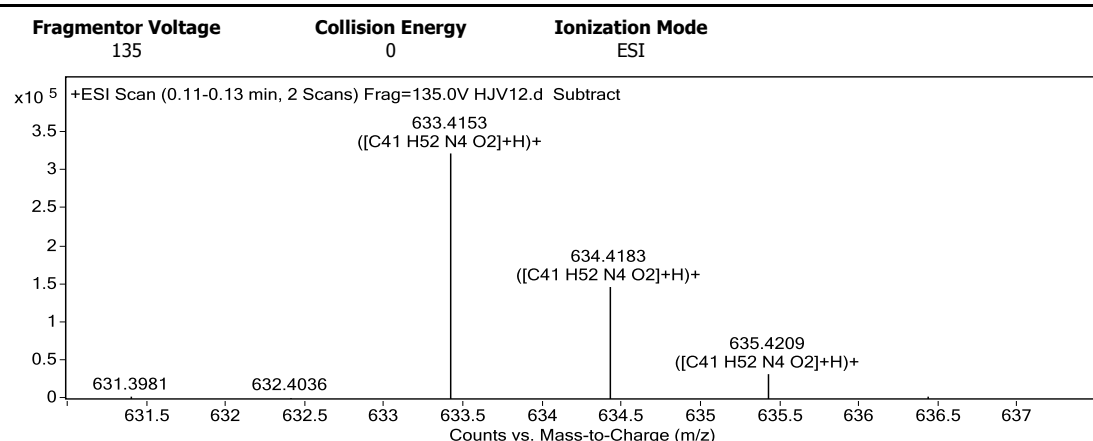
Qualitative Analysis Report

Data Filename	HJV12.d	Sample Name	HJV12
Sample Type	Sample	Position	P1-A8
Instrument Name	Instrument 1	User Name	
Acq Method	s.m	Acquired Time	8/5/2019 4:15:31 PM
IRM Calibration Status	Success	DA Method	Default.m

Comment

Sample Group Info.
Acquisition SW 6200 series TOF/6500 series
Version Q-TOF B.05.01 (B5125.2)

User Spectra



Peak List

m/z	z	Abund	Formula	Ion
317.2116	2	325584.34		
317.7129	2	162474.7		
318.2145	2	39909.68		
318.7154	2	5539.45		
633.4153	1	322475.75	C41 H52 N4 O2	(M+H)+
634.4183	1	147159.27	C41 H52 N4 O2	(M+H)+
635.4209	1	32267.08	C41 H52 N4 O2	(M+H)+
669.3907	1	7521.8		
671.3749	1	8166.5		
672.3784	1	4729.32		

Formula Calculator Element Limits

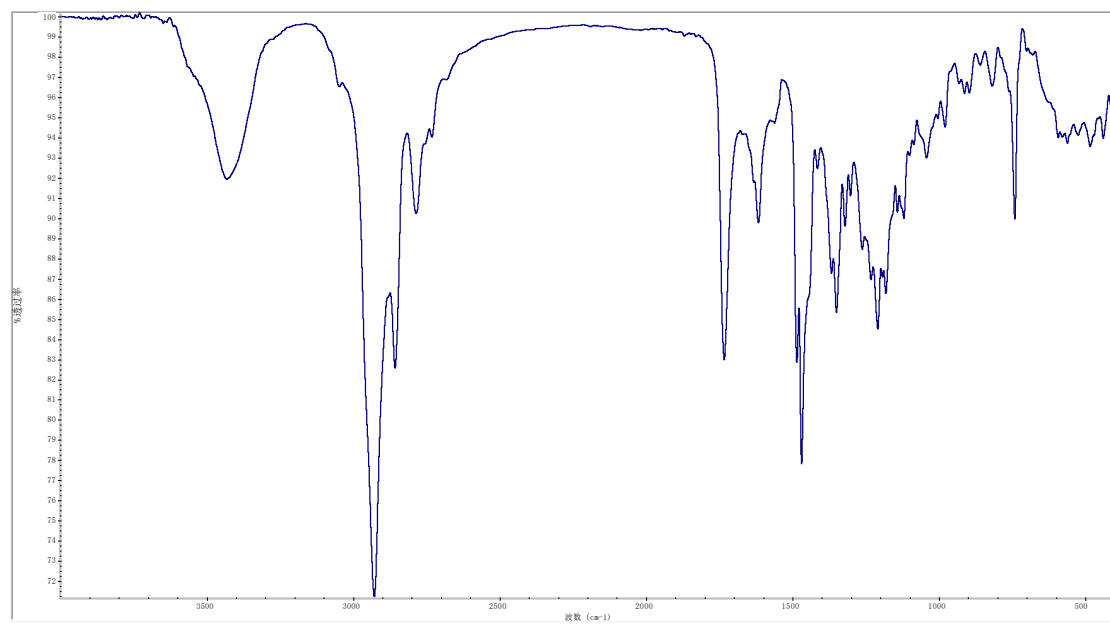
Element	Min	Max
C	3	60
H	0	120
O	0	30
N	0	8

Formula Calculator Results

Formula	CalculatedMass	CalculatedMz	Mz	Diff. (mDa)	Diff. (ppm)	DBE
C41 H52 N4 O2	632.4090	633.4163	633.4153	1.00	1.58	18.0000

--- End Of Report ---

Figure S3.8 IR (KBr disk) spectrum of 3.



Sample Name: HJV-12

KBr压片

采集时间: 星期五 6月 25 13:02:02 2021 (GMT+08:00)

仪器型号: NICOLET iS10

Software version: OMNIC 9.8.372

样品扫描次数: 16

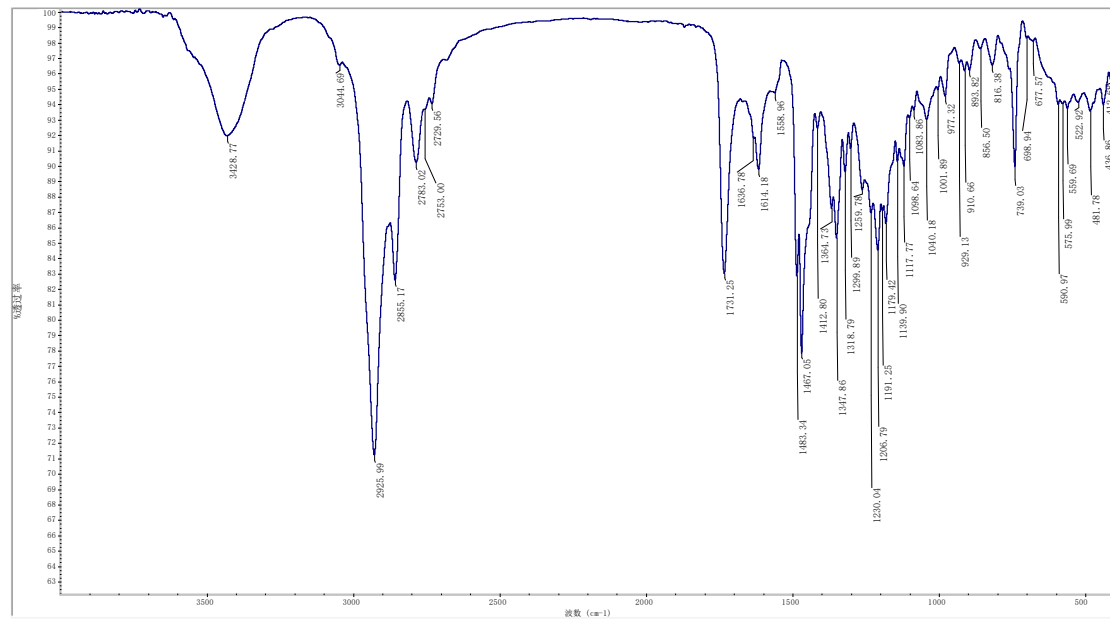
背景扫描次数: 16

分辨率: 4.000

采样增益: 1.0

动镜速度: 0.4747

光阑: 80.00



Sample Name: HJV-12

KBr压片

采集时间: 星期五 6月 25 13:02:02 2021 (GMT+08:00)

仪器型号: NICOLET iS10

Software version: OMNIC 9.8.372

样品扫描次数: 16

背景扫描次数: 16

分辨率: 4.000

采样增益: 1.0

动镜速度: 0.4747

光阑: 80.00

Figure S3.9 ECD spectrum of compound 3 in MeOH.

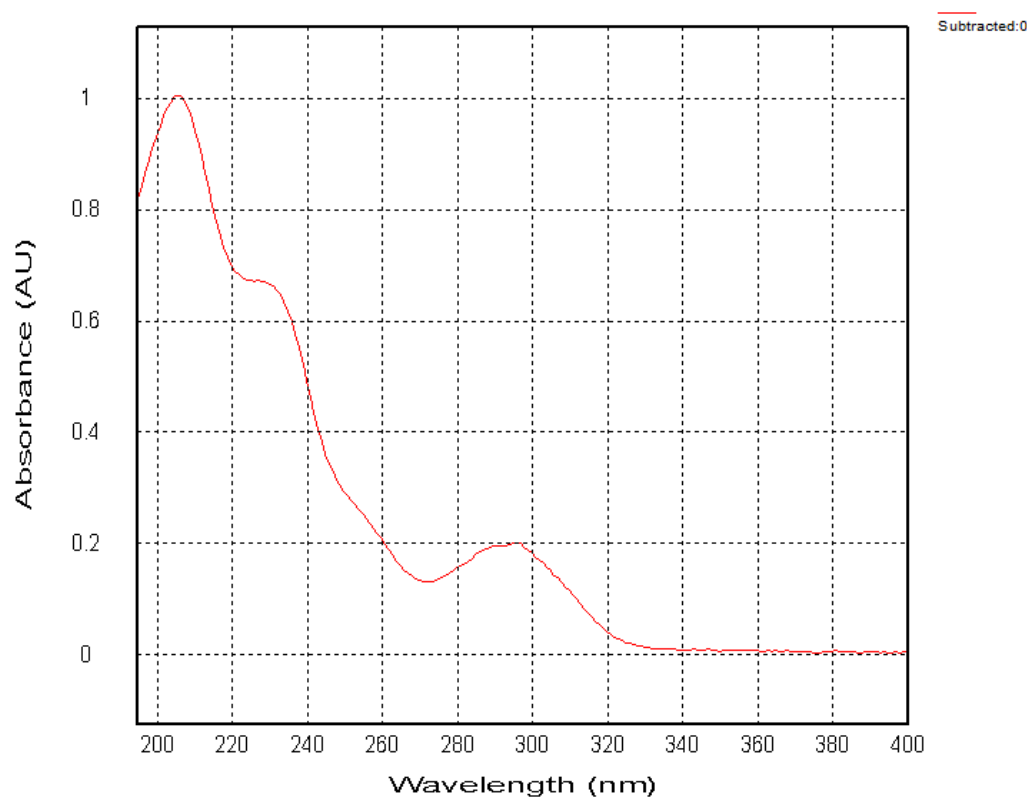
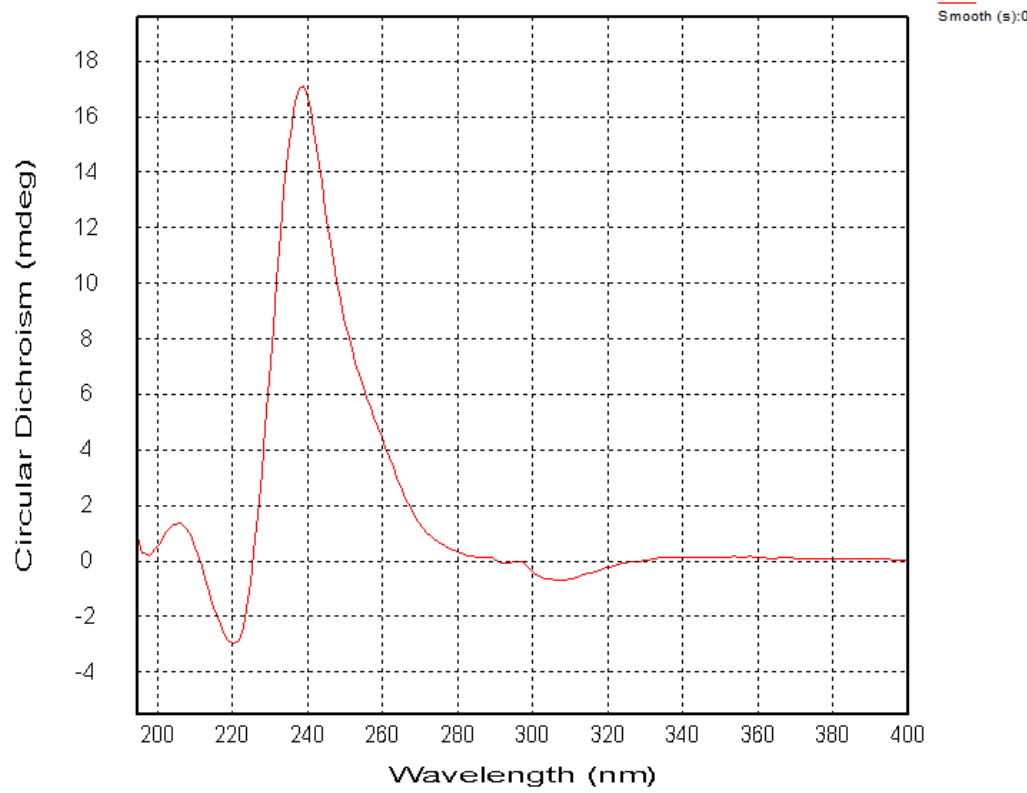


Figure S3.10 Comparison of the experimental ECD and calculated ECD spectra of 3.

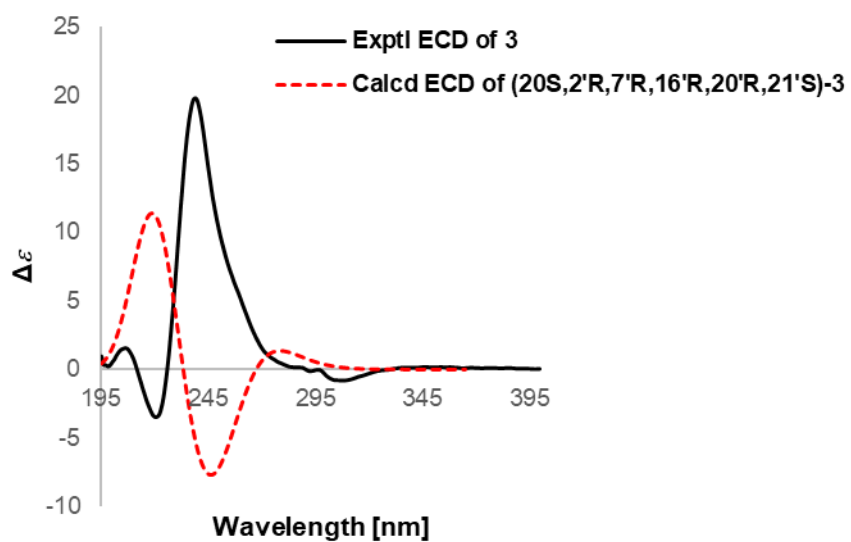
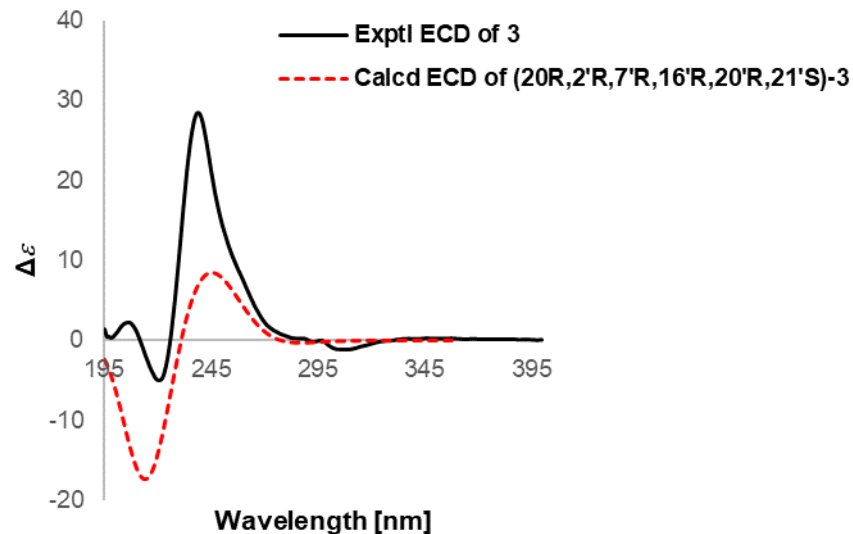


Figure S3.11 Optical rotation analysis of compound 3.

Rudolph Research Analytical

This sample was measured on an Autopol VI, Serial #91058
Manufactured by Rudolph Research Analytical, Hackettstown, NJ, USA.

Measurement Date : Tuesday, 26-JUL-2022

Set Temperature : 25.0

Time Delay : Disabled

Delay between Measurement : Disabled

<u>n</u>	<u>Average</u>	<u>Std.Dev.</u>	<u>% RSD</u>	<u>Maximum</u>	<u>Minimum</u>						
5	6.84	0.37	5.40	7.50	6.67						
S.No	Sample ID	Time	Result	Scale	OR °Arc	WLG.nm	Lg.mm	Conc.g/100ml	Temp.		
1	HJV-12	04:52:34 PM	7.50	SR	0.009	589	100.00	0.120	24.8		
2	HJV-12	04:52:41 PM	6.67	SR	0.008	589	100.00	0.120	24.8		
3	HJV-12	04:52:47 PM	6.67	SR	0.008	589	100.00	0.120	24.9		
4	HJV-12	04:52:53 PM	6.67	SR	0.008	589	100.00	0.120	24.9		
5	HJV-12	04:53:00 PM	6.67	SR	0.008	589	100.00	0.120	25.0		

Figure S3.12 The chiral HPLC chromatogram of **3**.

Chiral-phase resolution of **3** was carried out using the Daicel Chiraldapak IC column ($5 \mu\text{m}$; $10 \text{ mm} \times 250 \text{ mm}$) with 2-propanol-*n*-hexane (3:7) as the eluent.

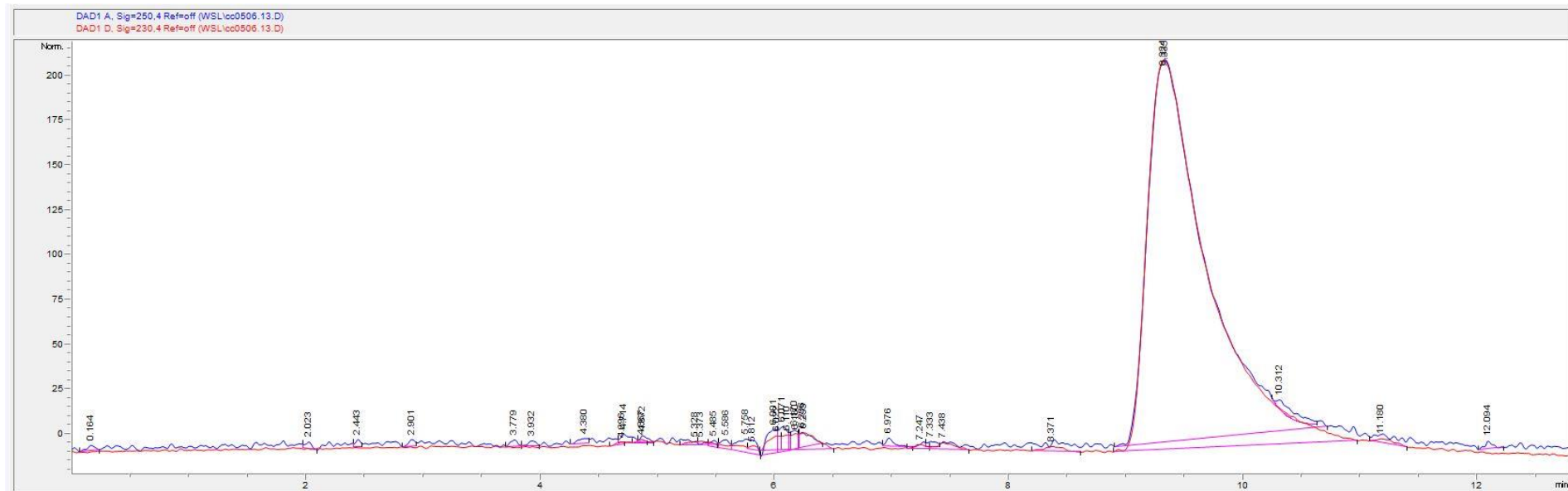


Figure S3.13 The molecular docking results of compound **3** with CDK5. (A) Two-dimensional ligand interaction diagram of compound **3** with the residues in the active site of CDK5. (B) Site view of the interactions observed between the residues in the active cavity of CDK5 and compound **3**.

